

ELECTRONIC STRUCTURE OF  
REACTIVE INTERMEDIATES:  
CARBONYL CARBENES AND LITHIUM  
CARBENES; THE ZERO-FIELD SPLITTING  
PARAMETERS OF METHYLENE

Dissertation for the Degree of Ph. D.  
MICHIGAN STATE UNIVERSITY  
RICHARD CHARLES LIEDTKE  
1975

**LIBRARY**  
**Michigan State**  
**University**

This is to certify that the  
thesis entitled  
**ELECTRONIC STRUCTURE OF REACTIVE INTERMEDIATES:  
CARBONYL CARBENES AND LITHIUM CARBENES;  
THE ZERO-FIELD SPLITTING PARAMETERS OF METHYLENE**

presented by

**Richard Charles Liedtke**

has been accepted towards fulfillment  
of the requirements for

Ph.D. degree in Chemical Physics

*James F. Harrison*  
Major professor

Date 1975 July 15

0-7639

BINDING BY  
HOAG & SONS'  
BOOK BINDERY INC.  
LIBRARY BINDERS  
SPRINGPORT, MICHIGAN

ABSTRACT

015551  
ELECTRONIC STRUCTURE OF REACTIVE INTERMEDIATES:  
CARBONYL CARBENES AND LITHIUM CARBENES;  
THE ZERO-FIELD SPLITTING PARAMETERS OF METHYLENE

By

Richard Charles Liedtke

Minimal basis ab initio SCF-CI calculations on the lowest states of the carbonyl carbene, :CHCOH, and its fluorine-substituted forms, :CHCOF and :CFCOH, yielded the state ordering  $E(^3A'') < E(^1A') < E(^1A'')$  for :CHCOH and :CHCOF, with the differential effects of correlation energy expected to make the  $^1A'$  state the ground state for :CFCOH. The state energy separations in :CHCOH were calculated to be 1.09 eV for  $^1A' + ^3A''$  and 1.39 eV for  $^1A'' + ^3A''$ . A geometry search for the :CHCOH states predicted equilibrium H-C-(COH) angles of  $\sim 125^\circ (^3A'')$ ,  $\sim 103^\circ (^1A')$ , and  $\sim 133^\circ (^1A'')$ , very similar to the :CH<sub>2</sub> values. The effects of fluorine substitution on the formyl group (:CHCOF) was found to have a minimal effect on the electronic structure of the low-lying states, while direct fluorine substitution (:CFCOH) resulted in a dramatic stabilization of the  $^1A'$  state relative to the A'' states. Significant polarization of the carbonyl group was found to accompany either substitution. The  $^1A'$  state of :CHCOH showed no spontaneous tendency to rearrange to ketene.

In addition, using a double-zeta quality basis plus a set of optimized Li p functions, restricted open-shell SCF calculations were done on the triplet ground states of the

lithium-substituted methylenes,  $\text{:CHLi}$  and  $\text{:CLi}_2$ , and the first excited triplet state ( $^3\Pi$ ) of  $\text{:CHLi}$ . The low-lying singlet states were constructed via a single-excitation CI within the set of virtual  $\pi$  orbitals from the ground state SCF. All the  $\text{:CHLi}$  states examined were found to have linear equilibrium geometries, a characteristic expected to apply more strongly to the states of  $\text{:CLi}_2$ . Open-shell SCF calculations on the stable fragments of both molecules indicated that all states except the  $^1\Sigma_g^+$  state of  $\text{:CLi}_2$  were at least nominally stable to dissociation.

A refinement of a previous calculation of the spin-spin contribution to the zero-field splitting parameters of  $^3B_1$  methylene was also done. The gaussian lobe function basis was retained, but the CI wave function was enlarged to the "best" 100 structures and improved via the iterative natural orbital technique. The ZFS parameters obtained ( $D=0.722 \text{ cm}^{-1}$ ;  $E=0.053 \text{ cm}^{-1}$ ) were in close agreement with the previous values and, with the inclusion of the most recent values for the spin-orbit contribution, in agreement with the range of experimental values.

ELECTRONIC STRUCTURE OF REACTIVE INTERMEDIATES:  
CARBONYL CARBENES AND LITHIUM CARBENES;  
THE ZERO-FIELD SPLITTING PARAMETERS OF METHYLENE

By

Richard Charles Liedtke

A DISSERTATION

Submitted to  
Michigan State University  
in partial fulfillment of the requirements  
for the degree of

DOCTOR OF PHILOSOPHY

Department of Physics  
Program in Chemical Physics

1975

To My Parents

## ACKNOWLEDGMENT

The author wishes to express his sincere appreciation to Dr. J. F. Harrison for his interest and guidance during the course of this research.

TABLE OF CONTENTS

Chapter	Page
LIST OF TABLES . . . . .	vi
LIST OF FIGURES. . . . .	ix
INTRODUCTION . . . . .	1
CHAPTER I - CARBONYL CARBENES. . . . .	4
A. Preliminaries. . . . .	4
B. :CHCOH . . . . .	7
C. :CHCOF . . . . .	22
D. :CFCOH . . . . .	34
E. Discussion . . . . .	44
CHAPTER II - LITHIUM CARBENES. . . . .	48
CHAPTER III - THE ZERO-FIELD SPLITTING PARAMETERS OF $^3B_1$ METHYLENE . . . . .	65
A. The Electron Spin-spin Interaction and the ZFS Parameters . . . . .	65
B. The Spin-spin Contribution to D and E for a CI Wave Function . . . . .	68
C. The ZFS Parameters of $^3B_1$ Methylene. . . . .	71
APPENDIX I . . . . .	76
A. The Closed Shell SCF (CSSCF) . . . . .	76
B. The Basis Set. . . . .	79
C. The CI . . . . .	80
D. Natural Orbitals . . . . .	101
APPENDIX II. . . . .	123
A. Basis Set. . . . .	123

Chapter	Page
B. The Restricted Open Shell SCF (ROSSCF) . . .	123
C. The Single Excitation CI (SECI). . . . .	127
APPENDIX III . . . . .	135
BIBLIOGRAPHY . . . . .	141

## LIST OF TABLES

Table		Page
1	Bond Lengths Fixed in Carbonyl Carbene Calculations . . . . .	6
2	:CHCOH SCF-MO's at $^3A''$ cis Equilibrium Geometry . . . . .	8
3	:CHCOH Equilibrium Geometries and CI Energies for the Three Lowest States, $^3A''$ , $^1A'$ , and $^1A''$ . . . . .	11
4	:CHCOH Largest Contributing Occupancies in the Three Lowest States . . . . .	15
5	:CHCOH (cis) Active NO's and Occupation Numbers for Three Lowest States. . . . .	18
6	:CHCOH (cis) Gross Mulliken Populations and Net Charges. . . . .	21
7	:CHCOF Active MO's and Orbital Energies. . . . .	24
8	:CHCOF Principal Contributing CI Structures for the Lowest States. . . . .	28
9	:CHCOF Active NO Occupation Numbers. . . . .	30
10	:CHCOF Gross Mulliken Populations and Net Charges. . . . .	33
11	:CFCHOH Active MO's and Orbital Energies at the $^3A''$ cis Geometry. . . . .	35
12	:CFCHOH Principal Contributing CI Structures for the Three Lowest States. . . . .	41

Table	Page
13	:CFCOH Active NO Occupation Numbers . . . . . 43
14	:CFCOH Gross Mulliken Populations and Net Charges . . . . . 45
15	Occupied MO's at Ground State Equilibrium Geometries: a) LiCH ( $^3\Sigma^-$ ) and b) Li <sub>2</sub> C ( $^3\Sigma_g^-$ ) . . . . . 50
16	Ground and Excited State Energies and Equilibrium Bond Lengths for LiCH and Li <sub>2</sub> C . . . . . 53
17	Gross Mulliken Populations and Net Charges for LiCH and Li <sub>2</sub> C . . . . . 60
18	Carbonyl Carbene Basis Set: STO-3G Coefficients and Scaled Exponents . . . . . 81
19	:CHCOH Determinantal Basis for All States. . . . . 84
20	:CHCOF $^3A''$ CI Structures. . . . . 88
21	:CHCOF $^1A'$ CI Structures. . . . . 92
22	:CHCOF $^1A''$ CI Structures. . . . . 97
23	:CFCOH $^3A''$ CI Structures. . . . . 102
24	:CFCOH $^1A'$ CI Structures. . . . . 108
25	:CFCOH $^1A''$ CI Structures. . . . . 115
26	Basis Set for LiCH and Li <sub>2</sub> C Calculations. . . . . 124
27	LiCH $^1\Delta$ SECI Structures . . . . . 129

Table		Page
28	LiCH $^1\Sigma^+$ SECI Structures . . . . .	130
29	LiCH $^1A'$ SECI Structures . . . . .	131
30	LiCH $^1A''$ SECI Structures . . . . .	132
31	Li <sub>2</sub> C $^1\Delta_g$ SECI Structures . . . . .	133
32	Li <sub>2</sub> C $^1\Sigma_g^+$ SECI Structures . . . . .	134

LIST OF FIGURES

Figure		Page
1	Coordinate System for Carbonyl Carbenes . . . . .	4
2	0-0 Energies for :CHCOH (cis) States . . .	13
3	:CHCOH Excitation Energies at $^3A''$ cis Geometry . . . . .	14
4	:CHCOH (cis) Electron Density Contour Maps for the Active a' NO's and the Total Density. . . . .	19
5	:CHCOF (cis) CI Energies for the States $^3A''$ , $^1A'$ , and $^1A''$ . . . . .	25
6	:CHCOF (cis) Excitation Energies at the $^3A''$ Geometry . . . . .	27
7	:CHCOF (cis) Electron Density Contour Maps for the Active a' NO's and the Total Density. . . . .	31
8	:CFCOH (cis) CI Energies for $^3A''$ , $^1A'$ , and $^1A''$ . . . . .	37
9	:CFCOH (cis) Excitation Energies at the $^3A''$ Geometry . . . . .	38
10	:CFCOH (cis) Excitation Energies at the $^1A'$ Geometry . . . . .	39

Figure	Page
11	:CFCOH Electron Density Contour Maps for Active NO's and Total Density at the $^3A''$ cis Geometry . . . . . 42
12	Effect of Fluorine Substitution on the Energy Levels of Carbonyl Carbenes. . . . . 46
13	LiCH ( $^3\Sigma^-$ ) Electron Density Contours for Non-Core MO's and the Total Density . . . . . 51
14	Li <sub>2</sub> C ( $^3\Sigma_g^-$ ) Electron Density Contours for Non-core MO's and the Total Density . . . . . 52
15	Excitation Energies at the Ground State Geometry for LiCH and Li <sub>2</sub> C. . . . . 55
16	LiCH State Energies <u>vs</u> $\theta_{Li-C-H}$ . . . . . 57
17	LiCH Orbital Energies <u>vs</u> $\theta_{Li-C-H}$ . . . . . 59
18	Correlation of LiCH Levels and Dissocia- tion Fragments. . . . . 62
19	Correlation of Li <sub>2</sub> C Levels and Dissociation Fragments. . . . . 63
20	Relation of D and E to the Zero-Field Level Splittings of a Triplet State . . . . . 68
21	:CH <sub>2</sub> ( $^3B_1$ ) Energy <u>vs</u> $\theta_{HCH}$ . . . . . 74
22	:CH <sub>2</sub> ( $^3B_1$ ) Spin-spin ZFS Parameters <u>vs</u> $\theta_{HCH}$ . . . . . 75

## INTRODUCTION

Methylene,  $\text{:CH}_2$ , is the parent species of a family of compounds called carbenes, which have the distinguishing property that they contain a formally divalent carbon. The term methylene appeared in chemistry as early as the 1830's, and the halocarbene,  $\text{:CCl}_2$ , was proposed by Geuther<sup>1</sup> in 1862 as an intermediate in the hydrolysis of chloroform. However, it was only about 1910 through the work of Staudinger that firm ground was laid in understanding the mechanisms of carbene chemistry. It was Staudinger and Kupfer<sup>2</sup> who obtained the first compelling evidence for the existence of free methylene. Except for the suggestions of Mulliken<sup>3</sup> in 1932, the theoretical investigation of carbene structure was virtually non-existent until the 1950's. After 1950, a prolific literature of divalent carbon has been seen to develop in both the experimental and theoretical aspects of carbene structure.

It was in 1950 that the first substantial spectroscopic evidence of the carbene  $\text{:CF}_2$  was obtained.<sup>4,5</sup> In 1959, Herzberg and Shoosmith<sup>6</sup> succeeded in recording the first absorption spectrum of methylene produced in the flash photolysis of diazomethane at low pressure. Herzberg and Johns<sup>7,8</sup> made a detailed analysis of the high resolution absorption spectra of both the singlet and triplet states, concluding that the ground state of  $\text{:CH}_2$  was a linear triplet

( ${}^3\Sigma_g^-$ ), and the first excited state a highly bent ( $\theta_{\text{HCH}}=103^\circ$ )  ${}^1A_1$ .

Consistent theoretical structure calculations of increasing accuracy,<sup>9,10</sup> supported by the first successful observation of an esr spectrum of matrix-isolated  $:\text{CH}_2$  by two groups<sup>11,12</sup> in 1970, prompted a reinterpretation of the absorption spectra by Herzberg in 1971.<sup>13</sup> He found that under the assumption of a bound  ${}^3A_2$  state, heterogeneously predissociated by a  ${}^3B_2$  state, an interpretation consistent with a bent  ${}^3B_1$  ground state could be made. Furthermore, under the new interpretation, the spectroscopic data predicted a  ${}^3B_1$  angle of  $136^\circ$  and a C-H bond length of 1.078 Å, in striking agreement with the theoretical values. This event was important in lending credibility to the predictive power of quantum chemical calculations.

It has been in the last two decades that quantum chemical calculation has developed into the powerful tool it is today. This fact is a consequence of the phenomenal development of high-speed reliable computing machines -- a development which has accelerated through the 1960's. Calculations on methylene have progressed from the extended Hückel results of Hoffman *et al.*<sup>14</sup> to the most recent and accurate *ab initio* study by Staemmler.<sup>15</sup>

It was in the light of the history of carbenes and the continuing interest in carbenes as reactive intermediates in organic chemistry that the work presented in this thesis was begun. The basic motivation was to extend the theoretical

understanding of carbene structure by examining the effects of substitution on carbonyl carbenes, the simplest example of which was taken to be  $\text{:CHCOH}$ . Of primary interest was the electronic character and the equilibrium geometry of the ground state and the lowest excited states, as well as the ordering and approximate excitation energies of those states. In addition, calculations were done on the lithium-substituted methylenes,  $\text{:CHLi}$  and  $\text{:CLi}_2$ , to examine the effect of a strong electron donor as a substituent on methylene. Also included is a refined calculation of the Zero-Field Splitting parameters of  $^3\text{B}_1$  methylene, first done by Harrison.<sup>16</sup> The importance of these parameters is connected with the esr work cited above, the value of which is unquestionable.

Good reviews of the structure and chemistry of carbenes may be found in the literature; a few of the most comprehensive are cited in the bibliography.<sup>17,18,19</sup>

CHAPTER I  
CARBONYL CARBENES

A. Preliminaries

Ab initio SCF-CI studies of three carbonyl carbenes were carried out to examine the effects on the carbene electronic structure arising from fluorine substitution. The three carbenes involved were :CHCOH, :CHCOF, and :CFCOH, written more generally as :CRCOR'. The coordinate system and relevant geometrical parameters are illustrated in Figure 1.

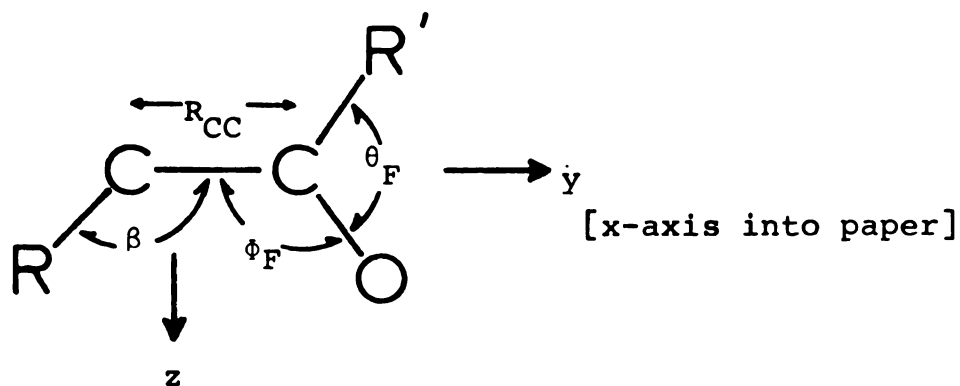


Figure 1. Coordinate System for Carbonyl Carbenes.

The molecules were taken to be planar for the states of interest, and only four of the many degrees of freedom were allowed to vary. As shown in Figure 1, the four parameters included all the angles and one bond length. Two of the angles,  $\theta_F$  and  $\phi_F$ , define the formyl group geometry; the third angle,  $\beta$ , is what was called the "carbene angle". Except for the carbon-carbon bond length,  $R_{CC}$ , all bond

lengths were fixed at predetermined values. Table 1 gives the bond length values used for each molecule.

For  $\beta \neq 180^\circ$ , it is useful to distinguish between two cases. Since it was desired to restrict  $\beta$  to be positive and  $\leq 180^\circ$ , the convention was adopted that for the substituent R and the oxygen on the same side of the carbon-carbon bond, the term "cis" would apply; the alternate case was termed "trans".

Appendix I contains a description of the basis functions used for this series of molecules as well as the closed shell self-consistent field (CSSCF) theory used to obtain the molecular orbitals (MO's). Also given is a description of the configuration interaction method (CI) for extending the SCF results. Briefly, the basis used was a minimal set of STO-3G functions described by Pople et al.,<sup>20</sup> constructed in a primitive basis of nuclear-centered cartesian gaussian functions (NCGTF). Appendix I also defines the approximate natural orbitals (NO's) discussed in this chapter and used to construct the atomic populations associated with the total CI electron density.

In this chapter, as well as the rest of the thesis, all results were obtained in atomic units (au), but some results are given in other units where noted.

Table 1. Bond Lengths Fixed in Carbonyl Carbene Calculations.<sup>a</sup>

Molecule	:CHCOH	:CHCOF	:CFCOH
R <sub>CO</sub>	2.340 <sup>b</sup>	2.340	2.340
R <sub>CF</sub> (formyl)	-----	2.532 <sup>c</sup>	-----
R <sub>CH</sub> (formyl)	2.060 <sup>b</sup>	-----	2.060
R <sub>CH</sub>	2.0787	2.0787	-----
R <sub>CF</sub>	-----	-----	2.457 <sup>d</sup>

<sup>a</sup>All values are in atomic units (bohrs).

<sup>b</sup>Shalhoub and Harrison.<sup>21</sup>

<sup>c</sup>Csizmadia.<sup>22</sup>

<sup>d</sup>Powell and Lide.<sup>23</sup>

B. :CHCOH

This molecule is the simplest carbonyl carbene (excluding :CCO), and, like its precursor :CH<sub>2</sub>, was found to have a bent triplet ground state. The MO's used to characterize the molecule were constructed via a CSSCF calculation. These MO's, their orbital energies at the ground state equilibrium geometry and approximate character are listed in Table 2. Following Hoffmann,<sup>14</sup> the MO of a' symmetry localized as a "lone pair" orbital on the carbene carbon is denoted "σ", while the a" MO localized roughly as an atomic p function on the carbene carbon is called "p". Three other MO's were given descriptive symbols reflecting their atomic associations: the 1a" ( $\pi_{CO}$ ) appears mainly as a CO bonding function in the formyl group; the 9a' ( $\sigma_O$ ) is strongly localized "p function" on oxygen perpendicular to the CO bond; and the 3a" MO ( $\pi^*$ ) is a virtual MO (i.e., unoccupied in the SCF determinant) displaying primarily anti-bonding character between the formyl carbon and oxygen. These five MO's are the only MO's whose occupation was allowed to change in the CI wave function, and therefore they are called the "active" MO's. The eight lowest-energy MO's were considered to represent the molecular core. The occupation of these "core" orbitals was "frozen" in the CI at two each. The electronic structure of the lowest excited states is usually determined by excitations from the valence electrons and not the "core". An unfortunate

Table 2. :CHCOH SCF MO's at  $^3A''$  cis Equilibrium Geometry

MO	Character	$-\epsilon$ (au)
1a'	 CORE	20.24
2a'		11.15
3a'		11.02
4a'		1.30
5a'		0.90
6a'		0.73
7a'		0.58
8a'		0.51
1a''	$\pi_{CO}$	0.47
9a'	$\sigma_O$	0.32
2a''	p	0.25
10a'	$\sigma$	-0.12
3a''	$\pi^*$	-0.31
11a'	 Unused virtual MO's	-0.58
12a'		-0.70

discovery near the end of the work on this molecule was that the SCF determinant used was not the lowest root. The lowest-energy single determinant has a doubly-occupied  $\sigma$  MO and an empty p MO. As a result, there was some question of the description of the  $\sigma$  MO. Some consideration of the orthogonality constraints on the  $\sigma$  system above the nine occupied a' MO's, the apparent character of the  $\sigma$  MO itself, and the power of the CI to adjust for such effects led to some confidence that the net result of the less desirable MO's was small. With regard to this discussion it is convenient to adopt another notational convention used by Hoffmann. Since it is usual in carbenes that the CSSCF determinant has either the  $\sigma$  or p MO as the highest occupied MO and the other as the lowest unoccupied MO, Hoffmann calls the carbene a " $\sigma^2$  carbene" if the highest occupied MO in the CSSCF is the  $\sigma$  MO and a " $p^2$  carbene" if the p MO holds that position. In those terms :CHCOH could be called a  $\sigma^2$  carbene.

To obtain the wave functions representative of the molecular electronic states, a CI calculation was done in a basis of 100 determinants constructed by permuting the six active electrons ( $3\alpha$  and  $3\beta$ ) among the ten active spin-orbitals (5 spatial MO's). A list of the determinants used can be found in Appendix I. Since only three a" MO's (one for each first-row atom) could be constructed in the minimal basis, all three were included in the active set to insure as much flexibility as the CI could afford.

For each of the three lowest states of :CHCOH ( $^3A''$ ,

$^1A'$ ,  $^1A''$ ), equilibrium geometries were found by a limited optimization of the four geometrical parameters with respect to the total energy. Each state was found to be bent ( $\beta \neq 180^\circ$ ), and the cis and trans equilibria were nearly degenerate in energy, with the equilibrium values of the geometrical parameters essentially identical. These results are displayed in Table 3. In contrast to a 1972 study of this molecule by Bodor and Dewar,<sup>24</sup> the first excited state,  $^1A'$ , did not display any spontaneous tendency to rearrange to ketene. Their work, using the semi-empirical MINDO/2 technique and a one-determinant closed shell representation of the  $^1A'$  state, predicted a barrierless migration of the formyl hydrogen to form singlet ground state ketene. Since ab initio SCF-CI results for  $:CH_2$  have shown that the first singlet ( $^1A_1$  for  $:CH_2$ ) is a strong mixture of both the  $\sigma^2$  and  $p^2$  closed shell determinants, results of calculations ignoring this fact are at least suspect.

The basic results of the  $:CHCOH$ , as reported here, are that  $:CHCOH$  has a  $^3A''$  strongly bent ground state ( $\beta \approx 125^\circ$ ); the first excited state is an even more strongly bent ( $\beta = 103^\circ$ )  $^1A'$ ; and the second excited state,  $^1A''$ , is still significantly bent ( $\beta \approx 133^\circ$ ). In addition, the effect of the formyl group is not significant in distinguishing the cis and trans conformations, the difference in energy between the two forms being  $\leq 2$  kcal/mole for any state. The results thus far are very close to the structural properties of the parent methylene.

Table 3.  $\text{:CHCOH}$  Equilibrium Geometries and CI Energies for the Three Lowest States,  $3A''$ ,  $1A'$ , and  $1A''$ .

State	E (au)	$\beta$	$R_{CC}$ (bohrs)	$\theta_F$	$\phi_F$
$3A''$ cis	-149.70592	126.9°	2.768	121.3°	121.7°
$3A''$ trans	-149.70507	124.8°	2.770	120.7°	125.1°
$1A'$ cis	-149.65874	103.7°	2.875	120.1°	122.9°
$1A'$ trans	-149.65588	103.3°	2.891	119.7°	121.2°
$1A''$ cis	-149.64559	134.2°	2.638	121.0°	121.4°
$1A''$ trans	-149.64751	132.0°	2.619	119.7°	125.9°

The predicted 0-0 transition energies are shown in Figure 2. Since the trans levels are nearly degenerate with their cis counterparts, they are not shown in the figure. The vertical excitation energies at the  $^3A''$  cis equilibrium geometry are displayed in Figure 3, which also includes the third and fourth excited states at the  $^3A''$  cis geometry.

The electronic structure of each state was analyzed by examining the constituent contributions to the CI wave function. The determinants are the obvious constituents of the wave function, but more fundamental are those combinations of determinants which are spin eigenfunctions and have the same symmetries as the state of interest. Such entities are called "structures". Each structure is composed of determinants defining the same distribution of electrons among the spatial MO's, i.e., defining a definite orbital occupancy. Table 4 lists the largest contributing "occupancies" and their weights in the CI wave function. In the table, only the active orbital occupations are given, the "core" being understood to be completely filled in each determinant. From the table, it can be seen that the  $A''$  states are dominated by the occupancy involving two unpaired electrons, one in the  $\sigma$  MO and one in the  $p$  MO. The next most important occupations in these two cases involve single and double excitations with respect to the dominant term, i.e., one or two electrons in the dominant occupancy may be considered to have been moved

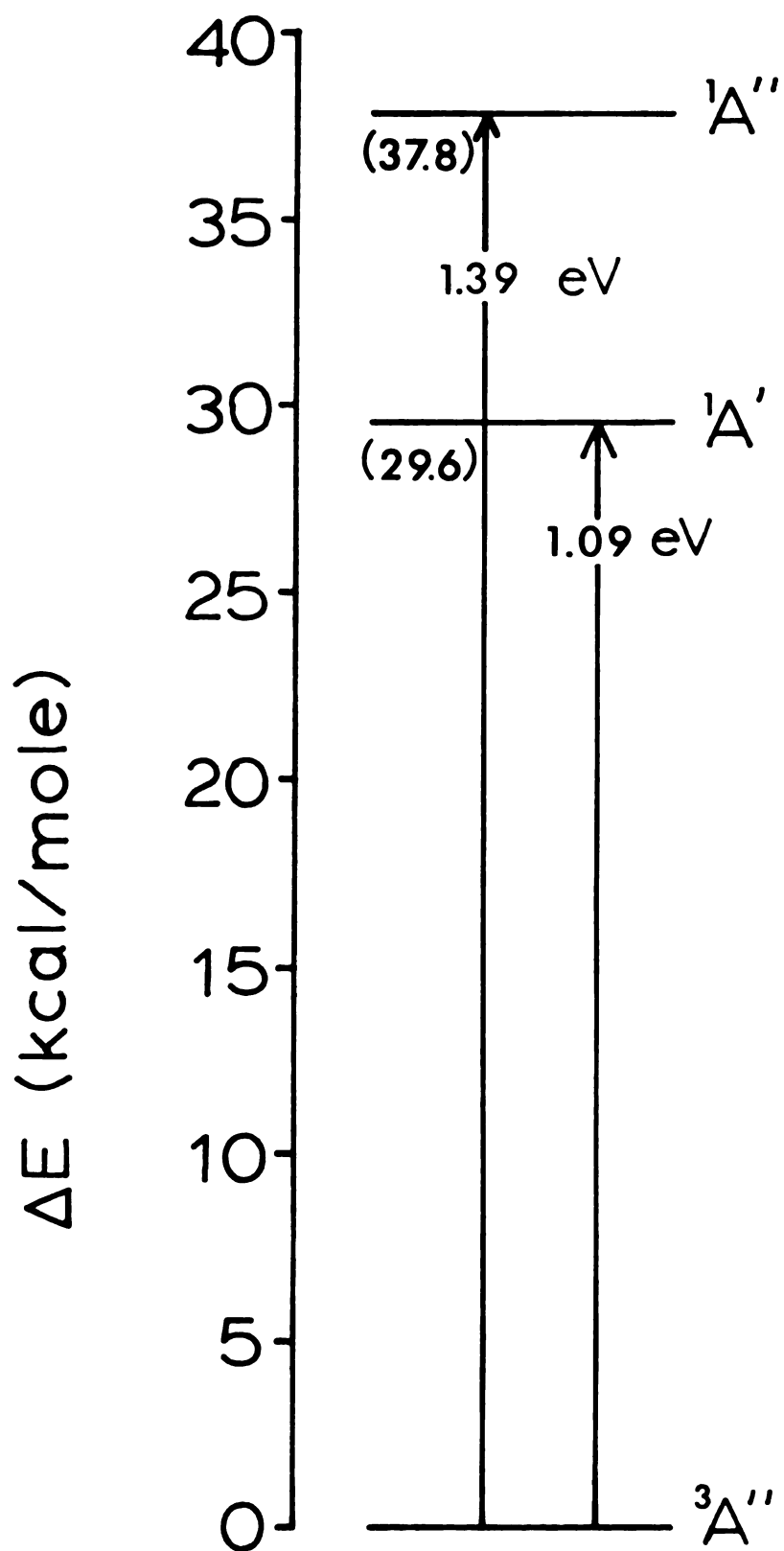


Figure 2. 0-0 Energies for  $\text{:CHCOH (cis)}$  States.

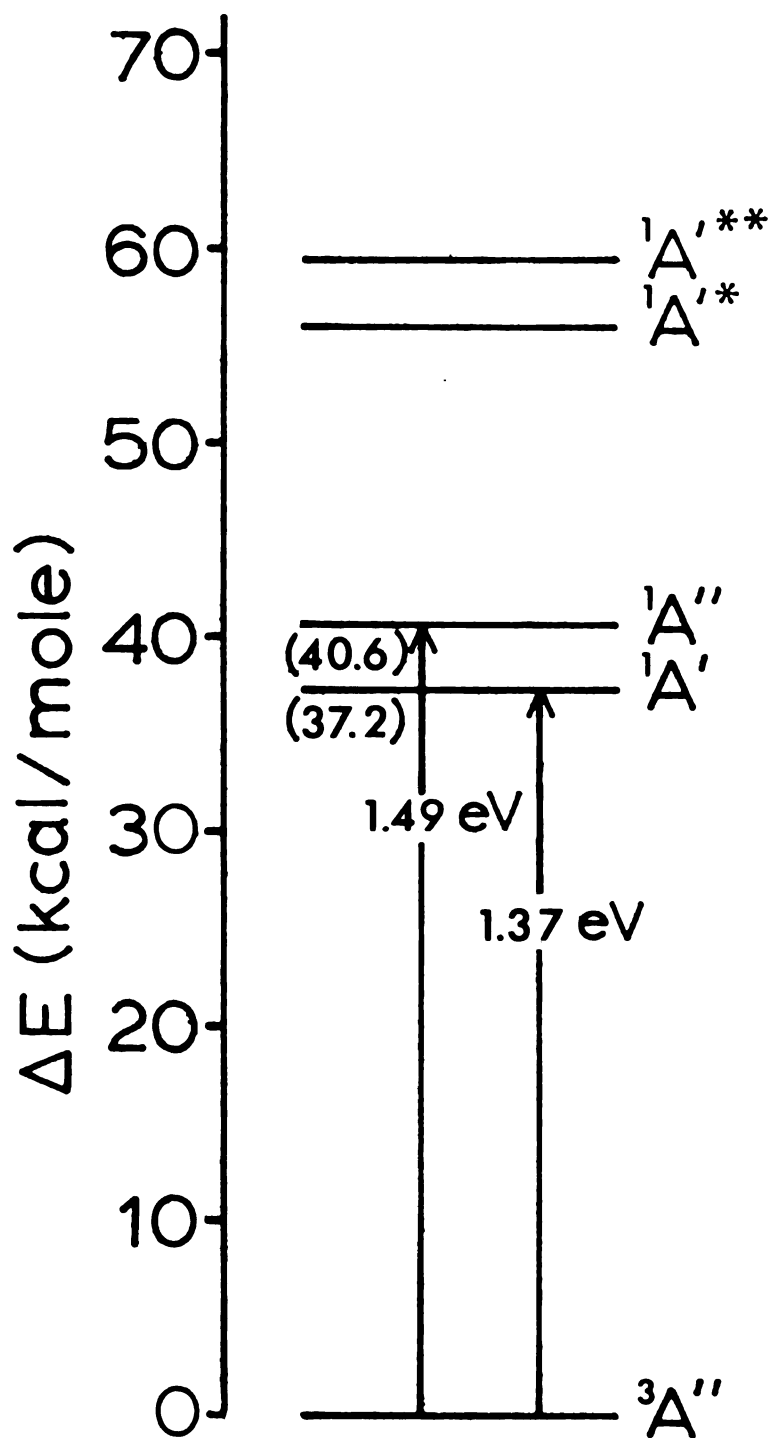


Figure 3.  $\text{:CHCOH}$  Excitation Energies at  ${}^3A''$  cis Geometry.

Table 4. :CHCOH Largest Contributing Occupancies in the Three Lowest States.

State	Structure Occupation					Coefficient
	$\pi_{CO}$	$\sigma_O$	p	$\sigma$	$\pi^*$	
$^3A''$ cis	2	2	1	1		0.936
		2	1	1	2	-0.182
	1	2	1	1	1	0.176
	1	2	2	1		-0.150
$^1A'$ cis	2	2		2		0.890
	2	2	2			-0.272
	1	2	1	2		-0.218
		2		2	2	-0.176
		2	1	2	1	-0.175
$^1A''$ cis	2	2	1	1		0.908
	2	2		1	1	0.249
	1	2	1	1	1 (a)	0.211
	1	2	1	1	1 (b)	0.163
		2	1	1	2	0.148

to higher energy MO's of the same symmetry. The excitations serve two roles in the CI wave function, they correct the MO description, which may be inappropriate for the state of interest, and they allow for the correlation of electrons of opposite spins - an effect not achieved completely by the SCF wave function. The single excitations usually only contribute via the first role, while the doubles participate in both. For the two  $A''$  states of  $:CHCOH$  under consideration, the MO's are derived from a closed shell SCF wavefunction, and the large contributors outside of the dominant occupancy are principally involved with refining the MO's to describe open shell states.

Turning to the  ${}^1A'$  state, a different situation becomes apparent; namely, that the second largest contributing occupancy is not describable as a double excitation refining the  $\sigma$  MO. The MO excited to is of a different symmetry type. Hence, the second occupancy listed, the  $p^2$  determinant, contributes a completely different aspect of the electronic distribution in the  ${}^1A'$  state than does the dominant  $\sigma^2$  determinant. The  $\sigma^2$  and  $p^2$  determinants represent different character in terms of preferred geometries; the  $p^2$  has a linear ( $\beta \approx 180^\circ$ ) equilibrium, while the  $\sigma^2$  is strongly bent ( $\beta \approx 100^\circ$ ). The conclusion is that just one of these determinants could not even qualitatively represent the essential electronic structure of the  ${}^1A'$  state of  $:CHCOH$ . In reference to the  ${}^1A''$  state entries in Table 4, the two rows labelled a) and b) indicate that for four unpaired

electrons there are two completely different ways to couple the spins so as to form a  $^1A''$  structure.

Another way to analyze a CI wavefunction is to construct its NO's, i.e., the eigenfunctions of the one-particle density matrix. They provide the simplicity of a set of one-particle functions, usually more localized than the MO's, but with non-integral occupations. Along with their eigenvalues, called occupation numbers, the NO's yield the same electron density distribution as the CI wave function, and therefore are convenient for use in Mulliken atomic population analyses.

For the  $^3A''$ ,  $^1A'$ , and  $^1A''$  states of :CHCOH, Table 5 lists the NO's corresponding to the MO active set along with their occupation numbers. Electron density contour maps of the  $a'$  NO's and the total CI density of the  $^3A''$  cis state are shown in Figure 4. The contour values range from 0.005 electrons/(bohr)<sup>3</sup> to 0.075 electrons/(bohr)<sup>3</sup> in steps of 0.01 electrons/(bohr)<sup>3</sup>. These contour values are used consistently throughout the thesis and seem to be appropriate to electron densities in the valence region.

For the  $A''$  states, the  $\sigma$  and  $p$  NO's are strongly localized on the carbene carbon, and their occupation numbers (both essentially one) indicates the unpaired spin is therefore also associated with the carbene carbon. For the  $^1A'$  state, it is apparent that although the  $\sigma$  NO is very important, the  $p$  NO contains a substantial contribution. The significance of the  $p$  NO is important in the chemical properties of carbenes, since the electrophilicity of singlet carbenes

Table 5. :CHCOH (cis) Active NO's and Occupation Numbers  
for Three Lowest States

NO	State		
	$^3A''$	$^1A'$	$^1A''$
$\pi_{CO}$	1.870	1.859	1.881
$\sigma_O$	1.994	1.989	1.991
p	1.002	0.229	1.003
$\sigma$	1.004	1.829	1.008
$\pi^*$	0.129	0.093	0.117

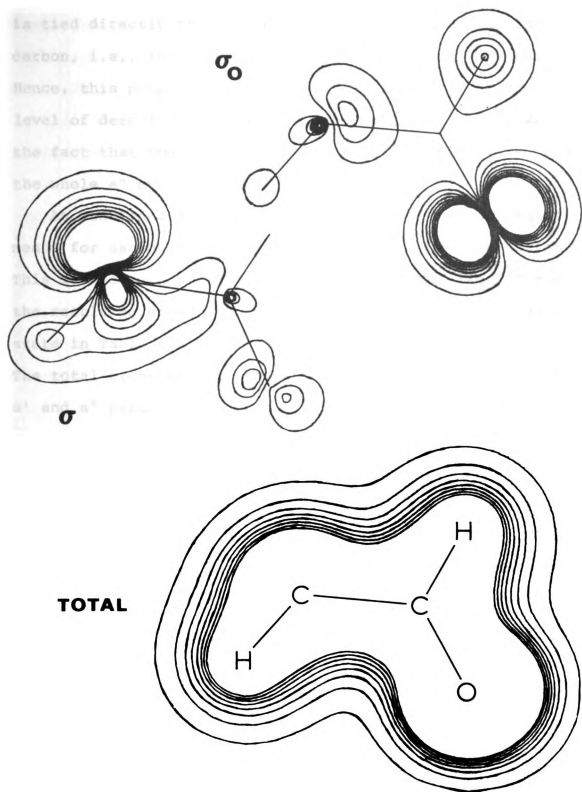


Figure 4. :CHCOH (cis) Electron Density Contour Maps for the Active  $\sigma$ ' NO's and the Total Density.

is tied directly to the amount of  $a''$  density on the carbene carbon, i.e., less density indicates greater electrophilicity. Hence, this property is not dealt with properly at the SCF level of description. Also of note, although not shown, is the fact that the p NO of the  $^1A'$  state is delocalized over the whole  $a''$  system.

As mentioned above, the NO's provide a very convenient means for assigning electron populations to atomic centers. This was done, according to the method of Mulliken,<sup>25</sup> and the resulting gross atomic populations are given for each state in Table 6, divided into  $a'$  and  $a''$  contributions. The total gross atomic populations are just the sum of the  $a'$  and  $a''$  parts for each atom. Also given is the net charge on each atomic center. Again, in the results given so far, no significant differences were seen for the trans configurations. In the table, the carbene carbon and its associated hydrogen are listed first and subscripted with a "c". The population analysis reveals small net charges on any atomic center (indicative of covalent bonding), a carbene carbon slightly negative in the  $A''$  states and positive in the  $A'$  state, and a consistently negative oxygen (not surprising since oxygen is the most electronegative element present). Here again the significance of the  $a''$  density (0.20 electron) on the carbene carbon in the  $^1A'$  state indicates a less electrophilic character than the  $\sigma^2$  SCF would predict.

The equilibrium geometries and energy ordering of the

Table 6. :CHCOH (cis) Gross Mulliken Populations and Net Charges.

Center	$3A''$			$1A'$			$1A''$		
	$n_{a'}$	$n_{a''}$	$\delta$	$n_{a'}$	$n_{a''}$	$\delta$	$n_{a'}$	$n_{a''}$	$\delta$
H <sub>C</sub>	.95	-----	+0.05	1.02	-----	-.02	.94	-----	+0.06
C <sub>C</sub>	5.09	.95	-.04	5.72	.20	+0.08	5.13	.89	-.02
C	5.01	.95	+0.04	5.10	.92	-.01	5.00	1.02	-.02
O	6.99	1.10	-.09	7.02	1.06	-.08	6.97	1.08	-.06
H	.96	-----	+0.04	.96	-----	+0.04	.96	-----	+0.04

low-lying states, as well as the essential electronic structure of :CHCOH was seen to be very close to those of the precursor, :CH<sub>2</sub>. It should be remarked that differences in the correlation energies of the three states investigated would have the probable result of lowering the <sup>1</sup>A' state energy relative to the A" states. This relative lowering, expected to be mainly due to the pair correlation of the doubly-occupied σ MO in the <sup>1</sup>A' state, was anticipated to be several tenths of an eV, certainly less than 1 eV, and therefore not enough to change the prediction of a <sup>3</sup>A" ground state. The effect of the formyl group was not disruptive of the methylene-like electronic structure.

### C. :CHCOF

Fluorine was substituted for hydrogen in the formyl group of :CHCOH. In the series of molecules treated in this chapter, :CHCOF may be called the indirectly-substituted carbene, the substitution site not being on the carbene carbon itself. The C-F bond length was taken as that listed in Table 1. A preliminary geometry search near the <sup>3</sup>A" cis equilibrium geometry of :CHCOH indicated negligible differences in geometry for the :CHCOF <sup>3</sup>A" equilibrium. With this datum in mind and the intent of determining the electronic structure of these compounds rather than their detailed geometries, it was decided to adopt the equilibrium geometries of the states of :CHCOH

in the calculations on :CHCOF and :CFCOH (discussed in the next section).

The basis set increase associated with the fluorine resulted in one a" and three a' functions added to the MO set. Of these new MO's, the fluorine non-bonding a' MO and the new a" (essentially an atomic p function) were added to the active MO's in the CI. Table 7 lists the active MO's for :CHCOF, their symbolic description, and their orbital energies at the  $^3A''$  cis assumed equilibrium geometry. The :CHCOF active MO's, although given similar symbols, differed in some significant aspects from the corresponding MO's of :CHCOH. The  $\pi_{CO}$  was more like a F-O anti-bonding function; the p MO became more delocalized onto the formyl carbon; and the  $\pi^*$  became essentially a C-C antibonding MO. The  $\sigma_O$  and  $\sigma$  MO's retained their localized character. In short the fluorine substitution generally effected a re-characterization of the a" orbitals in the CSSCF description.

The CI wave function was constructed using the set of seven active MO's  $\{p_F \sigma_F \pi_{CO} \sigma_O \sigma p \pi^*\}$  to form structures of the required symmetries. With the  $\sigma_F$  doubly-occupied, all single and double excitations off the SCF determinant ( $\sigma^2$ ) were formed using six active MO's. Then two singlet and two triplet structures involving excitations from the  $\sigma_F$  were added. This procedure resulted in a total of 214 structures. A more detailed breakdown is given in Appendix I.

The CI energies for the  $^3A''$ ,  $^1A'$ , and  $^1A''$  states are compared for the cis geometry in Figure 5. Again the energy

Table 7. :CHCOF Active MO's and Orbital Energies.

MO	Character	$-\epsilon$ (au)
1a''	p <sub>F</sub>	0.597
11a'	$\sigma$ <sub>F</sub>	0.480
12a'	$\sigma$ <sub>O</sub>	0.421
2a''	$\pi$	0.413
13a'	$\sigma$	0.289
3a''	p	-0.131
4a''	$\pi^*$	-0.357

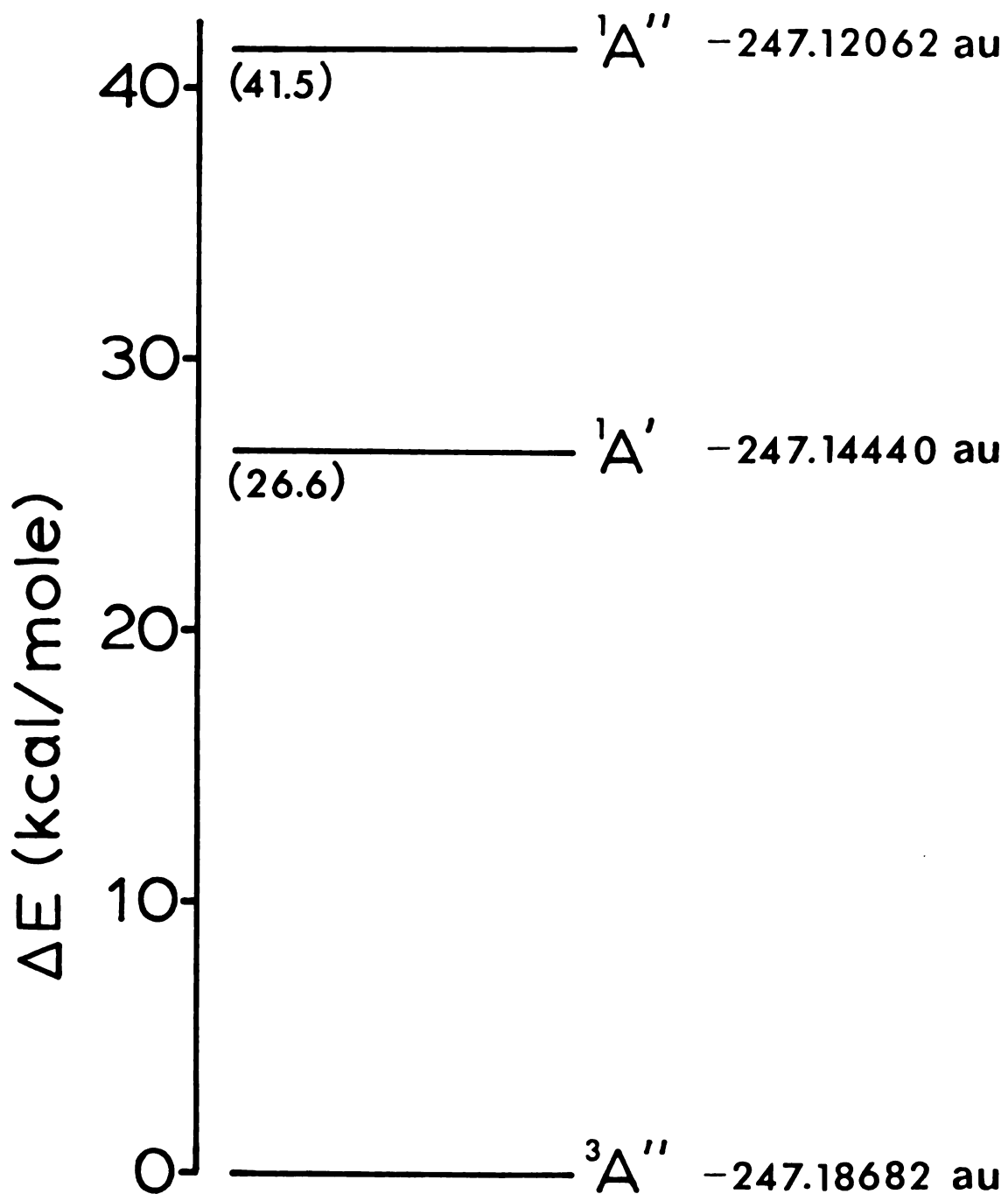


Figure 5.  $:\text{CHCOF}$  (cis) CI Energies for the States  $^3\text{A}''$ ,  $^1\text{A}'$ , and  $^1\text{A}''$ .

differences between the cis and trans geometries for each state are less than 2 kcal/mole for the  $^3A''$  state and less than 1/2 kcal/mole for the singlets. Because of the problem of selection of the SCF determinant for :CHCOH mentioned earlier, the lowering of the  $^1A'$  state relative to the  $A''$  states was difficult to interpret in terms of the fluorine substitution effects. The vertical excitation energies at the  $^3A''$  cis geometry are illustrated in Figure 6, which indicates the appearance of the first excited triplet ( $^3A'$ ) at an excitation energy of about 3.23 eV. In terms of relative energies, the indirectly-substituted fluorine did not cause any significant departures from the :CHCOH results.

An examination of the electronic structure was begun by an analysis of the important structures in the CI wave function for each state. Table 8 lists the principal structures by specifying their active MO occupation and includes their weight in the wave function. It is immediately apparent that the  $A''$  states contain a strong second structure. The effect of the second structure in both cases is to correct the  $a''$  MO's, which are presumably not close to optimal as a one-particle basis to describe the  $a''$  density of the  $A''$  states. The  $\sigma^2$  structure in the  $^1A'$  state has increased in weight relative to :CHCOH, but, again, that may easily be due to the :CHCOH SCF problem, so no conclusions are drawn.

The information in the CI wave function was again extracted through the construction and examination of its

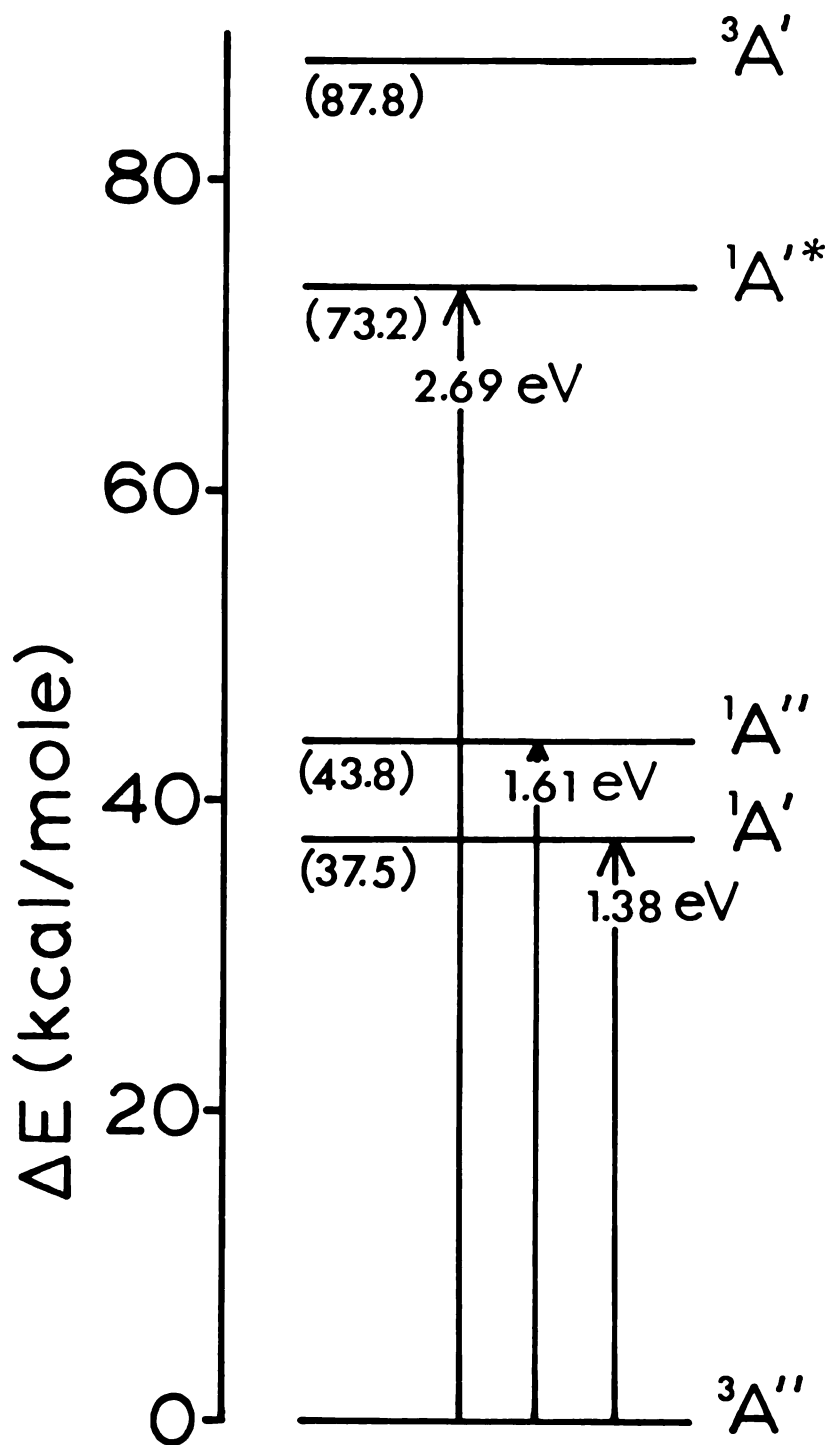


Figure 6.  $\text{:CHCOF (cis)}$  Excitation Energies at the  ${}^3A''$  Geometry.

Table 8. :CHCOF Principal Contributing CI Structures for the Lowest States.

State	Structure Occupation							Coef.
	p <sub>F</sub>	σ <sub>F</sub>	σ <sub>O</sub>	π <sub>CO</sub>	σ	p	π*	
<sup>3</sup> A" cis	2	2	2	2	1	1		.874
	2	2	2	2	1		1	-.365
	2	2	2		1	2	1	.132
	2	2	2	1	1	2		-.127
<sup>1</sup> A' cis	2	2	2		1	1	2	-.114
	2	2	2	2	2			.930
	2	2	2	2		2		-.199
	2	2	2		2	1	1	-.147
	2	2	2		2	2		-.132
	2	2	2	2		1	1	.110
<sup>1</sup> A" cis	2	2	2	2	1	1		.859
	2	2	2	1	1	2		-.347
	2	2	2	2	1		1	.165
	2	2	2	1	1	1	1	.163
	1	2	2	2	1	2		-.145

NO's. The active NO's and their occupation numbers for each state are listed in Table 9. The A" states are described essentially by doubly-occupied NO's up to the  $\sigma$  and p NO's, which each host one electron. The  $\sigma$  NO is slightly delocalized onto the oxygen, but is roughly unchanged from its MO counterpart, as can be seen in Figure 7. The significant changes induced by the CI were to localize the a" unpaired electron in the A" states on the carbene carbon, the p NO for :CHCOF appearing almost identical to the p NO for :CHCOH. Thus, the distribution of unpaired spins is essentially restricted to the carbene carbon and isolated from the influence of the substituted fluorine. The effect on the  $^1A'$  state is small. The  $\sigma$  NO for the  $^1A'$  state is mainly restricted to the carbene carbon and the p NO is very similar to the :CHCOH p NO.

The apparent effects of indirect substitution seemed very small, and an examination of the charge distribution was made using a Mulliken population analysis of the NO's for each state. The results are shown in Table 10. Comparing the populations of :CHCOF with those of :CHCOH, in the A" states there is seen to be a general shift of a' density from the hydrogen and both carbons to the more electronegative fluorine and oxygen, accompanied by a small return of charge from fluorine in the a" system. The electronegativity of the oxygen seems to have been enhanced in the presence of the fluorine. The result for the formyl carbon, attached to both oxygen and fluorine, is the most

Table 9. :CHCOF Active NO Occupation Numbers

NO	State		
	$3_{A''}$	$1_{A'}$	$1_{A''}$
$\sigma_F$	2.000	2.000	2.000
$p_F$	1.999	1.999	1.999
$\sigma_O$	1.994	1.995	1.990
$\pi_{CO}$	1.874	1.859	1.878
$\sigma$	1.005	1.870	1.009
$p$	1.002	0.083	1.005
$\pi_{CO}^*$	0.126	0.193	0.119

Table 10. :CHCOF Gross Mulliken Populations and Net Charges.

Center	$3A''$			$1A'$			$1A''$		
	$n_{a'}$	$n_{a''}$	$\delta$	$n_{a'}$	$n_{a''}$	$\delta$	$n_{a'}$	$n_{a''}$	$\delta$
H <sub>C</sub>	.93	----	+0.07	.97	----	+0.03	.92	----	+0.07
C <sub>C</sub>	4.94	1.09	-.04	5.82	.17	+0.01	5.09	.93	-.02
C	4.73	1.01	+0.26	4.78	.99	+0.23	4.72	1.06	+0.22
O	7.05	1.11	-.16	7.08	1.07	-.15	7.06	1.08	-.14
F	7.21	1.92	-.13	7.22	1.90	-.13	7.21	1.93	-.13

profound, causing it to be about a quarter of an electron deficient. For the  $^1A'$  state, the gross result is similar, with the interesting additional result that the  $a''$  population on the carbene carbon appears to have decreased slightly, suggesting an electrophilicity equal to or greater than that of the  $^1A'$  state of  $:CHCOH$ . An obvious phenomenon, common to all three states, is the strong polarization of the CO group in the direction  $C^+O^-$ . It would seem that the CO group "insulates" the carbene carbon vicinity, harboring the  $\sigma$  and  $p$  electrons, from the strong effects of the fluorine, and thus ameliorating greatly any changes in the basic electronic structure of the low-lying states.

#### D. $:CFCOH$

In this case, the fluorine was substituted directly on the carbene carbon. The C-F bond length assumed is given in Table 1. As done for  $:CHCOF$ , the geometries used were those found for  $:CHCOH$ .

Although the same number of MO's resulted from the SCF calculation as in  $:CHCOF$ , the presence of the fluorine adjacent to the carbene carbon required a greater flexibility of the  $\sigma_F$  MO in CI excitations. The set of active MO's, listed in Table 11, was increased to nine MO's, including the two highest  $a'$  virtual MO's.

Table 11. :CFCOH Active MO's and Orbital Energies at the  
 $3A''$  cis Geometry

MO	Character	$-\epsilon$ (au)
1a''	( $p_F$ ) Fluorine p orbital	.571
11a'	( $\sigma_F$ ) Fluorine non-bonding	.570
2a''	( $\pi_{CO}$ ) C formyl-O bonding	.461
12a'	( $\sigma_O$ ) Oxygen non-bonding	.410
13a'	( $\sigma$ ) Carbene "lone pair"	.264
3a''	(p) $\nu$ Carbene p orbital	-.149
4a''	( $\pi^*$ ) C-C anti-bonding	-.365
14a'	( $\sigma'$ ) a' virtual	-.559
15a'	( $\sigma''$ ) a' virtual	-.689

The structures possible using the active MO's were too numerous to handle within the limits of technology and expense, so that the arrangements of the  $5\alpha$  and  $5\beta$  electrons among the 18 available spin-orbitals were restricted as follows. All possible excitations were formed within the first seven MO's, deleting all excitations beyond singles and doubles off the SCF  $\sigma^2$  determinant. Then several selected double excitations into the  $\sigma'$  and  $\sigma''$  MO's were added. The result was a total of 319 structures of all four possible spin and spatial symmetries. Appendix I gives the distribution over symmetry type and lists all the structures.

The O-O transition energies and absolute state energies for the three lowest states at their cis geometries are illustrated in Figure 8. As before, the cis and trans configurations of each state differed by an insignificant amount -- less than 1 kcal/mole in this molecule. The dramatically increased stability of the  $^1A'$  state relative to the  $A''$  states is immediately apparent and reflects some significant change in the basic electronic structure in this directly-substituted molecule relative to the two previous molecules. In fact, the differential effects of the inclusion of correlation energy would almost certainly predict a  $^1A'$  ground state. For this reason, the vertical excitation energies at both the  $^3A''$  cis and  $^1A'$  cis geometries have been included (Figures 9 and 10, respectively).

The principal structures (on the basis of coefficient)

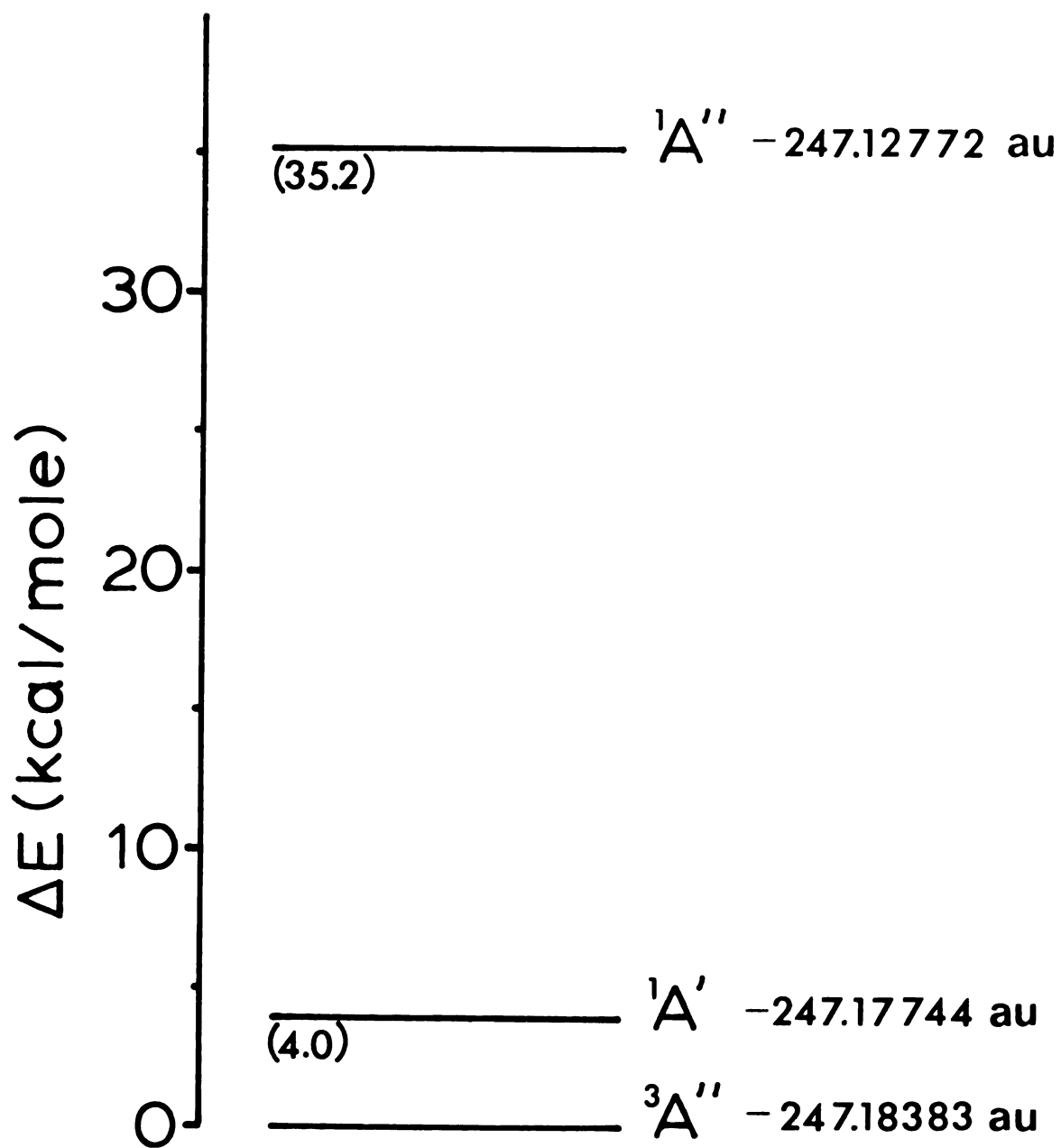


Figure 8.  $\text{:CF}_3\text{OH}$  (cis) CI Energies for the States  $^3A''$ ,  $^1A'$ , and  $^1A''$ .

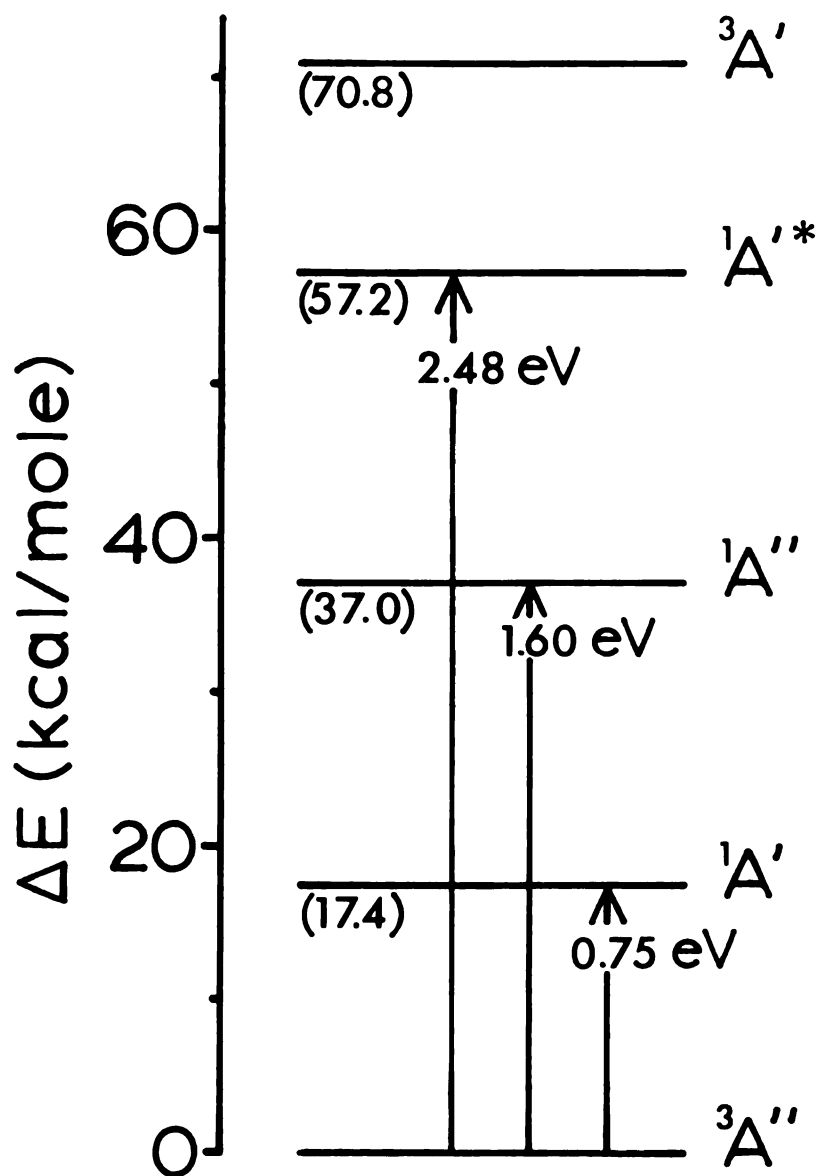


Figure 9.  $\text{:CFCOH (cis)}$  Excitation Energies at the  ${}^3A''$  Geometry.

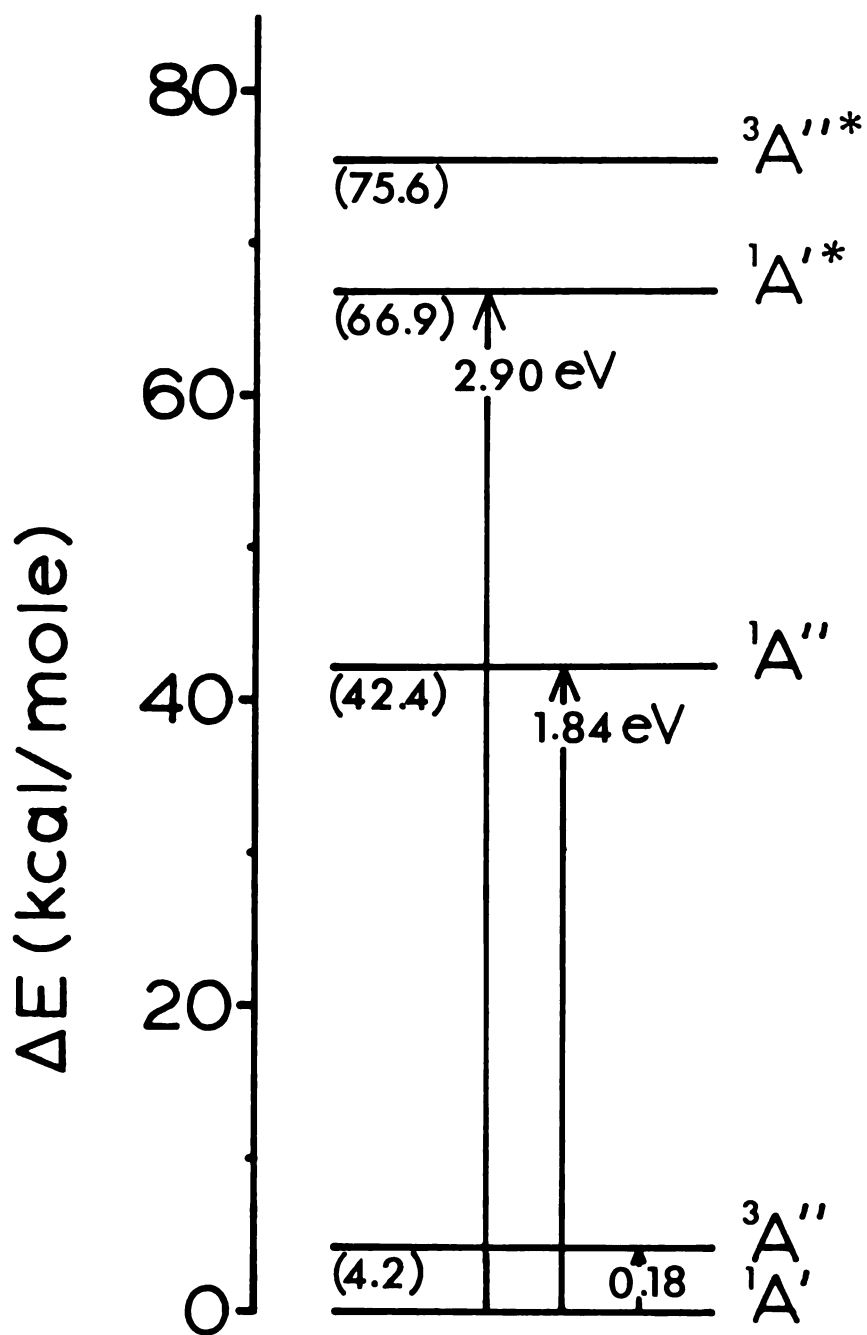


Figure 10.  $\text{:CFCOH (cis)}$  Excitation Energies at the  ${}^1A'$  Geometry.

in the CI wave functions of each state are given in Table 12. Due to the delocalized nature of the  $a''$  MO's, the  $A''$  states require a large orbital correction structure, appearing in each case as a single excitation within the  $a''$  system. The  ${}^1A'$  state is more strongly dominated by the  $\sigma^2$  SCF determinant, the  $\sigma$  MO having become significantly stabilized by the adjacent fluorine; and the  $p^2$  determinant has faded in significance as a component in the qualitative electronic structure.

Partly accounting for the decreased  ${}^1A'' + {}^3A''$  energy is the delocalization of both the  $\sigma$  and  $p$  NO's onto the fluorine. This argument can be made in terms of the NO's because, if the CI were redone in the NO basis, the  $\sigma p$  structure would be much more dominant than it was for the MO's. Since the  ${}^1A'' + {}^3A''$  energy for a  $\sigma p$  occupancy is just  $2K_{\sigma p}$  (twice the exchange integral for the  $\sigma$  and  $p$  orbitals), which diminishes in magnitude as the average distance between  $\sigma$  and  $p$  electrons, the delocalization of the  $\sigma$  and  $p$  NO's is a significant factor in decreasing the  ${}^1A'' + {}^3A''$  energy. Figure 11 shows electron density contours for the  $a'$  NO's and the total electron density at the  ${}^3A''$  cis geometry. The active NO's and their occupation numbers are listed in Table 13. The relative unimportance of the  $\sigma'$  and  $\sigma''$  NO's in the  $A''$  states is apparent from their near-zero occupation numbers, reflecting a very small mixing of the  $\sigma'$  and  $\sigma''$  MO's in the lower  $a'$  MO's. It is interesting to notice that the  $\pi^*$  NO (mostly C-O

Table 12. :CFCOH Principal Contributing CI Structures for the Three Lowest States.

State	Structure Occupation							Coef.
	P <sub>F</sub>	σ <sub>F</sub>	π <sub>CO</sub>	σ <sub>O</sub>	σ	p	π*	
<sup>3</sup> A" cis	2	2	2	2	1	1		.864
	2	2	2	2	1		1	-.375
	2	2		2	1	2	1	.161
	2	2	1	2	1	2		-.152
	2	2		2	1	1	2	-.129
	2	2	2	1	2		1	.119
<sup>1</sup> A' cis	2	2	2	2	2			.950
	2	2		2	2	1	1	.169
	2	2		2	2	2		-.161
	2	2	2	2		2		-.103
	2	2		2	2		2	-.098
<sup>1</sup> A" cis	2	2	2	2	1	1		.868
	2	2	1	2	1	2		.344
	2	2	1	2	1	1	1	.173
	2	2	2	2	1		1	-.164
	2	2		2	1	2	1	.113
	2	2	1	2	1		2	-.107

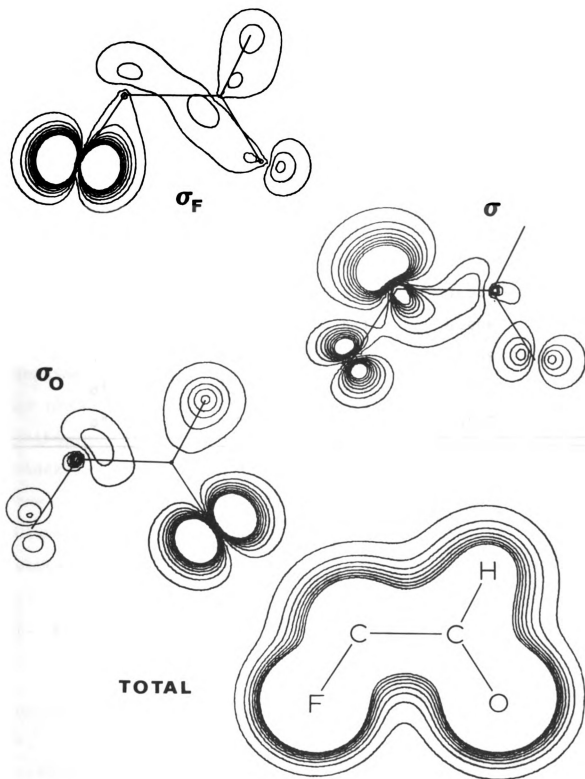


Figure 11.  $\text{:CFCOH}$  Electron Density Contour Maps for Active NO's and Total Density at the  $^3A'$  cis Geometry.

Table 13. :CFCOH Active NO Occupation Numbers

NO	State		
	$^3A''$	$^1A'$	$^1A''$
$\sigma_F$	1.999	2.000	1.998
$p_F$	1.998	1.989	1.996
$\sigma_O$	1.986	1.996	1.984
$\pi_{CO}$	1.874	1.863	1.890
$\sigma$	1.012	1.959	1.017
$p$	.999	.044	1.008
$\pi^*$	.132	.149	.108
$\sigma'$	.000	---	.000
$\sigma''$	.000	---	.000

anti-bonding) has a larger occupation in the  $^1A'$  state than does the p (localized on the carbene carbon) -- a situation also found in the  $:CHCOF$   $^1A'$  state and associated with the increased ionic character of the C-O bond in the fluorine-substituted species.

The Mulliken population analysis, summarized in Table 14, shows the effects on the charge density due to direct fluorine substitution. As in  $:CHCOF$ , the fluorine draws substantial charge through the  $a'$  system and returns a smaller amount to the  $a''$  system, which doubles the carbene carbon  $a''$  density in the  $^1A'$  state relative to  $:CHCOF$  and implies a much less electrophilic  $^1A'$  than either  $:CHCOF$  or  $:CHCOH$ . There is still a significant C-O polarization, although not as severe as in  $:CHCOF$ . The effect on the electronic structure is undoubtedly the stabilization of the  $\sigma$  orbital by the fluorine, leading to the transition energies shifts and a singlet, instead of a triplet, ground state.

#### E. Discussion

The effects of fluorine substitution on the relative energies of the low-lying states are summarized in Figure 12. It should be repeated that the expected result of including the correlation energy is to lower the  $^1A'$  state relative to the  $A''$  states for each molecule, leading to a  $^1A'$  ground state for  $:CFCOH$ . The results of direct

Table 14. :CFCOH Gross Mulliken Populations and Net Charges.

Center	$3A''$			$1A'$			$1A''$		
	$n_{a'}$	$n_{a''}$	$\delta$	$n_{a'}$	$n_{a''}$	$\delta$	$n_{a'}$	$n_{a''}$	$\delta$
F	7.20	1.90	-.10	7.33	1.74	-.07	7.18	1.88	-.06
C <sub>C</sub>	4.87	1.02	+.12	5.55	.34	+.11	4.89	.96	+.15
C	4.92	1.01	+.07	4.99	.96	+.05	4.91	1.08	+.00
O	7.08	1.08	-.16	7.13	1.02	-.15	7.09	1.08	-.16
H	.94	-----	+.06	.95	-----	+.05	.93	-----	+.07

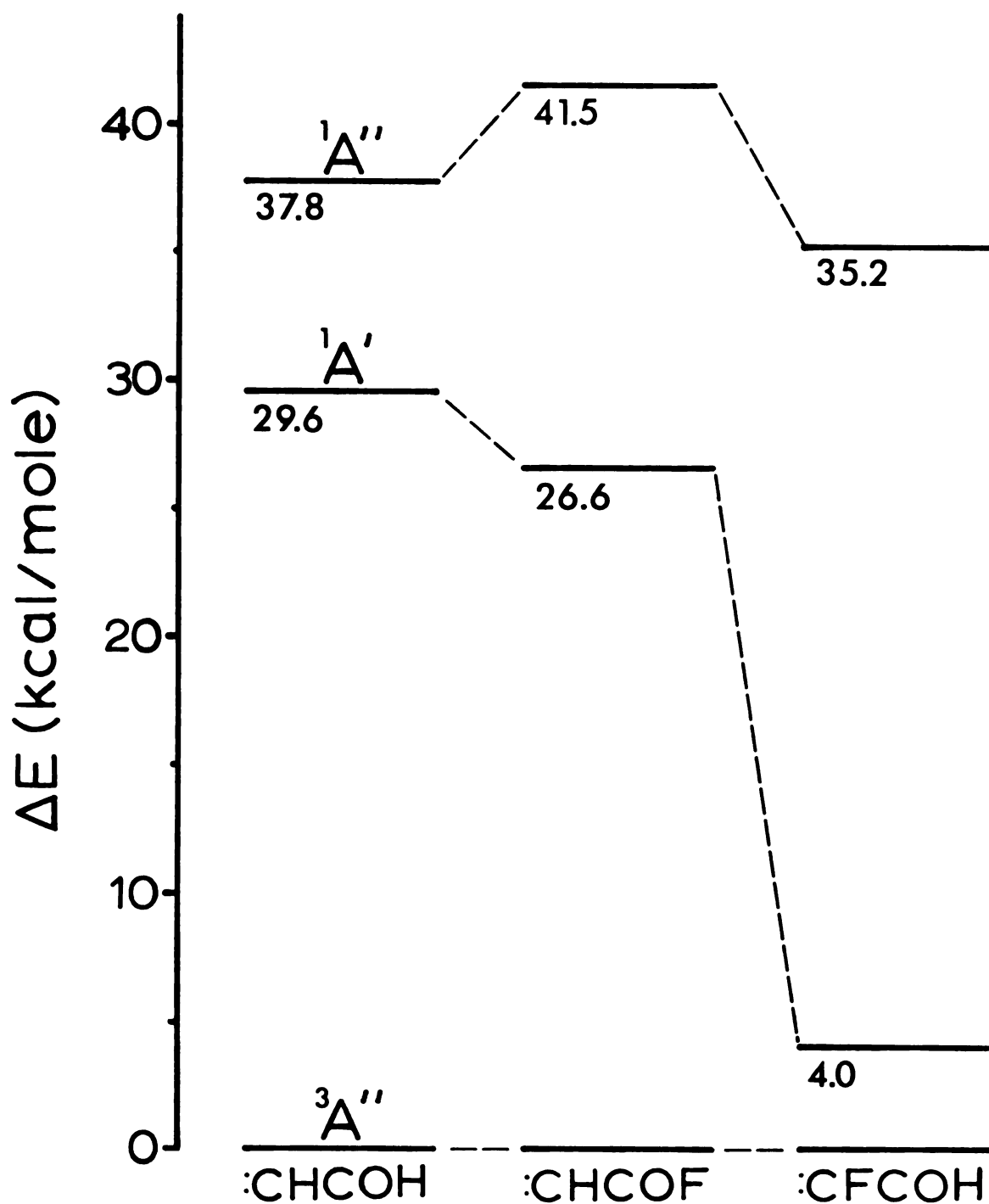


Figure 12. Effect of Fluorine Substitution on the Energy Levels of Carbonyl Carbenes.

fluorine substitution are very close to those found in studies on methylene.<sup>26</sup> The effects of indirect substitution are significant in demonstrating the insulating properties of the carbonyl group and the resulting minimal effect on the electronic structure of the low-lying states. A parallel study on carbonyl nitrenes (isoelectronic with the carbenes) by Shalhoub and Harrison<sup>21</sup> revealed a similar effect. In their study,  $\text{CH}_3$  and  $\text{OCH}_3$  were also used as substituents, with the result that the  $A''$  states were insensitive to such substitutions. In their study the analogous  $p$  and  $\sigma$  orbitals on nitrogen were localized on that center. It is this localization of the critical one particle densities, common to both the carbenes and nitrenes which makes the carbonyl group so effective in minimizing substituent effects on the gross electronic structure and perhaps the chemical reactivity.

Two interesting studies should be pursued to extend this work. One is the investigation of the barrier to formation of ketene, discussed earlier. Experimentally, there is no evidence for the presence of the reactive singlet carbonyl carbene, but ketene is found to be present. In this regard, a theoretical investigation of the rearrangement barrier in the  $^1A'$  state would be helpful. A second rearrangement reaction which could be followed theoretically is the formation of the heterocycle oxirene. The stability and electronic characterization of that species as an intermediate is also of interest in reactions involving the Wolff rearrangement.

## CHAPTER II

### LITHIUM CARBENES

In this chapter, the results of an ab initio SCF study of lithium-substituted methylene are presented. Lithium has as its first unoccupied atomic orbital a low-lying p-type function. Hence, the two molecules studied, LiCH and Li<sub>2</sub>C, were expected to be characterized by low-lying excited states. Also, in contrast to the mainly electro-negative substituents of Chapter 1, lithium is a good electron donor and it was anticipated that a substantial amount of  $\sigma$  electron density would shift from lithium to carbon, and some amount would be returned to lithium via the  $\pi$  system.

The level of calculation for the triplet ground states of both molecules and the first excited triplet of LiCH was that of a restricted open-shell SCF (ROSSCF). The basis set of contracted nuclear-centered cartesian gaussian functions was of double zeta quality and included one 4-component lithium p function, whose exponents and coefficients were optimized by Williams<sup>27</sup> in an SCF calculation of the lithium <sup>2</sup>P state. The other excited state wave-functions were constructed via a single excitation CI (SECI) calculation using the ground state MO's. Further details of the basis set, CI wave functions and calculational methods can be found in Appendix II.

All the states examined for these molecules were linear and at least nominally bound. The ground states were found to be of  $^3\Sigma^-$  symmetry ( $^3\Sigma^-$  for LiCH,  $^3\Sigma_g^-$  for Li<sub>2</sub>C). Table 15 contains a list of the ground state MO's and their orbital energies for both molecules at their equilibrium geometries. Figures 13 and 14 display electron density contour maps of the MO's above the atomic core orbitals and the total molecular density for LiCH and Li<sub>2</sub>C, respectively. In LiCH, the two MO's which primarily determine the bonding characteristics are the  $3\sigma$  (covalent C-H bonding) and the highly ionic  $4\sigma$  (C-Li bonding). For Li<sub>2</sub>C, which has no covalent bonds, two ionic C-Li bonding orbitals, similar to the  $4\sigma$  in LiCH, can be formed as linear combinations of the  $2\sigma_u$  and  $3\sigma_g$  MO's. These characteristics are apparent in the contour maps.

From the ground state electronic configurations of LiCH and Li<sub>2</sub>C, each having an occupancy describable as ( $\sigma$  core)<sup>2</sup>( $\pi_x$ )<sup>1</sup>( $\pi_z$ )<sup>1</sup>, with the two single electrons triplet coupled, a doubly degenerate  $^1\Delta$  and a non-degenerate  $^1\Sigma^+$  state can be constructed by alternate couplings of the  $\pi$  electrons. Virtual orbital representations of these states were constructed and improved via SECI calculations within the  $\pi$  orbitals. Table 16 gives the ground and excited state energies and equilibrium bond lengths for both molecules. The fact that no  $\sigma$  excitations were allowed in the SECI wave functions undoubtedly contributed to the nearly identical geometries of the three lowest states

Table 15. Occupied MO's at Ground State Equilibrium Geometries: a) LiCH ( $^3\Sigma^-$ ) and b) Li<sub>2</sub>C ( $^3\Sigma_g^-$ ).

a)		
MO	Character	$-\epsilon$ (au)
1 $\sigma$	Carbon 1s	11.123
2 $\sigma$	Lithium 1s	2.461
3 $\sigma$	C-H bonding	.581
4 $\sigma$	C-Li bonding (ionic)	.305
$\pi_x$	Carbon p <sub>x</sub>	.042
$\pi_z$	Carbon p <sub>z</sub>	.042
b)		
1 $\sigma_g$	Carbon 1s	11.093
2 $\sigma_g$	Li-Li bonding $\sigma$	2.409
1 $\sigma_u$	Li-Li anti-bonding $\sigma$	2.409
3 $\sigma_g$	Carbon 2s	.395
2 $\sigma_u$	Carbon p <sub>y</sub> (ionic)	.164
$\pi_{x_g}$	Carbon p <sub>x</sub>	.006
$\pi_{z_g}$	Carbon p <sub>z</sub>	.006

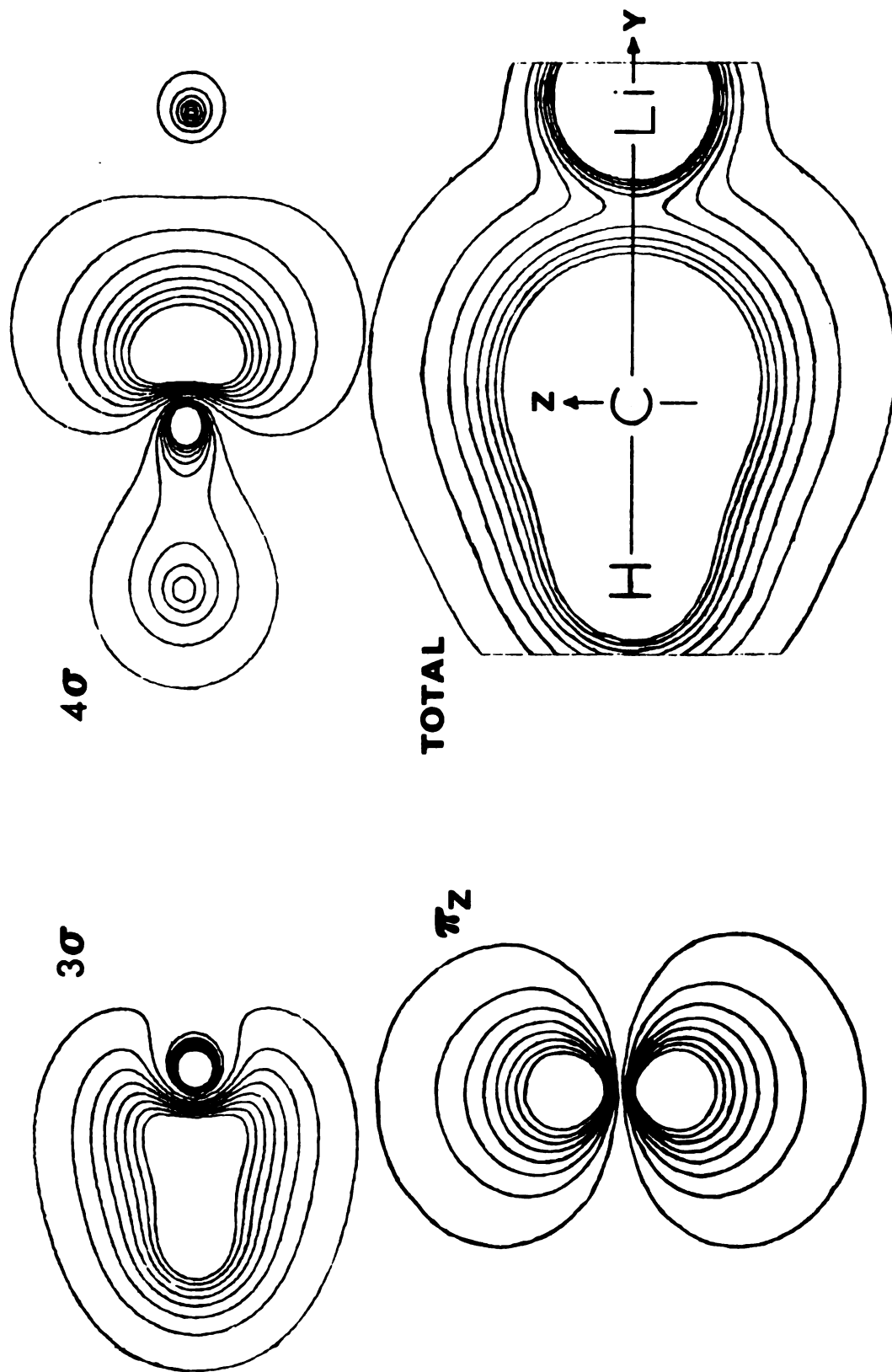


Figure 13. LiCH ( $^3\Sigma^-$ ) Electron Density Contours for Non-Core MO's and the Total Density.

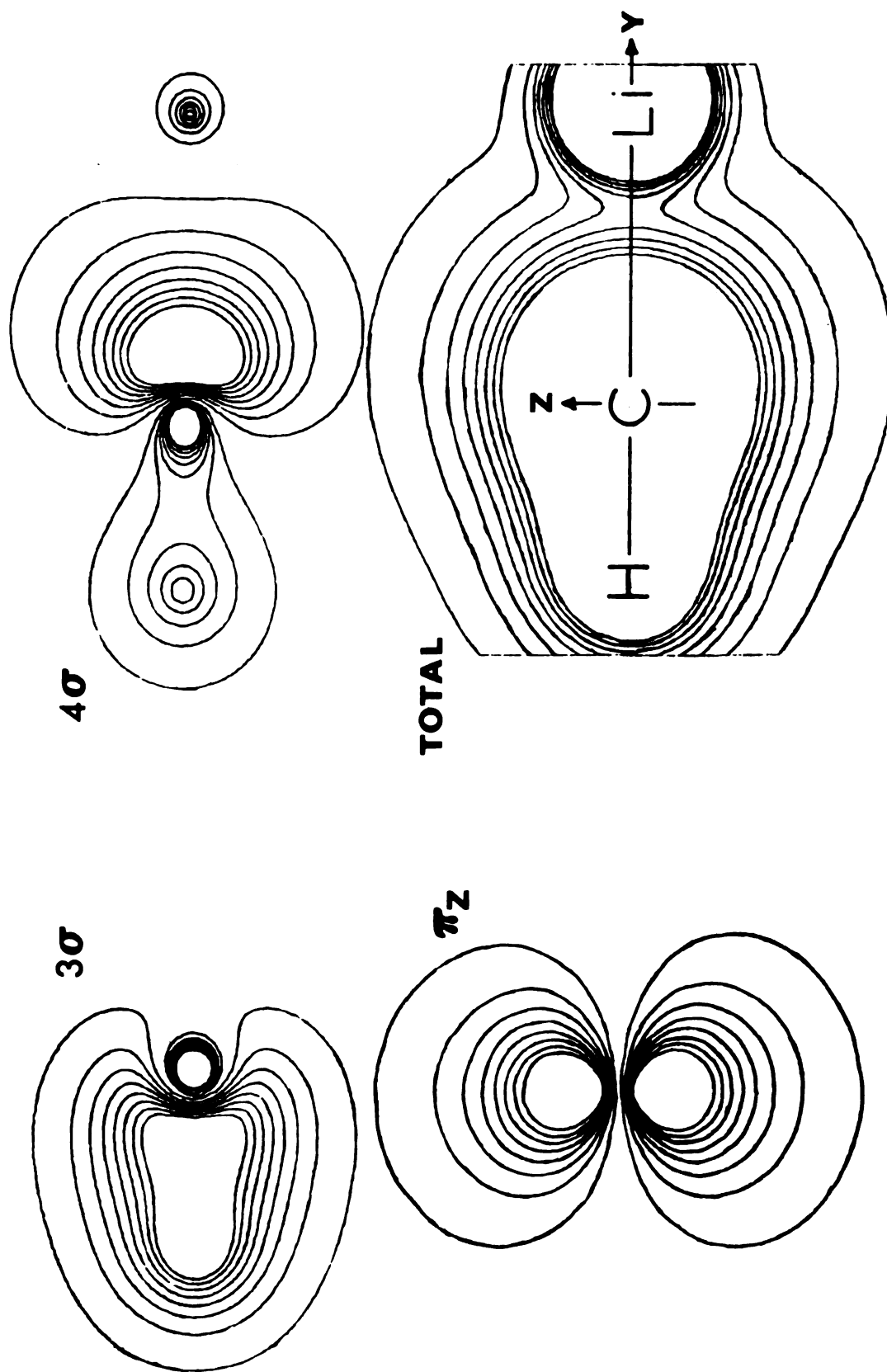


Figure 13. LiCH ( $^3\Sigma^-$ ) Electron Density Contours for Non-Core MO's and the Total Density.

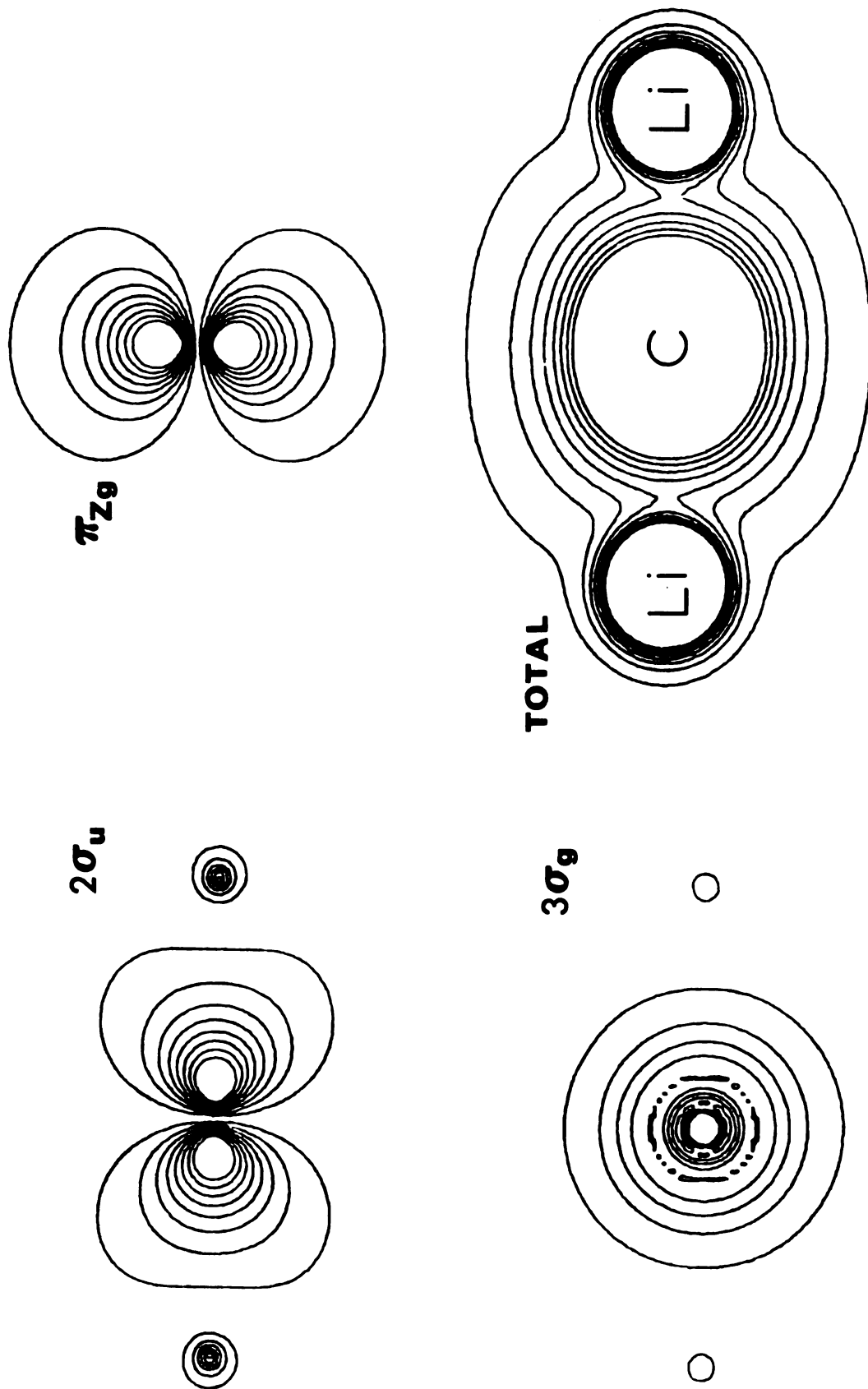


Figure 14.  $\text{Li}_2\text{C}$  ( ${}^3\Sigma_g^-$ ) Electron Density Contours for Non-core MO's and the Total Density.

Table 16. Ground and Excited State Energies and Equilibrium Bond Lengths for LiCH and Li<sub>2</sub>C.

Molecule	State	Energy (au)	R <sub>C-Li</sub> (bohrs)	R <sub>C-H</sub> (bohrs)
LiCH	<sup>3</sup> Π	-45.69713	4.40	2.08
	<sup>1</sup> Σ <sup>+</sup>	-45.69438	3.58	2.06
	<sup>1</sup> Δ	-45.73662	3.59	2.06
	<sup>3</sup> Σ <sup>-</sup>	-45.78154	3.59	2.07
Li <sub>2</sub> C	<sup>1</sup> Σ <sub>g</sub> <sup>+</sup>	-52.53350	3.73	----
	<sup>1</sup> Δ <sub>g</sub>	-52.56700	3.76	----
	<sup>3</sup> Σ <sub>g</sub> <sup>-</sup>	-52.60479	3.78	----

of each molecule. As a consequence, the 0-0 transition energies are the same as the vertical excitation energies. An energy level diagram illustrating both sets of energies is given in Figure 15 for both molecules. It is seen that the excitation energies,  $E(^1\Sigma_g^+) - E(^1\Delta_g)$  and  $E(^1\Delta_g) - E(^3\Sigma_g^-)$ , in  $\text{Li}_2\text{C}$  are smaller than the corresponding separations in  $\text{LiCH}$ . This result is due to the delocalization of the occupied  $\pi$  MO in  $\text{Li}_2\text{C}$  compared to  $\text{LiCH}$ . Outside of small corrections due to the single excitations, the two differences are largely determined by the exchange integral connecting the two occupied  $\pi$  MO's:

$$\Delta E \sim 2K_{\pi_x \pi_z}.$$

For  $\text{LiCH}$ ,  $2K_{\pi_x \pi_z} = 1.27$  eV, and for  $\text{Li}_2\text{C}$ ,  $2K_{\pi_x \pi_z} = 1.08$  eV. Hence, the extent to which  $\pi$  density can become more diffuse on carbon or delocalize to the lithium has a rather significant effect on the predicted relative energies of the lowest excited states. The expected effect of the inclusion of correlation energy would be to preferentially lower the  $^1\Delta$  state relative to the  $\Sigma$  states by some fraction of an eV, which would not be sufficient to alter the predicted state ordering, but it would reduce the singlet-triplet splitting. This correlation energy difference is principally the pair correlation energy associated with the  $\pi$  MO.

$\text{LiCH}$  was bent from its linear equilibrium geometry

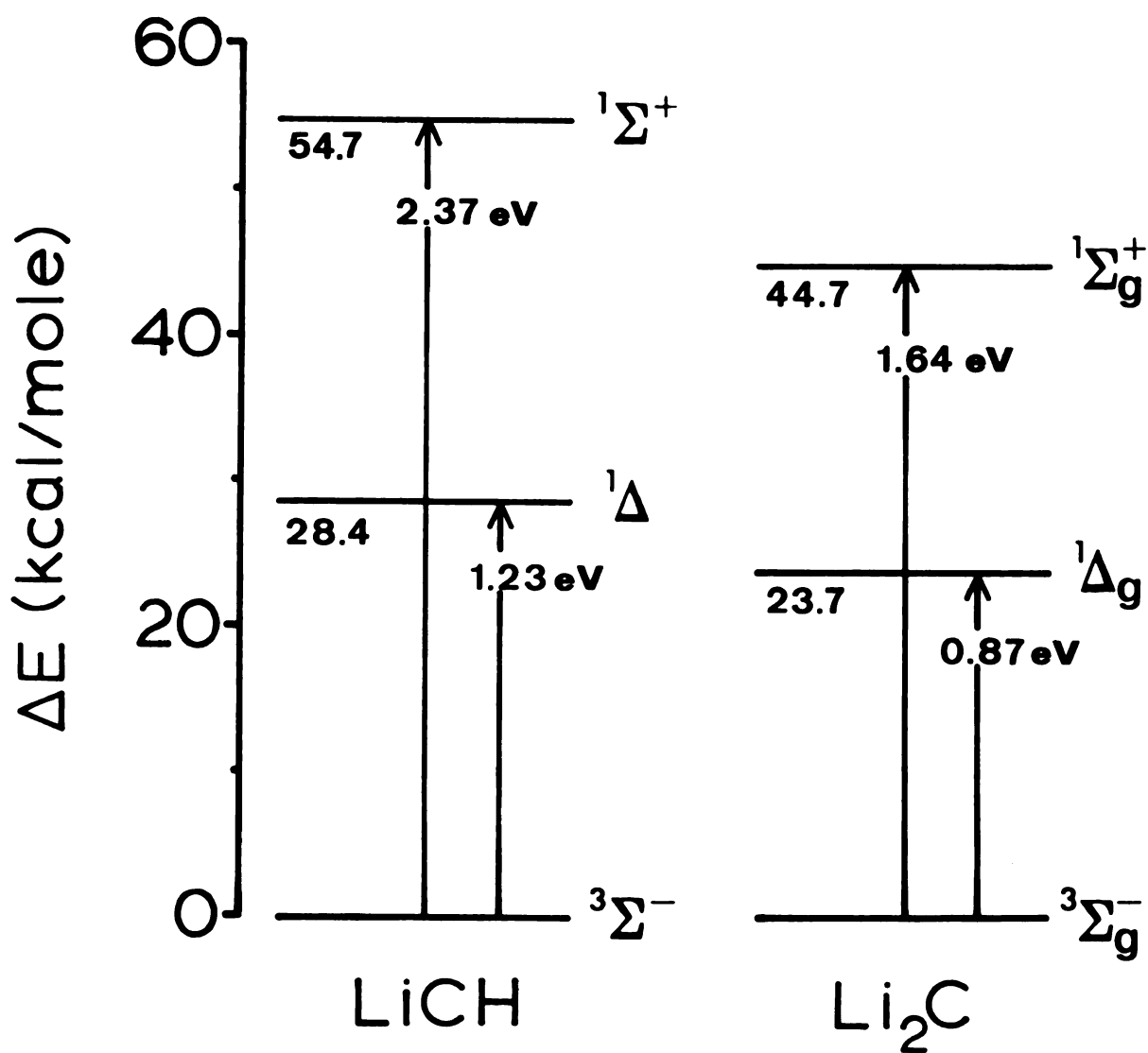


Figure 15. Excitation Energies at the Ground State Geometry for LiCH and Li<sub>2</sub>C.

holding the bond lengths fixed. The resulting energy dependence vs angle is shown in Figure 16. The preference for a linear configuration is difficult to rationalize because several small effects are involved, and their magnitudes are not reliably estimated at present. Consideration of the stabilization of the in-plane  $\pi$  MO through acquisition of s-character, stabilization of the bonding  $3\sigma$  and  $4\sigma$  MO's due to loss of s-character, the effects of incomplete orbital following, and bond-bond repulsion must all be taken into account with a good estimate of their relative importance. Without attempting such a task here, it does seem possible to give an argument as to why these ionic lithium-substituted methylenes should prefer linear geometries as compared to methylene itself, which is predicted by theoretical calculations to be bent in the states analogous to those considered here. The differences are mainly due to the ionic nature of the bonding in the lithium carbenes. The ionic bond is manifested as an electron pair closely associated with the carbon and hybridized in a roughly sp manner. Upon bending, the nuclear-nuclear repulsion between Li and H is more effective with the Li positively-charged. Also, if the ionic MO is less faithful in following the Li nucleus than a covalent MO would be (although plausible, this effect needs verification), the result would be less s-character acquired by the in-plane  $\pi$  MO. All of these differences imply an increased destabilization on bending compared

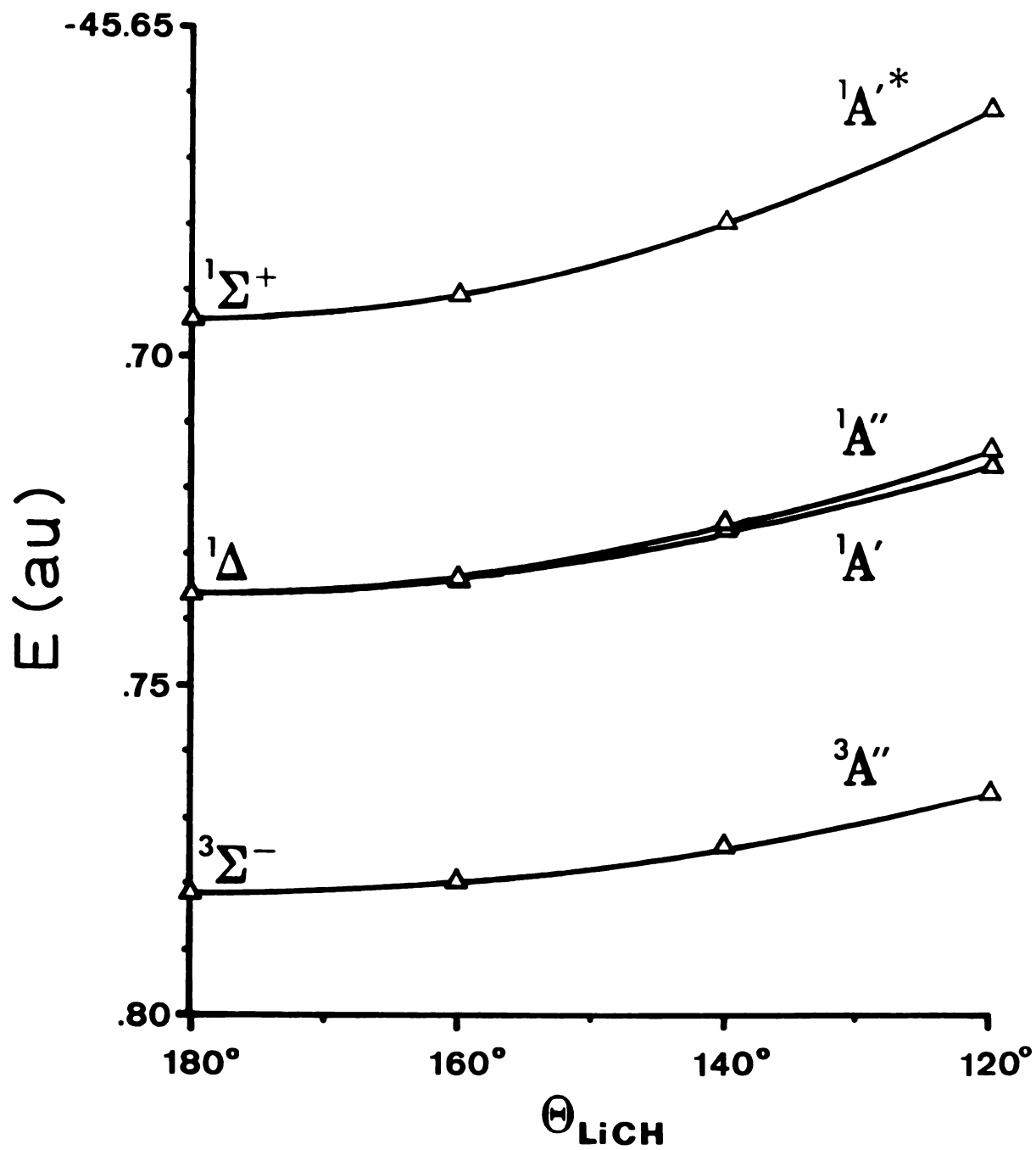


Figure 16. LiCH State Energies vs  $\theta_{\text{Li-C-H}}$ .

to methylene. For  $\text{Li}_2\text{C}$ , with two ionic bonds, the effect would be expected to increase. A Walsh diagram of the LiCH MO's above the  $2a'$  MO is included in Figure 17.

In examining the charge distribution of the lithium carbenes, a Mulliken population analysis was made of the ground state wavefunction. The results are summarized in Table 17, which lists the net atomic populations broken down into the  $\sigma$  orbital contribution, the  $\pi$  orbital contribution, and the net atomic charge. It is seen in LiCH that the Li loses about 0.9 electrons through the  $\sigma$  system and regains only about 0.1 electron via the  $\pi$  MO's. Since the carbon extracts about 0.1 electron from H, it is left with an excess charge of  $\sim 0.9$  electron. In going to the  $\text{Li}_2\text{C}$  system, the excess charge on C has increased to 1.2 electrons, which is the result of drawing over 0.7 electrons from each Li through the  $\sigma$  MO's and losing about 0.12 electrons to each Li via the  $\pi$  MO's. The overall result is less  $\sigma$  charge shifted to C and a greater  $\pi$  delocalization for  $\text{Li}_2\text{C}$  as compared to LiCH. However, this  $\pi$  delocalization is not apparent in the  $\pi$  MO contour plots because in neither case does the Li contribution reach the density of the lowest contour, 0.005 electrons/(bohr)<sup>3</sup>.

The  $^3\Pi$  state of LiCH was examined at the ROSSCF level because its electronic configuration was essentially different than the three lowest states and because as the first allowed transition from the ground state, a better transition energy was desired. The results showed its C-Li

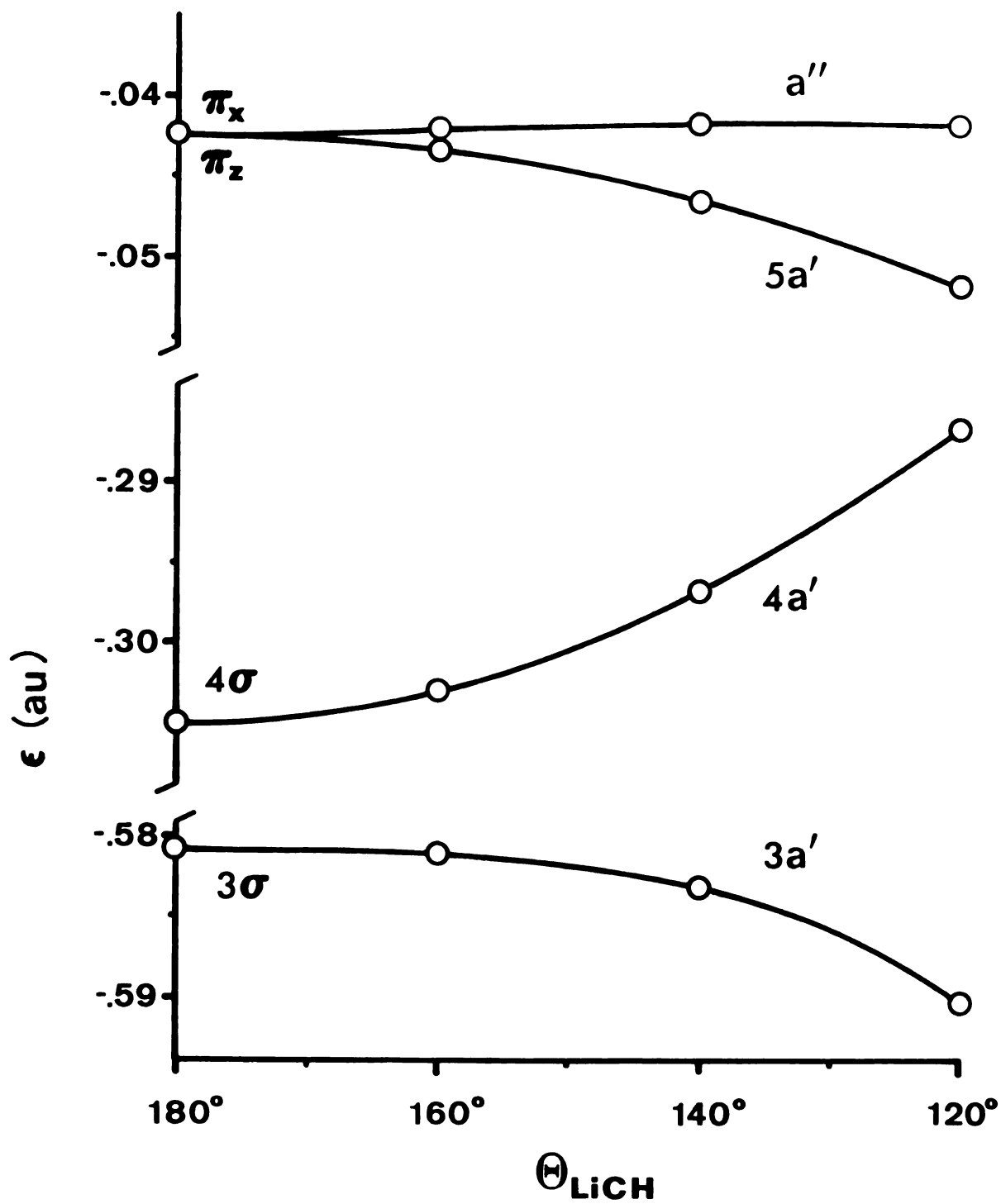


Figure 17. LiCH Orbital Energies vs  $\theta_{\text{Li-C-H}}$

Table 17. Gross Mulliken Populations and Net Charges for LiCH and Li<sub>2</sub>C.

<u>LiCH <math>^3\Sigma^-</math></u>				
Atom	$n_\sigma$	$n_{\pi_x}$	$n_{\pi_z}$	$\delta$
C	4.995	0.950	0.950	-0.895
Li	2.110	0.050	0.050	+0.789
H	0.894	-----	-----	+0.106

<u>Li<sub>2</sub>C</u>				
C	5.453	0.878	0.878	-1.208
Li	2.274	0.061	0.061	+0.604

bond length to be dramatically longer than the  $^3\Sigma^-$  (4.40 bohr compared to 3.59 bohr). It was also found to be bound by only 5 kcal/mole with respect to  $\text{Li}(^2\text{S})+\text{CH}(^2\Pi)$ , into which it smoothly dissociates. Hence, it was expected that a vertical transition from the ground state would result in dissociation. The potential energy was found to be a very broad and shallow function of the C-Li bond length. The vertical transition energy to the  $^3\Pi$  from the  $^3\Sigma^-$  equilibrium is estimated to be about 60 kcal/mole (2.6 eV), which would lie in the energy continuum of the  $^3\Pi$  surface. The bonding in the  $^3\Pi$  state was found to be essentially different from the other states examined in that there was little charge displacement, i.e., the Li was almost neutral. The long and shallow Li-(C-H) stretching potential and the substantial sp hybridization of the Li "2s" electron indicates a bonding based on a dipole-induced dipole attraction.

Heats of formation of the two molecules were estimated by determining the ROSSCF ground state equilibrium energies of the most stable dissociation fragments and calculating the dissociation energies. The calculated  $\Delta E$ 's differ from the corresponding  $\Delta H$ 's by an amount roughly 1 to 2 kcal/mole, which was less than the resolution of these calculations. Figures 18 and 19 correlate the levels of LiCH and  $\text{Li}_2\text{C}$ , respectively, to their lowest energy stable fragments. It is seen that  $^3\Sigma^-$  LiCH is much stabler to dissociation than  $\text{Li}_2\text{C}$ , and all the states examined, barring the

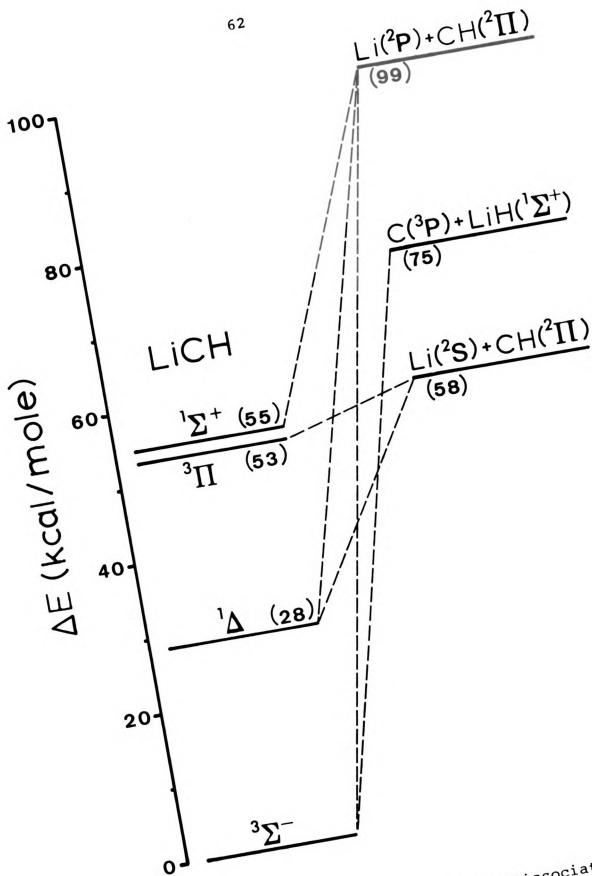


Figure 18. Correlation of LiCH Levels and Dissociation Fragments.

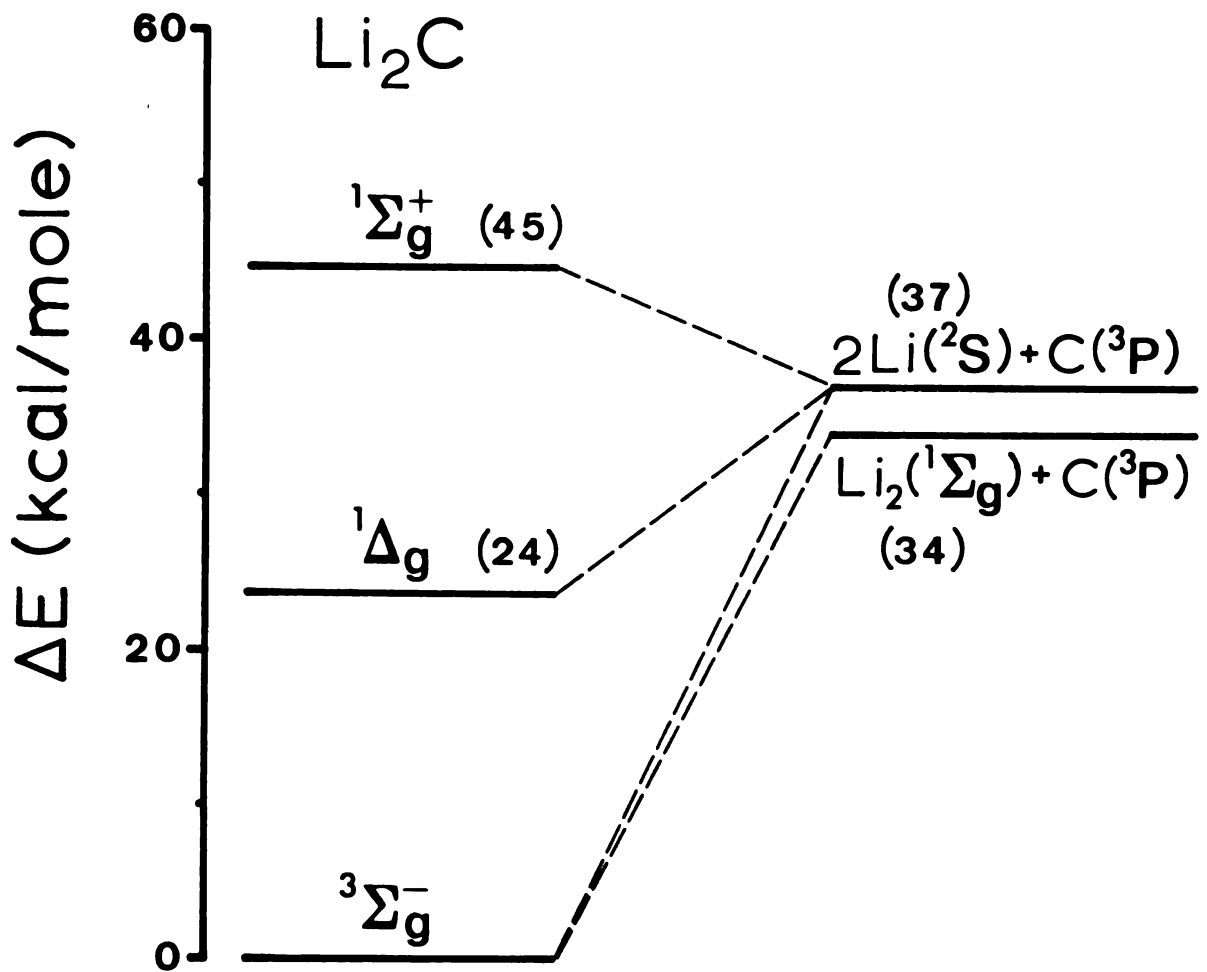


Figure 19. Correlation of  $\text{Li}_2\text{C}$  Levels and Dissociation Fragments.

$\text{Li}_2\text{C } ^1\Sigma_g^+$ , appear at least nominally stable.

Although lithium carbenes have not been observed experimentally, their generation does not a priori seem unattainable. As with several other carbenes produced in the laboratory, a promising technique would be the photolysis (or pyrolysis) of a diazo precursor, such as  $\text{N}_2\text{CLi}_2$  in this case. The synthesis of that precursor may not be possible, but that question would require an experimental answer.

CHAPTER III  
 THE ZERO-FIELD SPLITTING PARAMETERS  
 OF  $^3B_1$  METHYLENE

A. The Electron Spin-spin Interaction and the ZFS Parameters

Each electron has a magnetic dipole moment,  $\bar{\mu}$ , associated with its intrinsic spin,  $\bar{s}$ ; the relation connecting the two is  $\bar{\mu} = -g\beta\bar{s}$ . In any system containing two or more electrons, each pair of electronic magnetic dipoles interact through their associated magnetic fields. This interaction is called the electron spin-spin interaction, and the corresponding quantum mechanical energy operator is given by

$$\hat{H}_{ss} = \frac{1}{2}g^2\beta^2 \left\{ \sum_{\kappa}^{\text{all } e^-} \sum_{\lambda}^{\text{all } e^-} \left[ \frac{\hat{s}_{\kappa} \cdot \hat{s}_{\lambda}}{r_{\kappa\lambda}^3} - \frac{3(\hat{s}_{\kappa} \cdot \hat{r}_{\kappa\lambda})(\hat{s}_{\lambda} \cdot \hat{r}_{\kappa\lambda})}{r_{\kappa\lambda}^5} \right] \right\}$$

where  $g$  is the electronic  $g$ -factor, and  $\beta$  is the Bohr magneton ( $\beta = e\hbar/2m_e c$ ).  $r_{\kappa\lambda}$  is the distance between electrons  $\kappa$  and  $\lambda$ . The range of the interaction is quite short, dropping off as  $1/r_{\kappa\lambda}^3$ .

In practice, an empirical "spin Hamiltonian" is used which includes both the spin-spin and spin-orbit interactions. This empirical Hamiltonian has the form

$$\hat{H}_s = D(\hat{S}_z^2 - \frac{1}{3}\hat{S}^2) + E(\hat{S}_x^2 - \hat{S}_y^2),$$

where  $\hat{S}$  is the total electronic spin of the molecular system,

and D and E are constants into which all the information concerning the spatial distribution of the spin density has been compressed. It has been demonstrated that  $\hat{H}_{ss}$  can be reduced to this form,<sup>28,29</sup> in which case D and E are given (for a two-electron wave function  $\phi(1,2)$ ) by:

$$D = \frac{3}{4} g^2 \beta^2 \langle \phi | \frac{\hat{r}_{12}^2 - 3\hat{z}_{12}^2}{\hat{r}_{12}^5} | \phi \rangle$$

$$E = \frac{3}{4} g^2 \beta^2 \langle \phi | \frac{\hat{y}_{12}^2 - \hat{x}_{12}^2}{\hat{r}_{12}^5} | \phi \rangle$$

It is apparent that if the x and y directions are indistinguishable in the molecule (axial symmetry about z), then  $E \equiv 0$ . Also, if there is complete spatial isotropy in the electronic distribution,  $D \equiv 0$ . To the extent that D and E differ from zero, their magnitudes are a measure of the diffuseness of the net unpaired electronic spin density.

Other properties of the spin Hamiltonian can be gleaned from an examination of the general matrix element  $\langle SM_s | \hat{H}_s | S'M'_s \rangle$ . Writing  $\hat{S}_x^2 - \hat{S}_y^2$  as  $\frac{1}{2}(\hat{S}_+^2 + \hat{S}_-^2)$ , it is seen that

$$\hat{H}_s |00\rangle = D(0 - \frac{1}{3} \cdot 0) + E(0) \equiv 0,$$

and

$$\hat{H}_s | \frac{1}{2} \pm \frac{1}{2} \rangle \leq D(\frac{1}{4} - \frac{1}{3} \cdot \frac{3}{4}) + E(0) \equiv 0.$$

Thus there is no correction to the molecular energy levels for molecules having  $S < 1$ . Also,

$$\hat{H}_S |SM_S\rangle \propto |SM'_S\rangle,$$

indicating that mixing of spin states occurs only within a spin multiplet and does not mix states of different  $S$ . The energy shift of each level within a spin multiplet is given by  $D(M_S^2 - \frac{1}{3} S(S+1))$  and is a result of the first term in  $\hat{H}_S$ . The second term causes a mixing of the multiplet components which differ by  $\pm 2$  in their  $M_S$  value:

$$\langle SM_S | \hat{H}_S | SM_{S\pm 2} \rangle = \frac{E}{2} \sqrt{(S+M_S\mp 2)(S+M_S\pm 2+1)}.$$

In general, then, it is apparent that the spin-spin interaction causes a splitting of the Zeeman multiplets for  $S \geq 1$  in molecules possessing spatial anisotropy -- even in the absence of externally applied fields. This last observation justifies the name "Zero-field Parameters" (ZFS) for  $D$  and  $E$ .

For molecules containing only "low  $Z$ " nuclei, the spin-spin interaction is the dominant contributor to the ZFS parameters. However, the spin-orbit interaction will also contribute, and its strength increases roughly as  $Z^4$ , where " $Z$ " refers to the charge of the nuclei in the molecule considered. Since both of these effects are small in common molecules of interest in, say, organic chemistry, (i.e., in

the order of  $\text{cm}^{-1}$  energies), they are treated effectively in terms of perturbation theory. In those terms, the spin-spin interaction contributes in first order while the spin-orbit effects don't appear until second order corrections are accounted for.

A useful diagram of the perturbed multiplet levels can be constructed which relates the level splittings to the measured quantities D and E:

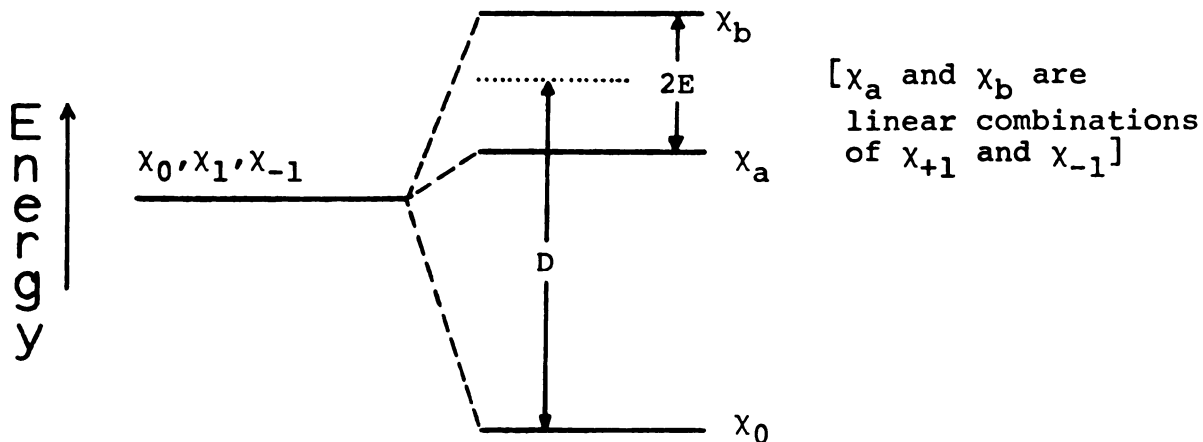


Figure 20. Relation of D and E to the Zero-Field Level Splittings of a Triplet State.

### B. The Spin-Spin Contribution to D and E for a CI Wave Function

In demonstrating the essential equivalence of  $\hat{H}_{ss}$  and  $\hat{H}_s$ , McLachlan<sup>29</sup> develops a function,  $S(\bar{r}_1, \bar{r}_2)$ , which is identical to the "coupling anisotropy" function of McWeeny.<sup>30</sup>

As McLachlan derives it,

$$S(\bar{r}_1, \bar{r}_2) = \frac{1}{S(2S-1)} \langle SS\alpha | \sum_{u \neq v} \{ 3\hat{s}_{zu}\hat{s}_{zv} - \hat{s}_u \cdot \hat{s}_v \} \delta(\bar{r}_u - \bar{r}_1) \\ \times \delta(\bar{r}_v - \bar{r}_2) | SS\alpha \rangle,$$

where  $|SS\alpha\rangle$  is the state of total spin  $S$  in its "standard state", i.e., with  $M_S = S$ , and  $\alpha$  denotes its non-spin quantum numbers. Since the  $M_S = 0$  component was preferred in the techniques used in this thesis,  $S(\bar{r}_1, \bar{r}_2)$  was used with a normalization factor appropriate to  $M_S = 0$  wave functions, i.e.,  $1/S(2S-1)$  was replaced by  $-1/S(S+1)$ . Correspondingly, a wave function describable as  $|S 0 \alpha\rangle$  replaced  $|SS\alpha\rangle$ . Of course, this choice of  $M_S = 0$  would not be applicable in the case of a wave function having non-integral spin.

$S(\bar{r}_1, \bar{r}_2)$  can be used to construct D and E as follows:

$$D = \frac{3}{4} g^2 \beta^2 \iint \left( \frac{r_{12}^2 - 3z_{12}^2}{r_{12}^5} \right) S(\bar{r}_1, \bar{r}_2) d\bar{r}_1 d\bar{r}_2 \\ E = \frac{3}{4} g^2 \beta^2 \iint \left( \frac{y_{12}^2 - x_{12}^2}{r_{12}^5} \right) S(\bar{r}_1, \bar{r}_2) d\bar{r}_1 d\bar{r}_2,$$

where  $S(\bar{r}_1, \bar{r}_2)$  can be written explicitly as:

$$S(r_1, r_2) = \frac{-1}{S(S+1)} \int \dots \int \Psi_S^{*M_S=0}(\tau_1, \tau_2, \dots, \tau_N) \\ \times \left\{ \sum_{u \neq v}^N [3\hat{s}_{zu}\hat{s}_{zv} - \hat{s}_u \cdot \hat{s}_v] \delta(\bar{r}_u - \bar{r}_1) \delta(\bar{r}_v - \bar{r}_2) \right\} \Psi_S^{M_S=0}(\tau_1, \tau_2, \dots, \tau_N) \\ d\tau_1 d\tau_2 d\tau_3 \dots d\tau_N, \quad (\text{III.B.1})$$

where  $N$  is the number of electrons in the system, and the integration is done over the space and spin coordinates,  $\tau_i$ , of all electrons. The wave functions employed in this work were CI wave functions and have the general form

$$\Psi = \sum_K c_K D_K,$$

where  $D_K$  is a Slater determinant of one-particle functions. For such wave functions,  $S(\bar{r}_1, \bar{r}_2)$  reduces to

$$S(\bar{r}_1, \bar{r}_2) = \sum_{ij\ell m} a_{ijkl} \phi_i^*(\bar{r}_1) \phi_j(\bar{r}_1) \phi_k^*(\bar{r}_2) \phi_\ell(\bar{r}_2), \quad (\text{III.B.2})$$

where the  $a_{ijkl}$  are determined by the  $c_K$  in the expression for  $\Psi$  and by factors arising from the spin integrations over the  $\phi$ 's in each term of  $S$ . Hence,  $D$  takes the form (and  $E$ , in a similar way)

$$D = \frac{3}{4} g^2 \beta^2 \sum_{ijkl} a_{ijkl} \iint \phi_i^*(\bar{r}_1) \phi_j(\bar{r}_1) \left( \frac{r_{12}^2 - 3z_{12}^2}{r_{12}^5} \right) \phi_k^*(\bar{r}_2) \phi_\ell(\bar{r}_2) d\bar{r}_1 d\bar{r}_2.$$

The author wrote a program to construct the set of  $a_{ijkl}$  from a CI wave function; and using an existing routine for calculating the spatial integrals in a gaussian lobe function (GLF) basis,  $D$  and  $E$  were obtained for the ground  ${}^3B_1$  state of  $:\text{CH}_2$ . For further details on the construction of the  $a_{ijkl}$ , see Appendix III.

### C. The ZFS Parameters of $^3B_1$ Methylene

The apparent conflict which developed between theory and experiment concerning the electronic structure of methylene has been gradually finding resolution. The initial interpretation of the electronic spectra of methylene by Herzberg<sup>7</sup> suggested a linear  $^3\Sigma_g^-$  ground state, while the rapidly-improving theoretical calculations indicated a bent triplet ground state ( $^3B_1$ ;  $\theta \sim 140^\circ$ ). This situation remained stale-mated until the esr spectrum was observed<sup>11,12</sup> in 1970, supporting the common belief in a triplet ground state. The ZFS parameters were the critical measurements in determining the question of the bond angle. The experimental values of D and E for methylene trapped in a matrix at low temperature were found to be  $0.69 \text{ cm}^{-1}$  and  $0.003 \text{ cm}^{-1}$ , respectively. A previous semi-quantitative estimate had been made by Higuchi.<sup>31</sup> The low experimental value of E, suggesting a nearly linear triplet state, must be corrected for motional effects. The result is an experimental value of  $0.074 \text{ cm}^{-1}$  in a xenon matrix and  $0.021 \text{ cm}^{-1}$  in  $\text{SF}_6$ . An ab initio calculation using an eight structure CI was carried out by Harrison,<sup>32</sup> who found the spin-spin contribution to D and E at  $\theta_{\text{HCH}} = 132.5^\circ$  (the determined equilibrium bond angle) to be  $0.71 \text{ cm}^{-1}$  and  $0.05 \text{ cm}^{-1}$ , respectively. When the spin-orbit contribution (expected to be much less significant) is added to Harrison's value for D, the theoretical prediction of  $0.776 \text{ cm}^{-1}$  (using  $D_{\text{SO}} = 0.066 \text{ cm}^{-1}$  from the latest

calculation by Hameka and Hall<sup>33</sup> at  $\theta_{\text{HCH}} = 135^\circ$ ) agrees well with the average experimental value of  $0.76 \pm .02 \text{ cm}^{-1}$ .

The results obtained in a xenon lattice are not included in the average because of the abnormally large spin-orbit contribution induced by the xenon host.

The calculations described in this chapter were undertaken to verify the essential correctness of Harrison's results. The double zeta set of GLF was retained but the CI procedure was extended to include the 100 most energetically important structures (based on their first order contribution to the  ${}^3B_1$  energy) selected from the set of single and double excitations with respect to the dominant  ${}^3B_1$  structure represented by the orbital occupation

$$(1a_1)^2(2a_1)^2(1b_2)^2(3a_1)^1(1b_1)^1.$$

Of the 14 MO's resulting from the closed shell restricted SCF calculation, the  $1a_1$  was held doubly occupied and the  $7a_1$  and  $8a_1$  were maintained empty in the construction of the excitations. Using the NO's obtained from the CI wave function as a basis; the selection of the "best" 100 structures was repeated, and a CI calculation done. This procedure, first introduced by Bender and Davidson<sup>34</sup> is called the iterative natural orbital technique and has the property that it produces a CI energy lowering for one or more iterations but, at some point, begins to diverge, i.e., the CI energy increases with iteration. In the case described

here, one iteration gave the lowest CI energy; the second iteration energy was somewhat higher (see Figure 21).

With a C-H bond length fixed at 1.05 Å, the minimum CI energy was interpolated to correspond to a  $\theta_{\text{HCH}}$  value of 132.5°. The calculation of the ZFS parameters at this bond angle, using the first iteration CI wave function (CI-NO1), gave  $D = 0.722 \text{ cm}^{-1}$  and  $E = 0.053 \text{ cm}^{-1}$ , supporting the earlier eight structure CI results. Figure 22 exhibits the angular dependence of D and E as calculated from the CI wave function for each iteration, and it also includes the eight structure results (CI<sub>0</sub>). The results of this extended calculation are also consistent with the range of experimental results for D, using the same spin-orbit contributions as above.

Subsequent to the results described here, Langhoff and Davidson<sup>35</sup> have calculated the spin-spin values of D and E based on a 575 configuration iterative NO CI wave function at 135°. They report  $D_{\text{ss}} = 0.781 \text{ cm}^{-1}$  and  $E_{\text{ss}} = 0.050 \text{ cm}^{-1}$ . Although this puts the theoretical value of D somewhat higher than the experimental results, it does help confirm the essential stability of the theoretical method.

With the theoretically predicted spin-spin contributions fairly well defined, the appearance of a sound value of the spin-orbit part is of most importance in making a firm comparison with the experimental results.

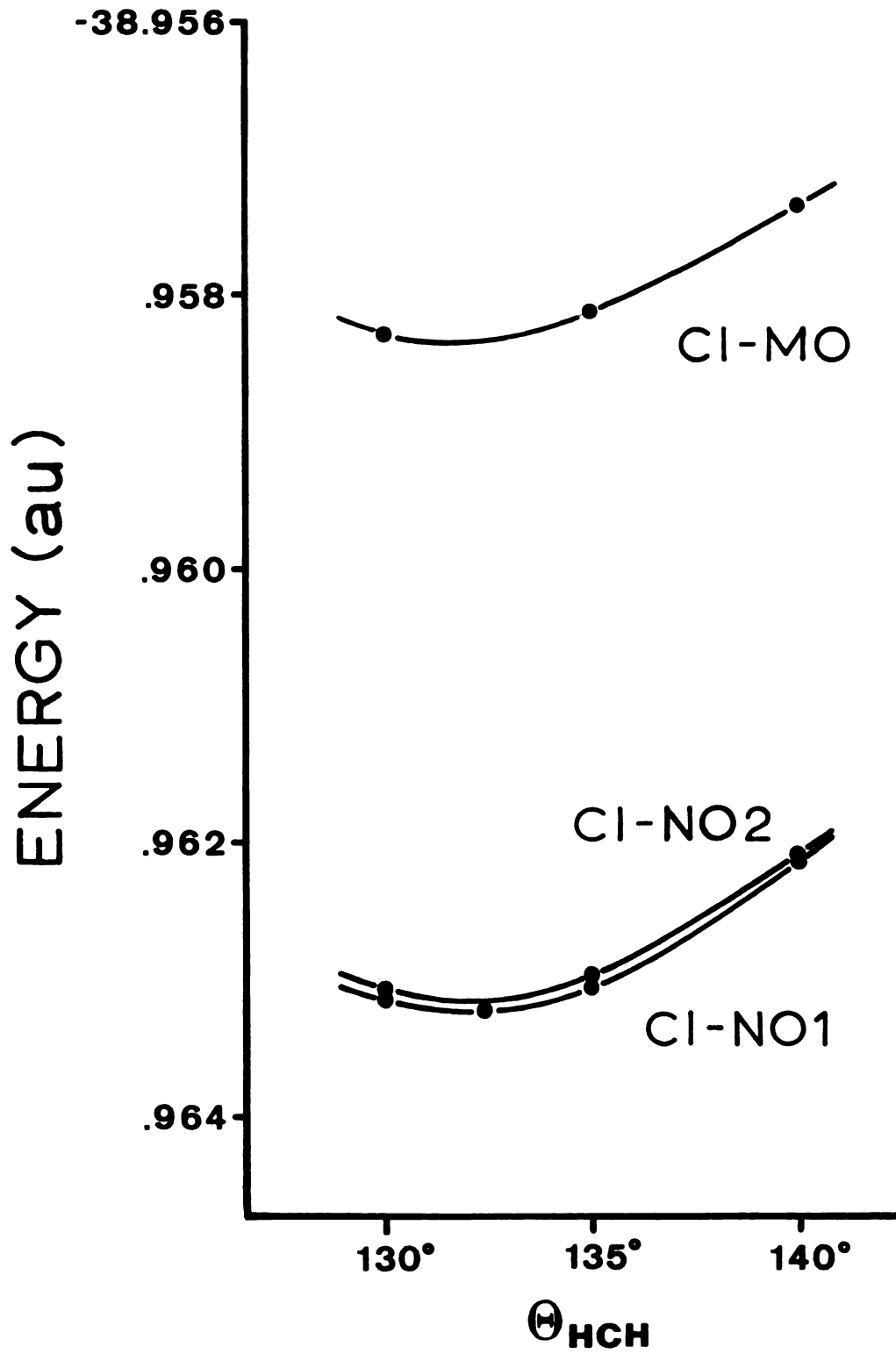


Figure 21.  ${}^{\cdot}\text{CH}_2$  ( ${}^3B_1$ ) Energy vs  $\theta_{\text{HCH}}$ .

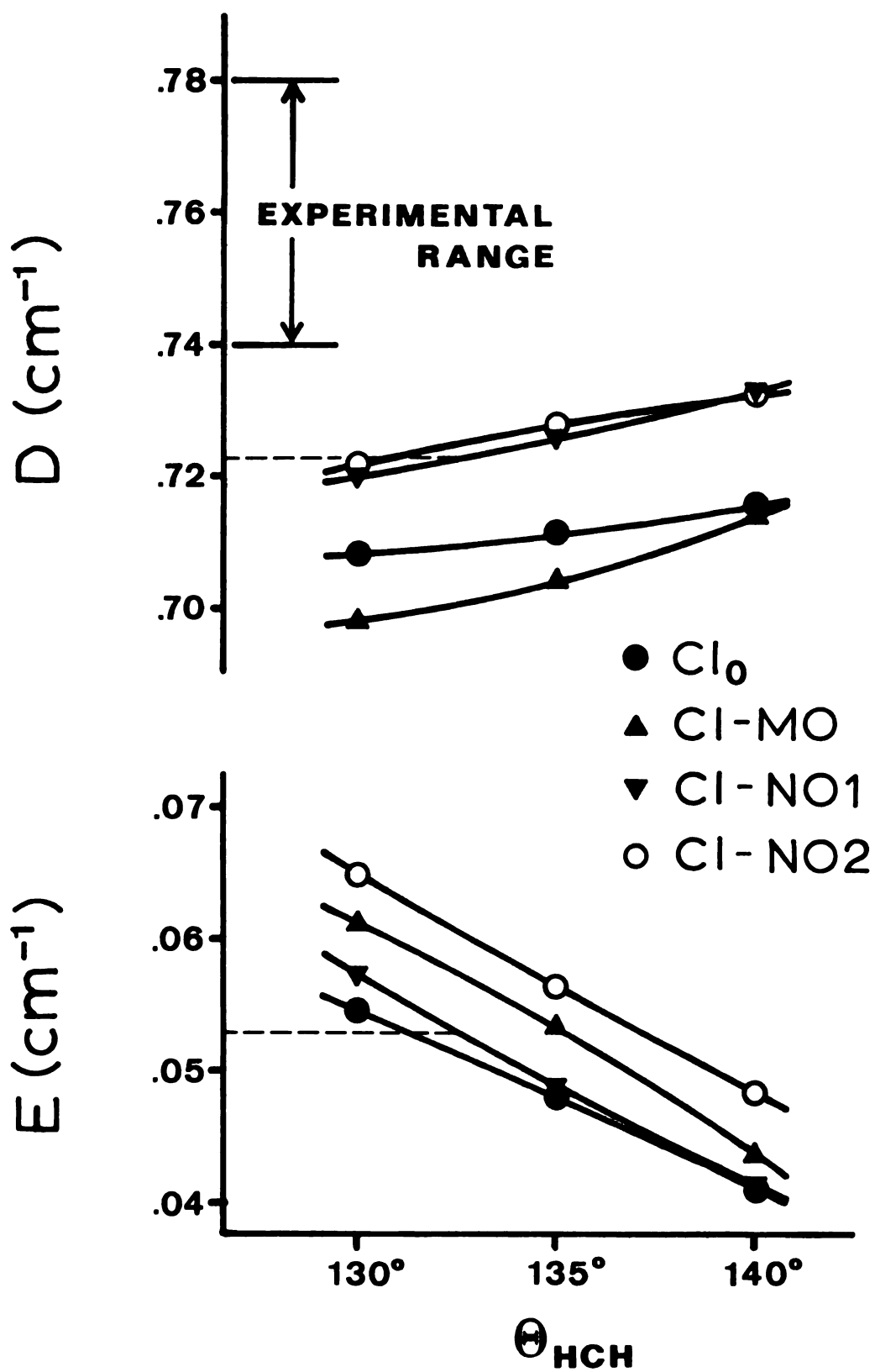


Figure 22.  $:\text{CH}_2$  ( ${}^3\text{B}_1$ ) Spin-spin ZFS Parameters vs  $\theta_{\text{HCH}}$ .

## APPENDICES

## APPENDIX I

### A. The Closed Shell SCF (CSSCF)

The quantum mechanical description of molecules is commonly done in terms of the solutions of the time-independent Schrödinger Equation with the purely electrostatic hamiltonian

$$\hat{H} = -\frac{1}{2} \sum_{i=1}^N \nabla_i^2 - \sum_{a=1}^M \sum_{i=1}^N \frac{Z_a}{r_{ai}} + \frac{1}{2} \sum_{i=1}^N \sum_{j=1}^N \frac{1}{r_{ij}} + \frac{1}{2} \sum_{a=1}^M \sum_{b=1}^M \frac{Z_a Z_b}{r_{ab}},$$

where atomic units are employed ( $e = 1$ ,  $m_e = 1$ ,  $\hbar = 1$ ).  $N$  is the number of electrons in the system,  $M$  the number of nuclei,  $Z_a$  is the multiple of the unit charge carried by each nucleus, and the  $r$ 's are interparticle distances. The nuclei are assumed to be fixed at some pre-chosen positions so that their coordinates become parameters in the problem. With the  $r_{ab}$  fixed, the last term, the nuclear repulsion energy, is simply a constant and doesn't affect the wave function solution by being neglected until the end. Of the first three terms, the first two are sums of one-electron operators (depending on the coordinates of only one electron). Because of the way the third term couples the coordinates of pairs of electrons, there is no exact mathematical way to write the part of  $\hat{H}$  involving electron

coordinates as a sum over one-electron operators. Hence, there is no finite procedure which can yield an exact solution,  $\Psi(\bar{r}_1, \bar{r}_2, \dots, \bar{r}_N)$ , for the Schrödinger Equation

$$\hat{H}\Psi = E\Psi. \quad (E \text{ constant}).$$

Approximate solutions are obtained by the Hartree-Fock method which replaces the exact electron-electron potential with an "effective" electron repulsion potential, in which each electron feels not the force of other electrons as point charges but only their "smeared out" charge densities. This modification requires a knowledge of the solutions before constructing the potentials used in  $\hat{H}$  and transforms  $\hat{H}$  into a sum of effective one-electron operators, which permits separation of the Schrödinger Equation into a coupled set of one-particle equations. The dependence of the hamiltonian on the solution makes the problem a pseudo-eigenvalue problem, expressed by:

$$\hat{H}(\Psi)\Psi = E_{\text{HF}}\Psi.$$

This equation (or set of equations) must be iteratively solved, beginning with an initial estimate of  $\Psi$ . When, or if, the procedure converges, the solution,  $\Psi$ , is called the self-consistent field (SCF) wave function. Multiple nuclei impose difficulties which restricted the numerical calculations to atomic systems. Molecular systems became generally

treatable when Roothaan<sup>36</sup> demonstrated the validity of a reformulation of the problem. In the alternate form, the one-particle solutions are written as expansions in a complete set of analytic functions satisfying the general boundary conditions of the problem; the expansion coefficients are determined by a variational minimization of the total energy,  $E$ . The variational energy is equal to the Hartree-Fock energy,  $E_{\text{HF}}$ , and the variationally-determined coefficients describe the one-particle Hartree-Fock solutions. The numerical solution of a set of coupled integro-differential equations is thus transformed into a set of algebraic equations, solved by methods of linear algebra. Although the new formulation allows solution of molecular systems and yields solutions in terms of analytic functions (instead of numerical tables), in practice it can only be carried out approximately; any complete set of expansion functions is necessarily infinite for these problems, and the choice of a truncated set is a very serious qualification on the results obtained.

The SCF wave functions obtained for the carbonyl carbenes were constructed using the Hartree-Fock-Roothaan (HFR) method discussed above for the case of a restricted, closed-shell wave function, i.e., each  $\alpha$  spin electron was associated with a  $\beta$  spin electron having the same spatial distribution, and there were always an even number of electrons involved. The one particle SCF spatial functions

are

pli

the

B.

c

T

c

v

are called molecular orbitals (MO's); if the MO is multiplied by one of the  $\hat{S}_z$  eigenfunctions (called  $\alpha$  and  $\beta$ ), the function is called a spin-orbital (SO).

### B. The Basis Set

The basis functions employed in the carbonyl carbene calculations were the STO-3G functions of Pople et al.<sup>20</sup> These functions are linear combinations of nuclear-centered cartesian gaussian functions, least-squares fitted to individual unscaled Slater-type functions (STO's). The scaling factors,  $\zeta_i$ , used for each atomic shell were those suggested by Pople as the "best molecular" scale factors. The form of each such simulated STO is

$$\chi_i(r) = N_i \sum_{k=1}^3 d_{ik} e^{-\zeta_i^2 \alpha_{ik} r^2},$$

where  $N_i$  is a normalization constant,  $d_{ik}$  are the least-squares determined coefficients of each gaussian in the linear combination,  $\alpha_{ik}$  are the least-squares determined exponents,  $\zeta_i$  is the scale factor appropriate to the basis function  $\chi_i$ , and  $r$  is the radial distance of the electron from the nucleus on which  $\chi_i$  is centered. As  $\chi_i$  is written above, it has the angular isotropy of an s-type function. The spherical harmonics,  $Y_l^m$ , having  $l > 0$  (in real form) are obtained by incorporating appropriate products of cartesian coordinates into  $\chi_i$ , e.g., a  $p_x$  would contain the

additional factor  $x$ :

$$\chi_{p_x}(x,y,z) = N_i' x \sum_{k=1}^3 d_{ik} e^{-\zeta_i^2 \alpha_{ik} r^2}.$$

Table 18 contains the coefficients,  $d_{ik}$ , and scaled exponents,  $\alpha_{ik}' = \zeta_i^2 \alpha_{ik}$ , used for the basis functions on each type of nucleus included in the series of carbenes involved. The basis set for each molecule was minimal, which is to say that the number of basis functions included for each atom involved in the molecules was just enough to account for the occupied  $(n,l)$  subshells. Thus, H has only one basis function, an s-type function, while C through F have five -- two s functions and a set of three p-type functions ( $p_x$ ,  $p_y$ , and  $p_z$ ).

### C. The CI

One method used to extend the wave function beyond the Hartree-Fock level (HF), is to construct a trial function as a linear combination of single determinants, formed by replacing some of the SO's in the HF determinant by some of the "virtual orbitals" resulting from the SCF procedure. The inclusion of these "excitations" allow the electrons a flexibility not obtainable in the HF wave function and this consequently allows the recovery of the Coulomb correlation energy missing from the HF total energy,  $E_{HF}$ . Also, this extended wave function is sometimes necessary to represent

Table 18. Carbonyl Carbene Basis Set: STO-3G Coefficients and Scaled Exponents

Basis Function	$\alpha'$	d(s)	d(p)
Carbon 1s:	3.53053 13.04509 71.616818	.444635 .535328 .154329	
Carbon 2s,2p:	.22229 .68348 2.94125	.700115 .399513 -.0999672	.391957 .607684 .155916
Oxygen 1s:	6.44364 23.80886 130.70929	Same as Carbon 1s	
Oxygen 2s,2p:	.38039 1.16959 5.03315	Same as Carbon 2s	Same as Carbon 2p
Fluorine 1s:	8.216857 30.360801 166.67909	Same as Carbon 1s	
Fluorine 2s,2p:	.488589 1.502279 6.464805	Same as Carbon 2s	Same as Carbon 2p
Hydrogen 1s:	.15814 .58431 3.20783	Same as Carbon 1s	

molecular systems which are not even qualitatively described by a single determinantal wave function. This extended wave function is variationally determined by minimizing the expectation value of  $\hat{H}$ ,

$$E = \langle \phi_{CI} | \hat{H} | \phi_{CI} \rangle / \langle \phi_{CI} | \phi_{CI} \rangle,$$

with respect to the coefficients of each determinant. The basis for the CI wave function is then the set of all determinants derivable from the HF determinant by replacement of SO's occupied in that determinant by virtual SO's. However, it is also possible to alter this basis (as was done for the CI wave functions of :CHCOF and :FCOH) by choosing linear combinations of the determinants. This is done to facilitate the interpretation of the wave function. In the calculations in this thesis, the new basis elements of the CI are linear combinations of determinants having definite symmetry under the elements of the molecular point group and the spin operators  $\hat{S}^2$  and  $\hat{S}_z$ ; such linear combinations of determinants are called "structures"

It is important to note that usually the number of determinants in the basis is finite (if the SCF basis is finite), but usually it is too large to be fully employed, so a subset of the basis is used. That subset will be termed the CI basis here.

For :CHCOH, a determinantal basis was used. Since, given the SCF MO's, a determinant is completely specified by a list

of the occupied spin-orbitals, the description of the CI basis in the following tables consists in associating a "." (unoccupied) or a 1 (occupied) with each SO. The "active" MO's are those with variable occupation in the basis used. Hence, there is also a "core", consisting, in this work, of MO's always doubly occupied in the basis determinants. In the tables, each MO is associated with two adjacent positions, the first for the  $\alpha$  spin-orbital, the second for the  $\beta$  spin-orbital. The core is de-emphasized by leaving no blanks between its MO's; the active MO's are separated by blanks. The coefficient given in front of each determinant is its weight in the associated structure. Since for :CHCOH structures were not used, each determinant has a coefficient of 1.0.

The active MO's for :CHCOH were the set  $\{\pi_{CO} \sigma_O p \sigma \pi^*\}$ . There were six electrons ( $3\alpha$ ,  $3\beta$ ) distributed among these 10 SO's. The total number of arrangements was

$$\binom{5}{3} \binom{5}{3} = \left(\frac{5!}{3!2!}\right)^2 = 10^2 = 100.$$

These 100 determinants are given in Table 19.

A structure basis was chosen for :CHCOF. The set of active MO's was taken as  $\{p_F \sigma_F \sigma_O \pi_{CO} \sigma p \pi^*\}$  and hosted 10 electrons ( $5\alpha$  and  $5\beta$ ). First, leaving the  $\sigma_F$  doubly occupied, all determinants were formed having  $4\alpha$  and  $4\beta$  electrons distributed among the remaining six MO's. There are  $\binom{6}{4} \binom{6}{4} = 225$  such determinants. When structures are formed from these

Table 19. :CHCOH Determinantal Basis for all States.

			$\pi_{CO}$	$\sigma_O$	p	$\sigma$	$\pi^*$
1	1.	111111111111111111	11	11	11	..	..
2	1.	111111111111111111	11	11	1.	.1	..
3	1.	111111111111111111	11	1.	11	.1	..
4	1.	111111111111111111	1.	11	11	.1	..
5	1.	111111111111111111	11	11	1.	..	.1
6	1.	111111111111111111	11	1.	11	..	.1
7	1.	111111111111111111	1.	11	11	..	.1
8	1.	111111111111111111	11	1.	1.	.1	.1
9	1.	111111111111111111	1.	11	1.	.1	.1
10	1.	111111111111111111	1.	1.	11	.1	.1
11	1.	111111111111111111	11	11	.1	1.	..
12	1.	111111111111111111	11	11	..	11	..
13	1.	111111111111111111	11	1.	.1	11	..
14	1.	111111111111111111	1.	11	.1	11	..
15	1.	111111111111111111	11	11	..	1.	.1
16	1.	111111111111111111	11	1.	.1	1.	.1
17	1.	111111111111111111	1.	11	.1	1.	.1
18	1.	111111111111111111	11	1.	..	11	.1
19	1.	111111111111111111	1.	11	..	11	.1
20	1.	111111111111111111	1.	1.	.1	11	.1
21	1.	111111111111111111	11	.1	11	1.	..
22	1.	111111111111111111	11	.1	1.	11	..
23	1.	111111111111111111	11	..	11	11	..
24	1.	111111111111111111	1.	.1	11	11	..
25	1.	111111111111111111	11	.1	1.	1.	.1
26	1.	111111111111111111	11	..	11	1.	.1
27	1.	111111111111111111	1.	.1	11	1.	.1
28	1.	111111111111111111	11	..	1.	11	.1
29	1.	111111111111111111	1.	.1	1.	11	.1
30	1.	111111111111111111	1.	..	11	11	.1
31	1.	111111111111111111	.1	11	11	1.	..
32	1.	111111111111111111	.1	11	1.	11	..
33	1.	111111111111111111	.1	1.	11	11	..
34	1.	111111111111111111	..	11	11	11	..
35	1.	111111111111111111	.1	11	1.	1.	.1
36	1.	111111111111111111	.1	1.	11	1.	.1
37	1.	111111111111111111	..	11	11	1.	.1
38	1.	111111111111111111	.1	1.	1.	11	.1
39	1.	111111111111111111	..	11	1.	11	.1
40	1.	111111111111111111	..	1.	11	11	.1

Table 19 - Continued

			$\pi_{CO}$	$\sigma_O$	p	$\sigma$	$\pi^*$
41	1.	111111111111111111	11	11	.1	..	1.
42	1.	111111111111111111	11	11	..	.1	1.
43	1.	111111111111111111	11	1.	.1	.1	1.
44	1.	111111111111111111	1.	11	.1	.1	1.
45	1.	111111111111111111	11	11	..	..	11
46	1.	111111111111111111	11	1.	.1	..	11
47	1.	111111111111111111	1.	11	.1	..	11
48	1.	111111111111111111	11	1.	..	.1	11
49	1.	111111111111111111	1.	11	..	.1	11
50	1.	111111111111111111	1.	1.	.1	.1	11
51	1.	111111111111111111	11	.1	11	..	1.
52	1.	111111111111111111	11	.1	1.	.1	1.
53	1.	111111111111111111	11	..	11	.1	1.
54	1.	111111111111111111	1.	.1	11	.1	1.
55	1.	111111111111111111	11	.1	1.	..	11
56	1.	111111111111111111	11	..	11	..	11
57	1.	111111111111111111	1.	.1	11	..	11
58	1.	111111111111111111	11	..	1.	.1	11
59	1.	111111111111111111	1.	.1	1.	.1	11
60	1.	111111111111111111	1.	..	11	.1	11
61	1.	111111111111111111	.1	11	11	..	1.
62	1.	111111111111111111	.1	11	1.	.1	1.
63	1.	111111111111111111	.1	1.	11	.1	1.
64	1.	111111111111111111	..	11	11	.1	1.
65	1.	111111111111111111	.1	11	1.	..	11
66	1.	111111111111111111	.1	1.	11	..	11
67	1.	111111111111111111	..	11	11	..	11
68	1.	111111111111111111	.1	1.	1.	.1	11
69	1.	111111111111111111	..	11	1.	.1	11
70	1.	111111111111111111	..	1.	11	.1	11
71	1.	111111111111111111	11	.1	.1	1.	1.
72	1.	111111111111111111	11	.1	..	11	1.
73	1.	111111111111111111	11	..	.1	11	1.
74	1.	111111111111111111	1.	.1	.1	11	1.
75	1.	111111111111111111	11	.1	..	1.	11
76	1.	111111111111111111	11	..	.1	1.	11
77	1.	111111111111111111	1.	.1	.1	1.	11
78	1.	111111111111111111	11	..	..	11	11
79	1.	111111111111111111	1.	.1	..	11	11
80	1.	111111111111111111	1.	..	.1	11	11

Table 19 - Continued

			$\pi_{CO}$	$\sigma_O$	p	$\sigma$	$\pi^*$
81	1.	111111111111111111	.1	11	.1	1.	1.
82	1.	111111111111111111	.1	11	..	11	1.
83	1.	111111111111111111	.1	1.	.1	11	1.
84	1.	111111111111111111	..	11	.1	11	1.
85	1.	111111111111111111	.1	11	..	1.	11
86	1.	111111111111111111	.1	1.	.1	1.	11
87	1.	111111111111111111	..	11	.1	1.	11
88	1.	111111111111111111	.1	1.	..	11	11
89	1.	111111111111111111	..	11	..	11	11
90	1.	111111111111111111	..	1.	.1	11	11
91	1.	111111111111111111	.1	.1	11	1.	1.
92	1.	111111111111111111	.1	.1	1.	11	1.
93	1.	111111111111111111	.1	..	11	11	1.
94	1.	111111111111111111	..	.1	11	11	1.
95	1.	111111111111111111	.1	.1	1.	1.	11
96	1.	111111111111111111	.1	..	11	1.	11
97	1.	111111111111111111	..	.1	11	1.	11
98	1.	111111111111111111	.1	..	1.	11	11
99	1.	111111111111111111	..	.1	1.	11	11
100	1.	111111111111111111	..	..	11	11	11

determinants, the following distribution of symmetries is obtained:

	Singlet	Triplet	Quintet	Total
A'	57	49	7	113
A''	48	56	8	112
Total	105	105	15	225

The quintet spin structures were not included in the CI wave function. In addition, two singlet and two triplet structures involving single excitations from the  $\sigma_F$  were included, bringing the total number of structures in the CI basis to 214. In the tables listing these structures, two "core" MO's appear above the  $\sigma_F$  and  $p_F$  active MO's. Tables 20, 21 and 22 list the structures of  $^3A''$ ,  $^1A'$ , and  $^1A''$  symmetry, respectively.

The active orbital set for :CFCOH included nine MO's:  $\{\sigma_F p_F \pi_{CO} \sigma_O \sigma p \pi^* \sigma' \sigma''\}$ . In the CSSCF determinant, the first five were doubly occupied. The structure basis was constructed by, first, forming all excitations within the first seven active MO's excluding any quadruple excitations with respect to the SCF determinant and all structures of quintet spin. In addition, a few selected double excitations involving the  $\sigma'$  and  $\sigma''$  virtual MO's were added. The following breakdown of the structures obtained (the quintets

Table 20. :CHCOF  $^3A''$  CI Structure.

			$P_F$	$\sigma_F$	$\sigma_O$	$\pi_{CO}$	$\sigma$	$p$	$\pi^*$	
1	1.	11111111111111111111	11	11	1111	11	11	1.	.1	..
1	1.	11111111111111111111	11	11	1111	11	11	.1	1.	..
2	1.	11111111111111111111	11	11	1111	1.	.1	11	..	11
2	1.	11111111111111111111	11	11	1111	.1	1.	11	..	11
3	1.	11111111111111111111	11	11	1111	..	.1	1.	11	11
3	1.	11111111111111111111	11	11	1111	..	1.	.1	11	11
4	1.	11111111111111111111	11	11	1111	.1	1.	..	11	11
4	1.	11111111111111111111	11	11	1111	1.	.1	..	11	11
5	1.	11111111111111111111	11	11	1111	..	11	1.	.1	11
5	1.	11111111111111111111	11	11	1111	..	11	.1	1.	11
6	1.	11111111111111111111	11	11	1111	1.	..	11	.1	11
6	1.	11111111111111111111	11	11	1111	.1	..	11	1.	11
7	1.	11111111111111111111	11	11	1111	.1	11	..	1.	11
7	1.	11111111111111111111	11	11	1111	1.	11	..	.1	11
8	1.	11111111111111111111	11	11	1111	11	..	1.	.1	11
8	1.	11111111111111111111	11	11	1111	11	..	.1	1.	11
9	1.	11111111111111111111	..	11	1111	11	11	1.	.1	11
9	1.	11111111111111111111	..	11	1111	11	11	.1	1.	11
10	1.	11111111111111111111	..	11	1111	11	.1	1.	11	11
10	1.	11111111111111111111	..	11	1111	11	1.	.1	11	11
11	1.	11111111111111111111	..	11	1111	1.	.1	11	11	11
11	1.	11111111111111111111	..	11	1111	.1	1.	11	11	11
12	1.	11111111111111111111	..	11	1111	1.	11	11	.1	11
12	1.	11111111111111111111	..	11	1111	.1	11	11	1.	11
13	1.	11111111111111111111	.1	11	1111	1.	11	..	11	11
13	1.	11111111111111111111	1.	11	1111	.1	11	..	11	11
14	1.	11111111111111111111	.1	11	1111	..	11	1.	11	11
14	1.	11111111111111111111	1.	11	1111	..	11	.1	11	11
15	1.	11111111111111111111	.1	11	1111	1.	..	11	11	11
15	1.	11111111111111111111	1.	11	1111	.1	..	11	11	11
16	1.	11111111111111111111	.1	11	1111	11	..	1.	11	11
16	1.	11111111111111111111	1.	11	1111	11	..	.1	11	11

Table 20 - Continued

			P <sub>F</sub>	σ <sub>F</sub>		σ <sub>O</sub>	π <sub>CO</sub>	σ	P	π*
17	1.	11111111111111111111	.1	11	1111	1.	11	11	..	11
17	1.	11111111111111111111	1.	11	1111	.1	11	11	..	11
18	1.	11111111111111111111	.1	11	1111	11	11	1.	..	11
18	1.	11111111111111111111	1.	11	1111	11	11	.1	..	11
19	1.	11111111111111111111	..	11	1111	11	11	1.	11	.1
19	1.	11111111111111111111	..	11	1111	11	11	.1	11	1.
20	1.	11111111111111111111	..	11	1111	1.	11	11	11	.1
20	1.	11111111111111111111	..	11	1111	.1	11	11	11	1.
21	1.	11111111111111111111	11	11	1111	11	11	1.	..	.1
21	1.	11111111111111111111	11	11	1111	11	11	.1	..	1.
22	1.	11111111111111111111	11	11	1111	1.	11	11	..	.1
22	1.	11111111111111111111	11	11	1111	.1	11	11	..	1.
23	1.	11111111111111111111	11	11	1111	..	11	1.	11	.1
23	1.	11111111111111111111	11	11	1111	..	11	.1	11	1.
24	1.	11111111111111111111	11	11	1111	1.	..	11	11	.1
24	1.	11111111111111111111	11	11	1111	.1	..	11	11	1.
25	1.	11111111111111111111	11	11	1111	11	..	1.	11	.1
25	1.	11111111111111111111	11	11	1111	11	..	.1	11	1.
26	1.	11111111111111111111	11	11	1111	1.	11	..	11	.1
26	1.	11111111111111111111	11	11	1111	.1	11	..	11	1.
27	1.	11111111111111111111	.1	11	1111	11	11	1.	11	..
27	1.	11111111111111111111	1.	11	1111	11	11	.1	11	..
28	1.	11111111111111111111	.1	11	1111	1.	11	11	11	..
28	1.	11111111111111111111	1.	11	1111	.1	11	11	11	..
29	1.	11111111111111111111	11	11	1111	1.	.1	11	11	..
29	1.	11111111111111111111	11	11	1111	.1	1.	11	11	..
30	1.	11111111111111111111	11	11	1111	11	.1	1.	11	..
30	1.	11111111111111111111	11	11	1111	11	1.	.1	11	..
31	1.	11111111111111111111	11	11	1111	.1	11	11	1.	..
31	1.	11111111111111111111	11	11	1111	1.	11	11	.1	..
32	1.	11111111111111111111	11	11	1111	11	1.	.1	..	11
32	1.	11111111111111111111	11	11	1111	11	.1	1.	..	11

Table 20 - Continued

			$p_F$	$\sigma_F$	$\sigma_O$	$\pi_{CO}$	$\sigma$	$p$	$\pi^*$	
33	1.	11111111111111111111	11	1.	1111	11	11	11	.1	..
33	1.	11111111111111111111	11	.1	1111	11	11	11	1.	..
34	1.	11111111111111111111	1.	11	1111	.1	.1	11	1.	11
34	-1.	11111111111111111111	.1	11	1111	1.	1.	11	.1	11
35	1.	11111111111111111111	1.	11	1111	.1	1.	11	.1	11
35	-1.	11111111111111111111	.1	11	1111	1.	.1	11	1.	11
36	1.	11111111111111111111	1.	11	1111	1.	.1	11	.1	11
36	-1.	11111111111111111111	.1	11	1111	.1	1.	11	1.	11
37	1.	11111111111111111111	1.	11	1111	11	.1	.1	1.	11
37	-1.	11111111111111111111	.1	11	1111	11	1.	1.	.1	11
38	1.	11111111111111111111	1.	11	1111	11	.1	1.	.1	11
38	-1.	11111111111111111111	.1	11	1111	11	1.	.1	1.	11
39	1.	11111111111111111111	1.	11	1111	11	1.	.1	.1	11
39	-1.	11111111111111111111	.1	11	1111	11	.1	1.	1.	11
40	1.	11111111111111111111	11	11	1111	11	1.	.1	.1	1.
40	-1.	11111111111111111111	11	11	1111	11	.1	1.	1.	.1
41	1.	11111111111111111111	11	11	1111	11	1.	.1	1.	.1
41	-1.	11111111111111111111	11	11	1111	11	.1	1.	.1	1.
42	1.	11111111111111111111	11	11	1111	11	1.	1.	.1	.1
42	-1.	11111111111111111111	11	11	1111	11	.1	.1	1.	1.
43	1.	11111111111111111111	11	11	1111	1.	.1	11	.1	1.
43	-1.	11111111111111111111	11	11	1111	.1	1.	11	1.	.1
44	1.	11111111111111111111	11	11	1111	1.	.1	11	1.	.1
44	-1.	11111111111111111111	11	11	1111	.1	1.	11	.1	1.
45	1.	11111111111111111111	11	11	1111	1.	1.	11	.1	.1
45	-1.	11111111111111111111	11	11	1111	.1	.1	11	1.	1.
46	1.	11111111111111111111	1.	11	1111	11	11	.1	.1	1.
46	-1.	11111111111111111111	.1	11	1111	11	11	1.	1.	.1
47	1.	11111111111111111111	1.	11	1111	11	11	.1	1.	.1
47	-1.	11111111111111111111	.1	11	1111	11	11	1.	.1	1.
48	1.	11111111111111111111	1.	11	1111	11	11	1.	.1	.1
48	-1.	11111111111111111111	.1	11	1111	11	11	.1	1.	1.

Table 20 - Continued

			$p_F$	$\sigma_F$	$\sigma_O$	$\pi_{CO}$	$\sigma$	$p$	$\pi^*$	
49	1.	11111111111111111111	1.	11	1111	.1	11	11	.1	1.
49	-1.	11111111111111111111	.1	11	1111	1.	11	11	1.	.1
50	1.	11111111111111111111	1.	11	1111	.1	11	11	1.	.1
50	-1.	11111111111111111111	.1	11	1111	1.	11	11	.1	1.
51	1.	11111111111111111111	1.	11	1111	1.	11	11	.1	.1
51	-1.	11111111111111111111	.1	11	1111	.1	11	11	1.	1.
52	1.	11111111111111111111	1.	11	1111	11	.1	.1	11	1.
52	-1.	11111111111111111111	.1	11	1111	11	1.	1.	11	.1
53	1.	11111111111111111111	1.	11	1111	11	.1	1.	11	.1
53	-1.	11111111111111111111	.1	11	1111	11	1.	.1	11	1.
54	1.	11111111111111111111	1.	11	1111	11	1.	.1	11	.1
54	-1.	11111111111111111111	.1	11	1111	11	.1	1.	11	1.
55	1.	11111111111111111111	1.	11	1111	.1	.1	11	11	1.
55	-1.	11111111111111111111	.1	11	1111	1.	1.	11	11	.1
56	1.	11111111111111111111	1.	11	1111	.1	1.	11	11	.1
56	-1.	11111111111111111111	.1	11	1111	1.	.1	11	11	1.
57	1.	11111111111111111111	1.	11	1111	1.	.1	11	11	.1
57	-1.	11111111111111111111	.1	11	1111	.1	1.	11	11	1.

Table 21. :CHCOF  $^1A'$  CI Structures.

			$p_F$	$\sigma_F$		$\sigma_O$	$\pi_{CO}$	$\sigma$	$p$	$\pi^*$
1	1.	11111111111111111111	11	11	1111	11	11	11	..	..
2	1.	11111111111111111111	11	11	1111	11	11	..	11	..
3	1.	11111111111111111111	11	11	1111	11	..	11	11	..
4	1.	11111111111111111111	11	11	1111	..	11	11	11	..
5	1.	11111111111111111111	..	11	1111	11	11	11	11	..
6	1.	11111111111111111111	11	11	1111	11	11	..	..	11
7	1.	11111111111111111111	11	11	1111	11	..	11	..	11
8	1.	11111111111111111111	11	11	1111	..	11	11	..	11
9	1.	11111111111111111111	..	11	1111	11	11	11	..	11
10	1.	11111111111111111111	11	11	1111	11	..	..	11	11
11	1.	11111111111111111111	11	11	1111	..	11	..	11	11
12	1.	11111111111111111111	..	11	1111	11	11	..	11	11
13	1.	11111111111111111111	11	11	1111	..	..	11	11	11
14	1.	11111111111111111111	..	11	1111	11	..	11	11	11
15	1.	11111111111111111111	..	11	1111	..	11	11	11	11
16	1.	11111111111111111111	1.	11	1111	11	.1	11	11	..
16	-1.	11111111111111111111	.1	11	1111	11	1.	11	11	..
17	1.	11111111111111111111	1.	11	1111	..	.1	11	11	11
17	-1.	11111111111111111111	.1	11	1111	..	1.	11	11	11
18	1.	11111111111111111111	.1	11	1111	11	..	11	1.	11
18	-1.	11111111111111111111	1.	11	1111	11	..	11	.1	11
19	1.	11111111111111111111	.1	11	1111	11	..	11	11	1.
19	-1.	11111111111111111111	1.	11	1111	11	..	11	11	.1
20	1.	11111111111111111111	1.	11	1111	..	11	11	11	.1
20	-1.	11111111111111111111	.1	11	1111	..	11	11	11	1.
21	1.	11111111111111111111	1.	11	1111	..	11	11	.1	11
21	-1.	11111111111111111111	.1	11	1111	..	11	11	1.	11

Table 21 - Continued

			$p_F$	$\sigma_F$	$\sigma_O$	$\pi_{CO}$	$\sigma$	$p$	$\pi^*$
22	1.	11111111111111111111	1.	11	1111	11	11	..	11 .1
22	-1.	11111111111111111111	.1	11	1111	11	11	..	11 1.
23	1.	11111111111111111111	1.	11	1111	11	11	..	.1 11
23	-1.	11111111111111111111	.1	11	1111	11	11	..	1. 11
24	1.	11111111111111111111	1.	11	1111	11	.1	..	11 11
24	-1.	11111111111111111111	.1	11	1111	11	1.	..	11 11
25	1.	11111111111111111111	1.	11	1111	11	.1	11	.. 11
25	-1.	11111111111111111111	.1	11	1111	11	1.	11	.. 11
26	1.	11111111111111111111	1.	11	1111	11	11	11	.. .1
26	-1.	11111111111111111111	.1	11	1111	11	11	11	.. 1.
27	1.	11111111111111111111	1.	11	1111	11	11	11	.1 ..
27	-1.	11111111111111111111	.1	11	1111	11	11	11	1. ..
28	1.	11111111111111111111	..	11	1111	11	1.	11	.1 11
28	-1.	11111111111111111111	..	11	1111	11	.1	11	1. 11
29	1.	11111111111111111111	..	11	1111	1.	11	.1	11 11
29	-1.	11111111111111111111	..	11	1111	.1	11	1.	11 11
30	1.	11111111111111111111	..	11	1111	11	11	11	1. .1
30	-1.	11111111111111111111	..	11	1111	11	11	11	.1 1.
31	1.	11111111111111111111	..	11	1111	11	1.	11	11 .1
31	-1.	11111111111111111111	..	11	1111	11	.1	11	11 1.
32	1.	11111111111111111111	11	11	1111	..	1.	11	11 .1
32	-1.	11111111111111111111	11	11	1111	..	.1	11	11 1.
33	1.	11111111111111111111	11	11	1111	11	1.	..	11 .1
33	-1.	11111111111111111111	11	11	1111	11	.1	..	11 1.
34	1.	11111111111111111111	11	11	1111	..	11	11	1. .1
34	-1.	11111111111111111111	11	11	1111	..	11	11	.1 1.
35	1.	11111111111111111111	11	11	1111	11	11	..	1. .1
35	-1.	11111111111111111111	11	11	1111	11	11	..	.1 1.
36	1.	11111111111111111111	11	11	1111	11	1.	11	.. .1
36	-1.	11111111111111111111	11	11	1111	11	.1	11	.. 1.
37	1.	11111111111111111111	11	11	1111	11	..	11	1. .1
37	-1.	11111111111111111111	11	11	1111	11	..	11	.1 1.

Table 21 - Continued

			$p_F$	$\sigma_F$	$\sigma_O$	$\pi_{CO}$	$\sigma$	$p$	$\pi^*$
38	1.	11111111111111111111	11	11	1111	11	.1	11	1. ..
38	-1.	11111111111111111111	11	11	1111	11	1.	11	.1 ..
39	1.	11111111111111111111	11	11	1111	.1	11	1.	11 ..
39	-1.	11111111111111111111	11	11	1111	1.	11	.1	11 ..
40	1.	11111111111111111111	11	11	1111	1.	..	.1	11 11
40	-1.	11111111111111111111	11	11	1111	.1	..	1.	11 11
41	1.	11111111111111111111	11	11	1111	.1	11	1.	.. 11
41	-1.	11111111111111111111	11	11	1111	1.	11	.1	.. 11
42	1.	11111111111111111111	11	11	1111	11	.1	..	1. 11
42	-1.	11111111111111111111	11	11	1111	11	1.	..	.1 11
43	1.	11111111111111111111	11	11	1111	..	1.	11	.1 11
43	-1.	11111111111111111111	11	11	1111	..	.1	11	1. 11
44	1.	11111111111111111111	11	1.	1111	11	11	.1	11 ..
44	-1.	11111111111111111111	11	.1	1111	11	11	1.	11 ..
45	2.	11111111111111111111	1.	11	1111	11	1.	11	.1 .1
45	-1.	11111111111111111111	1.	11	1111	11	.1	11	1. .1
45	-1.	11111111111111111111	1.	11	1111	11	.1	11	.1 1.
45	-1.	11111111111111111111	.1	11	1111	11	1.	11	1. .1
45	-1.	11111111111111111111	.1	11	1111	11	1.	11	.1 1.
45	2.	11111111111111111111	.1	11	1111	11	.1	11	1. 1.
46	2.	11111111111111111111	11	11	1111	1.	11	1.	.1 .1
46	-1.	11111111111111111111	11	11	1111	1.	11	.1	1. .1
46	-1.	11111111111111111111	11	11	1111	1.	11	.1	.1 1.
46	-1.	11111111111111111111	11	11	1111	.1	11	1.	1. .1
46	-1.	11111111111111111111	11	11	1111	.1	11	1.	.1 1.
46	2.	11111111111111111111	11	11	1111	.1	11	.1	1. 1.
47	2.	11111111111111111111	11	11	1111	1.	1.	.1	11 .1
47	-1.	11111111111111111111	11	11	1111	1.	.1	1.	11 .1
47	-1.	11111111111111111111	11	11	1111	1.	.1	.1	11 1.
47	-1.	11111111111111111111	11	11	1111	.1	1.	1.	11 .1
47	-1.	11111111111111111111	11	11	1111	.1	1.	.1	11 1.
47	2.	11111111111111111111	11	11	1111	.1	.1	1.	11 1.
48	2.	11111111111111111111	1.	11	1111	1.	11	.1	11 .1
48	-1.	11111111111111111111	1.	11	1111	.1	11	1.	11 .1
48	-1.	11111111111111111111	1.	11	1111	.1	11	.1	11 1.
48	-1.	11111111111111111111	.1	11	1111	1.	11	1.	11 .1
48	-1.	11111111111111111111	.1	11	1111	1.	11	.1	11 1.
48	2.	11111111111111111111	.1	11	1111	.1	11	1.	11 1.

Table 21 - Continued

			$P_F$	$\sigma_F$		$\sigma_O$	$\pi_{CO}$	$\sigma$	$P$	$\pi^*$
49	2.	11111111111111111111	11	11	1111	1.	1.	.1	.1	11
49	-1.	11111111111111111111	11	11	1111	1.	.1	1.	.1	11
49	-1.	11111111111111111111	11	11	1111	1.	.1	.1	1.	11
49	-1.	11111111111111111111	11	11	1111	.1	1.	1.	.1	11
49	-1.	11111111111111111111	11	11	1111	.1	1.	.1	1.	11
49	2.	11111111111111111111	11	11	1111	.1	.1	1.	1.	11
50	2.	11111111111111111111	1.	11	1111	1.	11	.1	.1	11
50	-1.	11111111111111111111	1.	11	1111	.1	11	1.	.1	11
50	-1.	11111111111111111111	1.	11	1111	.1	11	.1	1.	11
50	-1.	11111111111111111111	.1	11	1111	1.	11	1.	.1	11
50	-1.	11111111111111111111	.1	11	1111	1.	11	.1	1.	11
50	2.	11111111111111111111	.1	11	1111	.1	11	1.	1.	11
51	2.	11111111111111111111	1.	11	1111	1.	.1	.1	11	11
51	-1.	11111111111111111111	1.	11	1111	.1	1.	.1	11	11
51	-1.	11111111111111111111	1.	11	1111	.1	.1	1.	11	11
51	-1.	11111111111111111111	.1	11	1111	1.	1.	.1	11	11
51	-1.	11111111111111111111	.1	11	1111	1.	.1	1.	11	11
51	2.	11111111111111111111	.1	11	1111	.1	1.	1.	11	11
52	1.	11111111111111111111	1.	11	1111	11	.1	11	1.	.1
52	-1.	11111111111111111111	1.	11	1111	11	.1	11	.1	1.
52	-1.	11111111111111111111	.1	11	1111	11	1.	11	1.	.1
52	1.	11111111111111111111	.1	11	1111	11	1.	11	.1	1.
53	1.	11111111111111111111	11	11	1111	1.	11	.1	1.	.1
53	-1.	11111111111111111111	11	11	1111	1.	11	.1	.1	1.
53	-1.	11111111111111111111	11	11	1111	.1	11	1.	1.	.1
53	1.	11111111111111111111	11	11	1111	.1	11	1.	.1	1.
54	1.	11111111111111111111	11	11	1111	1.	.1	1.	11	.1
54	-1.	11111111111111111111	11	11	1111	1.	.1	.1	11	1.
54	-1.	11111111111111111111	11	11	1111	.1	1.	1.	11	.1
54	1.	11111111111111111111	11	11	1111	.1	1.	.1	11	1.
55	1.	11111111111111111111	1.	11	1111	.1	11	1.	11	.1
55	-1.	11111111111111111111	1.	11	1111	.1	11	.1	11	1.
55	-1.	11111111111111111111	.1	11	1111	1.	11	1.	11	.1
55	1.	11111111111111111111	.1	11	1111	1.	11	.1	11	1.
56	1.	11111111111111111111	11	11	1111	1.	.1	1.	.1	11
56	-1.	11111111111111111111	11	11	1111	1.	.1	.1	1.	11
56	-1.	11111111111111111111	11	11	1111	.1	1.	1.	.1	11
56	1.	11111111111111111111	11	11	1111	.1	1.	.1	1.	11

Table 21 - Continued

			$P_F$	$\sigma_F$		$\sigma_O$	$\pi_{CO}$	$\sigma$	$P$	$\pi^*$
57	1.	11111111111111111111	1.	11	1111	.1	11	1.	.1	11
57	-1.	11111111111111111111	1.	11	1111	.1	11	.1	1.	11
57	-1.	11111111111111111111	.1	11	1111	1.	11	1.	.1	11
57	1.	11111111111111111111	.1	11	1111	1.	11	.1	1.	11
58	1.	11111111111111111111	1.	11	1111	.1	1.	.1	11	11
58	-1.	11111111111111111111	1.	11	1111	.1	.1	1.	11	11
58	-1.	11111111111111111111	.1	11	1111	1.	1.	.1	11	11
58	1.	11111111111111111111	.1	11	1111	1.	.1	1.	11	11

Table 22. :CHCOF  $^1A''$  CI Structures.

			$P_F$	$\sigma_F$	$\sigma_O$	$\pi_{CO}$	$\sigma$	$P$	$\pi^*$	
1	1.	11111111111111111111	11	11	1111	11	11	.1	1.	..
1	-1.	11111111111111111111	11	11	1111	11	11	1.	.1	..
2	1.	11111111111111111111	1.	11	1111	11	..	.1	11	11
2	-1.	11111111111111111111	.1	11	1111	11	..	1.	11	11
3	1.	11111111111111111111	1.	11	1111	11	11	.1	11	..
3	-1.	11111111111111111111	.1	11	1111	11	11	1.	11	..
4	1.	11111111111111111111	1.	11	1111	.1	..	11	11	11
4	-1.	11111111111111111111	.1	11	1111	1.	..	11	11	11
5	1.	11111111111111111111	1.	11	1111	..	11	.1	11	11
5	-1.	11111111111111111111	.1	11	1111	..	11	1.	11	11
6	1.	11111111111111111111	1.	11	1111	.1	11	..	11	11
6	-1.	11111111111111111111	.1	11	1111	1.	11	..	11	11
7	1.	11111111111111111111	1.	11	1111	.1	11	11	..	11
7	-1.	11111111111111111111	.1	11	1111	1.	11	11	..	11
8	1.	11111111111111111111	1.	11	1111	11	11	.1	..	11
8	-1.	11111111111111111111	.1	11	1111	11	11	1.	..	11
9	1.	11111111111111111111	..	11	1111	11	11	.1	1.	11
9	-1.	11111111111111111111	..	11	1111	11	11	1.	.1	11
10	1.	11111111111111111111	..	11	1111	1.	11	11	.1	11
10	-1.	11111111111111111111	..	11	1111	.1	11	11	1.	11
11	1.	11111111111111111111	..	11	1111	1.	.1	11	11	11
11	-1.	11111111111111111111	..	11	1111	.1	1.	11	11	11
12	1.	11111111111111111111	..	11	1111	11	.1	1.	11	11
12	-1.	11111111111111111111	..	11	1111	11	1.	.1	11	11
13	1.	11111111111111111111	..	11	1111	11	11	1.	11	.1
13	-1.	11111111111111111111	..	11	1111	11	11	.1	11	1.
14	1.	11111111111111111111	..	11	1111	1.	11	11	11	.1
14	-1.	11111111111111111111	..	11	1111	.1	11	11	11	1.
15	1.	11111111111111111111	11	11	1111	1.	..	11	11	.1
15	-1.	11111111111111111111	11	11	1111	.1	..	11	11	1.
16	1.	11111111111111111111	11	11	1111	1.	11	..	11	.1
16	-1.	11111111111111111111	11	11	1111	.1	11	..	11	1.

Table 22 - Continued.

			P <sub>F</sub>	σ <sub>F</sub>		σ <sub>O</sub>	π <sub>CO</sub>	σ	P	π*
17	1.	11111111111111111111	11	11	1111	..	11	1.	11	.1
17	-1.	11111111111111111111	11	11	1111	..	11	.1	11	1.
18	1.	11111111111111111111	11	11	1111	11	..	1.	11	.1
18	-1.	11111111111111111111	11	11	1111	11	..	.1	11	1.
19	1.	11111111111111111111	11	11	1111	1.	11	11	..	.1
19	-1.	11111111111111111111	11	11	1111	.1	11	11	..	1.
20	1.	11111111111111111111	11	11	1111	11	11	1.	..	.1
20	-1.	11111111111111111111	11	11	1111	11	11	.1	..	1.
21	1.	11111111111111111111	11	11	1111	.1	11	11	1.	..
21	-1.	11111111111111111111	11	11	1111	1.	11	11	.1	..
22	1.	11111111111111111111	11	11	1111	11	.1	1.	11	..
22	-1.	11111111111111111111	11	11	1111	11	1.	.1	11	..
23	1.	11111111111111111111	11	11	1111	.1	1.	11	11	..
23	-1.	11111111111111111111	11	11	1111	1.	.1	11	11	..
24	1.	11111111111111111111	.1	11	1111	1.	11	11	11	..
24	-1.	11111111111111111111	1.	11	1111	.1	11	11	11	..
25	1.	11111111111111111111	11	11	1111	1.	.1	..	11	11
25	-1.	11111111111111111111	11	11	1111	.1	1.	..	11	11
26	1.	11111111111111111111	11	11	1111	..	.1	1.	11	11
26	-1.	11111111111111111111	11	11	1111	..	1.	.1	11	11
27	1.	11111111111111111111	11	11	1111	11	.1	1.	..	11
27	-1.	11111111111111111111	11	11	1111	11	1.	.1	..	11
28	1.	11111111111111111111	11	11	1111	1.	.1	11	..	11
28	-1.	11111111111111111111	11	11	1111	.1	1.	11	..	11
29	1.	11111111111111111111	11	11	1111	.1	11	..	1.	11
29	-1.	11111111111111111111	11	11	1111	1.	11	..	.1	11
30	1.	11111111111111111111	11	11	1111	..	11	.1	1.	11
30	-1.	11111111111111111111	11	11	1111	..	11	1.	.1	11
31	1.	11111111111111111111	11	11	1111	11	..	.1	1.	11
31	-1.	11111111111111111111	11	11	1111	11	..	1.	.1	11
32	1.	11111111111111111111	11	11	1111	.1	..	11	1.	11
32	-1.	11111111111111111111	11	11	1111	1.	..	11	.1	11

Table 22 - Continued

			$P_F$	$\sigma_F$		$\sigma_O$	$\pi_{CO}$	$\sigma$	$p$	$\pi^*$
33	1.	11111111111111111111	11	1.	1111	11	11	11	.1	..
33	-1.	11111111111111111111	11	.1	1111	11	11	11	1.	..
34	2.	11111111111111111111	1.	11	1111	1.	11	11	.1	.1
34	-1.	11111111111111111111	1.	11	1111	.1	11	11	1.	.1
34	-1.	11111111111111111111	1.	11	1111	.1	11	11	.1	1.
34	-1.	11111111111111111111	.1	11	1111	1.	11	11	1.	.1
34	-1.	11111111111111111111	.1	11	1111	1.	11	11	.1	1.
34	2.	11111111111111111111	.1	11	1111	.1	11	11	1.	1.
35	2.	11111111111111111111	1.	11	1111	11	11	1.	.1	.1
35	-1.	11111111111111111111	1.	11	1111	11	11	.1	1.	.1
35	-1.	11111111111111111111	1.	11	1111	11	11	.1	.1	1.
35	-1.	11111111111111111111	.1	11	1111	11	11	1.	1.	.1
35	-1.	11111111111111111111	.1	11	1111	11	11	1.	.1	1.
35	2.	11111111111111111111	.1	11	1111	11	11	.1	1.	1.
36	2.	11111111111111111111	11	11	1111	1.	1.	11	.1	.1
36	-1.	11111111111111111111	11	11	1111	1.	.1	11	1.	.1
36	-1.	11111111111111111111	11	11	1111	1.	.1	11	.1	1.
36	-1.	11111111111111111111	11	11	1111	.1	1.	11	1.	.1
36	-1.	11111111111111111111	11	11	1111	.1	1.	11	.1	1.
36	2.	11111111111111111111	11	11	1111	.1	.1	11	1.	1.
37	2.	11111111111111111111	11	11	1111	11	1.	1.	.1	.1
37	-1.	11111111111111111111	11	11	1111	11	1.	.1	1.	.1
37	-1.	11111111111111111111	11	11	1111	11	1.	.1	.1	1.
37	-1.	11111111111111111111	11	11	1111	11	.1	1.	1.	.1
37	-1.	11111111111111111111	11	11	1111	11	.1	1.	.1	1.
37	2.	11111111111111111111	11	11	1111	11	.1	.1	1.	1.
38	2.	11111111111111111111	1.	11	1111	1.	.1	11	11	.1
38	-1.	11111111111111111111	1.	11	1111	.1	1.	11	11	.1
38	-1.	11111111111111111111	1.	11	1111	.1	.1	11	11	1.
38	-1.	11111111111111111111	.1	11	1111	1.	1.	11	11	.1
38	-1.	11111111111111111111	.1	11	1111	1.	.1	11	11	1.
38	2.	11111111111111111111	.1	11	1111	.1	1.	11	11	1.
39	2.	11111111111111111111	1.	11	1111	11	1.	.1	11	.1
39	-1.	11111111111111111111	1.	11	1111	11	.1	1.	11	.1
39	-1.	11111111111111111111	1.	11	1111	11	.1	.1	11	1.
39	-1.	11111111111111111111	.1	11	1111	11	1.	1.	11	.1
39	-1.	11111111111111111111	.1	11	1111	11	1.	.1	11	1.
39	2.	11111111111111111111	.1	11	1111	11	.1	1.	11	1.
40	2.	11111111111111111111	1.	11	1111	11	1.	.1	.1	11
40	-1.	11111111111111111111	1.	11	1111	11	.1	1.	.1	11
40	-1.	11111111111111111111	1.	11	1111	11	.1	.1	1.	11
40	-1.	11111111111111111111	.1	11	1111	11	1.	1.	.1	11
40	-1.	11111111111111111111	.1	11	1111	11	1.	.1	1.	11
40	2.	11111111111111111111	.1	11	1111	11	.1	1.	1.	11

Table 22 - Continued

			$P_F$	$\sigma_F$		$\sigma_O$	$\pi_{CO}$	$\sigma$	$P$	$\pi^*$
41	2.	11111111111111111111	1.	11	1111	1.	.1	11	.1	11
41	-1.	11111111111111111111	1.	11	1111	.1	1.	11	.1	11
41	-1.	11111111111111111111	1.	11	1111	.1	.1	11	1.	11
41	-1.	11111111111111111111	.1	11	1111	1.	1.	11	.1	11
41	-1.	11111111111111111111	.1	11	1111	1.	.1	11	1.	11
41	2.	11111111111111111111	.1	11	1111	.1	1.	11	1.	11
42	1.	11111111111111111111	1.	11	1111	.1	11	11	1.	.1
42	-1.	11111111111111111111	1.	11	1111	.1	11	11	.1	1.
42	-1.	11111111111111111111	.1	11	1111	1.	11	11	1.	.1
42	1.	11111111111111111111	.1	11	1111	1.	11	11	.1	1.
43	1.	11111111111111111111	1.	11	1111	11	11	.1	1.	.1
43	-1.	11111111111111111111	1.	11	1111	11	11	.1	.1	1.
43	-1.	11111111111111111111	.1	11	1111	11	11	1.	1.	.1
43	1.	11111111111111111111	.1	11	1111	11	11	1.	.1	1.
44	1.	11111111111111111111	11	11	1111	1.	.1	11	1.	.1
44	-1.	11111111111111111111	11	11	1111	1.	.1	11	.1	1.
44	-1.	11111111111111111111	11	11	1111	.1	1.	11	1.	.1
44	1.	11111111111111111111	11	11	1111	.1	1.	11	.1	1.
45	1.	11111111111111111111	11	11	1111	11	1.	.1	1.	.1
45	-1.	11111111111111111111	11	11	1111	11	1.	.1	.1	1.
45	-1.	11111111111111111111	11	11	1111	11	.1	1.	1.	.1
45	1.	11111111111111111111	11	11	1111	11	.1	1.	.1	1.
46	1.	11111111111111111111	1.	11	1111	.1	1.	11	11	.1
46	-1.	11111111111111111111	1.	11	1111	.1	.1	11	11	1.
46	-1.	11111111111111111111	.1	11	1111	1.	1.	11	11	.1
46	1.	11111111111111111111	.1	11	1111	1.	.1	11	11	1.
47	1.	11111111111111111111	1.	11	1111	11	.1	1.	11	.1
47	-1.	11111111111111111111	1.	11	1111	11	.1	.1	11	1.
47	-1.	11111111111111111111	.1	11	1111	11	1.	1.	11	.1
47	1.	11111111111111111111	.1	11	1111	11	1.	.1	11	1.
48	1.	11111111111111111111	1.	11	1111	11	.1	1.	.1	11
48	-1.	11111111111111111111	1.	11	1111	11	.1	.1	1.	11
48	-1.	11111111111111111111	.1	11	1111	11	1.	1.	.1	11
48	1.	11111111111111111111	.1	11	1111	11	1.	.1	1.	11
49	1.	11111111111111111111	1.	11	1111	.1	1.	11	.1	11
49	-1.	11111111111111111111	1.	11	1111	.1	.1	11	1.	11
49	-1.	11111111111111111111	.1	11	1111	1.	1.	11	.1	11
49	1.	11111111111111111111	.1	11	1111	1.	.1	11	1.	11

listed were not included in the CI):

	Singlet	Triplet	Quintet	Total
A'	76	81	16	173
A''	74	88	14	176
Total	150	169	30	349

The structures for the symmetries  ${}^3A''$ ,  ${}^1A'$ , and  ${}^1A''$  are displayed in Tables 23, 24, and 25, respectively.

#### D. Natural Orbitals

The natural orbitals (NO's) used in the population analyses and displayed in the electron density contour maps were obtained as the eigenfunctions of the one-particle density matrix for the CI wave function for each state. This procedure was carried out using a program written by the author of this thesis. It is technically inaccurate to call the NO's obtained "the NO's for the molecule" since that description is reserved for the eigenfunctions of the exact one-particle density matrix. However, the NO's constructed may be called "approximate NO's" or perhaps the NO's "for this approximate wave function". The occupation numbers are the eigenvalues of the one-particle density matrix corresponding to each NO. In a limited CI, the









































NO's and their eigenvalues contain a large amount of concise information about the CI wave function and are of value as a diagnostic device as well as a source of physical information about the electronic structure.

## APPENDIX II

### A. Basis Set

The basis chosen for the lithium carbenes was of roughly double zeta quality and consisted of a set of contracted nuclear-centered cartesian gaussian-type functions. Each function in the basis has the form

$$\chi_i = \sum_{m=1}^{n_i} d_{im} g(\alpha_{im}; r),$$

where  $g(\alpha_{im}; r)$  is a primitive normalized cartesian gaussian having an exponent  $\alpha_{im}$ , and where  $d_{im}$  is the contraction coefficient of that primitive in the basis function  $\chi_i$ . The exponents and contraction coefficients defining each basis function in the set used are given in Table 26. Except for the 4-component p function on Li, taken from Williams,<sup>27</sup> the primitives were the revised set of Huzinaga<sup>36</sup> contracted according to the method of Dunning.<sup>37</sup> Specifically, for carbon a (9s5p) set was contracted to a [4s/2p] set; for lithium, an (8s) set of primitives was contracted to [3s], and a (4s) set for hydrogen to [2s].

### B. The Restricted Open Shell SCF (ROSSCF)

The SCF results for the lithium carbenes were obtained using the ROSSCF routine (PA41) of the POLYATOM package of programs.



Table 26. Basis Set for LiCH and Li<sub>2</sub>C Calculations.

Atom	s-functions		p-functions	
	$\alpha_i$	$d_i$	$\alpha_i$	$d_i$
Li	1354.159	.00084731232	1.5343	.032763
	203.30116	.0065139116	.27499	.139005
	46.323493	.032726414	.073618	.500402
	13.133489	.11848646	.024026	.508552
	4.2477542	.29643380		
	1.4872743	.44723288		
	.54097490	1.0		
.047841890	1.0			
C	4240.3098	.0012152226	18.099144	.014760512
	637.77827	.0092731586	3.9769145	.091649350
	146.74534	.045279235	1.1450768	.30392714
	42.531428	.15492334	.36188831	.50711806
	14.184804	.35808349		
	2.0072531	.14932812	.11460548	1.0
	5.1756943	1.0		
.49677422	1.0			
.15348718	1.0			
H	19.2406	.032828		
	2.8992	.231208		
	.6534	.817238		
	.1776	1.0		

For a closed shell wave function (all electrons spin-paired) the set of one-particle equations are mixed by a matrix of Lagrangian multipliers. A unitary transformation on the occupied functions can be found which does not alter the physical meaning of the total wave function but effects a diagonalization of the multiplier matrix. The result is a set of pseudo-eigenvalue equations for the individual MO's. In the open shell problem, attempts to apply the same technique met with difficulties in eliminating the off-diagonal multipliers connecting the closed and open shell functions, which cannot be mixed in a unitary transformation without altering the total wave function. No exact method of constructing open shell Hartree-Fock-Roothaan wave functions existed until Roothaan<sup>38</sup> found a formulation of the problem requiring no approximations. It is Roothaan's method which is the basis for the program employed here.

An open shell wave function based on the independent particle approximation usually cannot be written as a single Slater determinant, and in the ROSSCF method, an expression representing the energy expectation value of the multi-determinantal wave function is variationally minimized with respect to the coefficients,  $C_{ij}$ , which relate the MO's to the fixed set of basis functions. This energy expression, in the Roothaan formulation, has the form

$$E = 2 \sum_k H_k + \sum_{kl} (2J_{kl} - K_{kl}) + f \left[ 2 \sum_m H_m + f \sum_{mn} (2a J_{mn} - bK_{mn}) + 2 \sum_{km} (2J_{km} - K_{km}) \right],$$

where the indices  $k$  and  $l$  run over the set of closed MO's,  $m$  and  $n$  run only over the open shell MO's, and  $f$ ,  $a$ , and  $b$  are parameters which are chosen to make the expression identical to the energy expectation value of the multi-determinantal wave function of interest. It should be noted that a set of  $f$ ,  $a$ , and  $b$  cannot be found for all multi-determinantal functions.

As an example, consider the  $\text{LiCH } ^3\Sigma^-$  ground state function. In terms of Slater determinants,

$$\psi(^3\Sigma^-) = \frac{1}{\sqrt{2}} \{ |1\sigma\bar{1}\sigma 2\sigma\bar{2}\sigma 3\sigma\bar{3}\sigma 4\sigma\bar{4}\sigma \pi_x \bar{\pi}_z | + |1\sigma\bar{1}\sigma 2\sigma\bar{2}\sigma 3\sigma\bar{3}\sigma 4\sigma\bar{4}\sigma \bar{\pi}_x \pi_z | \}$$

where  $|\dots|$  represents a Slater determinant of one-particle spin functions, the bar over a spatial function indicates a  $\beta$  spin function, no bar means  $\alpha$  spin. Here the spatial MO's  $\{1\sigma, 2\sigma, 3\sigma, 4\sigma\}$  are the set of closed orbitals, and the degenerate pair  $\{\pi_x, \pi_z\}$  are the partially filled open set (only 2 of the 4 possible spin-orbitals are occupied). The expectation value of the electronic energy for this function, written in terms of one-electron integrals,  $H_i$ , and coulomb,  $J_{ij}$ , and exchange  $K_{ij}$ , integrals is:

$$\begin{aligned}
E_{el} = & 2 \sum_i H_i + \sum_{i,j} (2J_{ij} - K_{ij}) \\
& + \sum_m H_m + J_{\pi_x, \pi_z} \\
& + \sum_i (J_{i, \pi_x} - K_{i, \pi_x} + J_{i, \pi_z} - K_{i, \pi_z})
\end{aligned}$$

$$i, j = \{1\sigma, 2\sigma, 3\sigma, 4\sigma\}$$

$$m = \{\pi_x, \pi_z\}.$$

Roothaan's energy expression will be identical if  $f = 1/2$ ,  $a = 1$ , and  $b = 2$ .

### C. The Single Excitation CI (SECI)

To obtain variational wave functions for the excited states, which again are open-shell functions, without the ROSSCF calculation to optimize the MO's, a multideterminantal trial function was explicitly constructed, and the expectation value of the electronic Hamiltonian over this function was minimized variationally with respect to the weighting coefficients of the determinants. In actuality, the trial function was constructed of structures, which are linear combinations of determinants and have a definite spatial and spin symmetry:

$$S_i = \sum_j a_{ij} D_j,$$

where the  $D_j$  are determinants and the  $a_{ij}$  are fixed in relative size for a particular choice of spatial and spin symmetry. The two-determinant function  $\Psi(^3\Sigma^-)$  given above is an example of a structure, with  $a_1 = 1$ ,  $a_2 = 1$ .

The structures for the LiCH linear states  $^1\Delta$  and  $^1\Sigma^+$  are listed in Tables 27 and 28. The  $^1A'$ ,  $^1A''$  structures for bent LiCH appear in Tables 29 and 30. Tables 31 and 32 list the  $\text{Li}_2\text{C}$  structures of  $^1\Delta_g$  and  $^1\Sigma_g^+$  symmetry. The format of each determinant and structure is as given in Appendix I.

Table 27. LiCH  $^1\Delta$  SECI Structures

	a	Core	$x_1$	$x_2$	$x_3$	$z_1$	$z_2$	$z_3$
1	1.	11111111.....	11	..	..	..	..	..
1	-1.	11111111.....	..	..	..	11	..	..
2	1.	11111111.....	1.	.1	..	..	..	..
2	-1.	11111111.....	.1	1.	..	..	..	..
2	-1.	11111111.....	..	..	..	1.	.1	..
2	1.	11111111.....	..	..	..	.1	1.	..
3	1.	11111111.....	1.	..	.1	..	..	..
3	-1.	11111111.....	.1	..	1.	..	..	..
3	-1.	11111111.....	..	..	..	1.	..	.1
3	1.	11111111.....	..	..	..	.1	..	1.

Table 28. LiCH  $1^+$  SECI Structures.

	a	core	$x_1$	$x_2$	$x_3$	$z_1$	$z_2$	$z_3$
1	1.	11111111.....	11	..	..	..	..	..
1	1.	11111111.....	..	..	..	11	..	..
2	1.	11111111.....	1.	.1	..	..	..	..
2	-1.	11111111.....	.1	1.	..	..	..	..
2	1.	11111111.....	..	..	..	1.	.1	..
2	-1.	11111111.....	..	..	..	.1	1.	..
3	1.	11111111.....	1.	..	.1	..	..	..
3	-1.	11111111.....	.1	..	1.	..	..	..
3	1.	11111111.....	..	..	..	1.	..	.1
3	-1.	11111111.....	..	..	..	.1	..	1.

Table 29. LiCH  $^1A'$  SECI Structures.

	a	CORE	$a_5'$	$a_6'$	$a_7'$	$a_8'$	$a_9'$	$a_{10}'$	$a_{11}'$	$a_{12}'$	$a_{13}'$	$a_{14}'$	$a_{15}'$	$a_1''$	$a_2''$	$a_3''$
1	1.	11111111	11	..	..	..	..	..	..	..	..	..	..	..	..	..
2	1.	11111111	..	..	..	..	..	..	..	..	..	..	..	11	..	..
3	1.	11111111	..	..	..	..	..	..	..	..	..	..	..	1.	.1	..
3	-1.	11111111	..	..	..	..	..	..	..	..	..	..	..	.1	1.	..
4	1.	11111111	..	..	..	..	..	..	..	..	..	..	..	1.	..	.1
4	-1.	11111111	..	..	..	..	..	..	..	..	..	..	..	.1	..	1.
5	1.	11111111	1.	.1	..	..	..	..	..	..	..	..	..	..	..	..
5	-1.	11111111	.1	1.	..	..	..	..	..	..	..	..	..	..	..	..
6	1.	11111111	1.	..	.1	..	..	..	..	..	..	..	..	..	..	..
6	-1.	11111111	.1	..	1.	..	..	..	..	..	..	..	..	..	..	..
7	1.	11111111	1.	..	..	.1	..	..	..	..	..	..	..	..	..	..
7	-1.	11111111	.1	..	..	1.	..	..	..	..	..	..	..	..	..	..
8	1.	11111111	1.	..	..	..	.1	..	..	..	..	..	..	..	..	..
8	-1.	11111111	.1	..	..	..	1.	..	..	..	..	..	..	..	..	..
9	1.	11111111	1.	..	..	..	..	.1	..	..	..	..	..	..	..	..
9	-1.	11111111	.1	..	..	..	..	1.	..	..	..	..	..	..	..	..
10	1.	11111111	1.	..	..	..	..	..	.1	..	..	..	..	..	..	..
10	-1.	11111111	.1	..	..	..	..	..	1.	..	..	..	..	..	..	..
11	1.	11111111	1.	..	..	..	..	..	..	.1	..	..	..	..	..	..
11	-1.	11111111	.1	..	..	..	..	..	..	1.	..	..	..	..	..	..
12	1.	11111111	1.	..	..	..	..	..	..	..	.1	..	..	..	..	..
12	-1.	11111111	.1	..	..	..	..	..	..	..	1.	..	..	..	..	..
13	1.	11111111	1.	..	..	..	..	..	..	..	..	.1	..	..	..	..
13	-1.	11111111	.1	..	..	..	..	..	..	..	..	1.	..	..	..	..
14	1.	11111111	1.	..	..	..	..	..	..	..	..	..	.1	..	..	..
14	-1.	11111111	.1	..	..	..	..	..	..	..	..	..	1.	..	..	..

Table 30. LiCH  $^1A''$  SECI Structures.

	a	CORE	$a'_5$	$a'_6$	$a'_7$	$a'_8$	$a'_9$	$a'_{10}$	$a'_{11}$	$a'_{12}$	$a'_{13}$	$a'_{14}$	$a'_{15}$	$a''_1$	$a''_2$	$a''_3$
1	1.	11111111	1.	..	..	..	..	..	..	..	..	..	..	.1	..	..
1	-1.	11111111	.1	..	..	..	..	..	..	..	..	..	..	1.	..	..
2	1.	11111111	1.	..	..	..	..	..	..	..	..	..	..	..	.1	..
2	-1.	11111111	.1	..	..	..	..	..	..	..	..	..	..	..	1.	..
3	1.	11111111	1.	..	..	..	..	..	..	..	..	..	..	..	..	.1
3	-1.	11111111	.1	..	..	..	..	..	..	..	..	..	..	..	..	1.
4	1.	11111111	..	1.	..	..	..	..	..	..	..	..	..	.1	..	..
4	-1.	11111111	..	.1	..	..	..	..	..	..	..	..	..	1.	..	..
5	1.	11111111	..	..	1.	..	..	..	..	..	..	..	..	.1	..	..
5	-1.	11111111	..	..	.1	..	..	..	..	..	..	..	..	1.	..	..
6	1.	11111111	..	..	..	1.	..	..	..	..	..	..	..	.1	..	..
6	-1.	11111111	..	..	..	.1	..	..	..	..	..	..	..	1.	..	..
7	1.	11111111	..	..	..	..	1.	..	..	..	..	..	..	.1	..	..
7	-1.	11111111	..	..	..	..	.1	..	..	..	..	..	..	1.	..	..
8	1.	11111111	..	..	..	..	..	1.	..	..	..	..	..	.1	..	..
8	-1.	11111111	..	..	..	..	..	.1	..	..	..	..	..	1.	..	..
9	1.	11111111	..	..	..	..	..	..	1.	..	..	..	..	.1	..	..
9	-1.	11111111	..	..	..	..	..	..	.1	..	..	..	..	1.	..	..
10	1.	11111111	..	..	..	..	..	..	..	1.	..	..	..	.1	..	..
10	-1.	11111111	..	..	..	..	..	..	..	.1	..	..	..	1.	..	..
11	1.	11111111	..	..	..	..	..	..	..	..	1.	..	..	.1	..	..
11	-1.	11111111	..	..	..	..	..	..	..	..	.1	..	..	1.	..	..
12	1.	11111111	..	..	..	..	..	..	..	..	..	1.	..	.1	..	..
12	-1.	11111111	..	..	..	..	..	..	..	..	..	.1	..	1.	..	..
13	1.	11111111	..	..	..	..	..	..	..	..	..	..	1.	.1	..	..
13	-1.	11111111	..	..	..	..	..	..	..	..	..	..	.1	1.	..	..

Table 31.  $\text{Li}_2\text{C } ^1\Delta_g$  SECI Structures.

	a	CORE	$1x_g$	$1x_u$	$2x_g$	$2x_u$	$1z_g$	$1z_u$	$2z_g$	$2z_u$
1	1.	1111111111	11	..	..	..	..	..	..	..
1	-1.	1111111111	..	..	..	..	11	..	..	..
2	1.	1111111111	1.	.1	..	..	..	..	..	..
2	-1.	1111111111	.1	1.	..	..	..	..	..	..
2	-1.	1111111111	..	..	..	..	1.	.1	..	..
2	1.	1111111111	..	..	..	..	.1	1.	..	..
3	1.	1111111111	1.	..	.1	..	..	..	..	..
3	-1.	1111111111	.1	..	1.	..	..	..	..	..
3	-1.	1111111111	..	..	..	..	1.	..	.1	..
3	1.	1111111111	..	..	..	..	.1	..	1.	..
4	1.	1111111111	1.	..	..	.1	..	..	..	..
4	-1.	1111111111	.1	..	..	1.	..	..	..	..
4	-1.	1111111111	..	..	..	..	1.	..	..	.1
4	1.	1111111111	..	..	..	..	.1	..	..	1.

Table 32.  $\text{Li}_2\text{C } ^1\Sigma_g^+$  SECI Structures

	a	CORE	$x_g$	$x_u$	$x_g$	$x_u$	$z_g$	$z_u$	$z_g$	$z_u$
1	1.	1111111111	11	..	..	..	..	..	..	..
1	1.	1111111111	..	..	..	..	11	..	..	..
2	1.	1111111111	1.	.1	..	..	..	..	..	..
2	-1.	1111111111	.1	1.	..	..	..	..	..	..
2	1.	1111111111	..	..	..	..	1.	.1	..	..
2	-1.	1111111111	..	..	..	..	.1	1.	..	..
3	1.	1111111111	1.	..	.1	..	..	..	..	..
3	-1.	1111111111	.1	..	1.	..	..	..	..	..
3	1.	1111111111	..	..	..	..	1.	..	.1	..
3	-1.	1111111111	..	..	..	..	.1	..	1.	..
4	1.	1111111111	1.	..	..	.1	..	..	..	..
4	-1.	1111111111	.1	..	..	1.	..	..	..	..
4	1.	1111111111	..	..	..	..	1.	..	..	.1
4	-1.	1111111111	..	..	..	..	.1	..	..	1.

### APPENDIX III

To construct the  $a_{ijkl}$  in Equation III.B.2, given  $S(\bar{r}_1, \bar{r}_2)$  in the form of Equation III.B.1, it is sufficient for illustration to evaluate one term in the sum over the pairs of determinants:

$$\langle D_K | \sum_{u \neq v}^N \sum^N (3\hat{s}_{uz}\hat{s}_{vz} - \hat{s}_u \cdot \hat{s}_v) \delta(\bar{r}_u - \bar{r}_1) \delta(\bar{r}_v - \bar{r}_2) | D_L \rangle.$$

First, however, it is necessary to make some preliminary explanatory remarks essential to clarity.

The determinants are assumed to be of the form

$$D_K = A(\phi_1(1)\phi_2(2)\phi_3(3)\dots\phi_N(N)),$$

where  $A$  is the  $N$ -particle anti-symmetrizer, and the  $\phi_i$  are spin-orbitals forming an orthonormal set. Although each pair of spin-orbitals,  $\phi_i$  and  $\phi_j$ , are distinct for  $i \neq j$ , their space parts,  $\chi_i$  and  $\chi_j$ , may be identical.

Also it is convenient to rewrite the spin part of the two particle operator as follows:

$$3\hat{s}_{uz}\hat{s}_{vz} - \hat{s}_u \cdot \hat{s}_v = 2\hat{s}_{uz}\hat{s}_{vz} - \frac{1}{2}(\hat{s}_{u+}\hat{s}_{v-} + \hat{s}_{u-}\hat{s}_{v+}).$$

The contribution due to a pair of determinants over a two-particle operator is given by the well-known Slater-Condon rules, by which three cases can be distinguished.

Defining

$$\hat{O}(u,v) \equiv [2\hat{s}_{uz}\hat{s}_{vz} - \frac{1}{2}(\hat{s}_{u+}\hat{s}_{v-} + \hat{s}_{u-}\hat{s}_{v+})] \delta(\bar{r}_u - \bar{r}_1) \delta(\bar{r}_v - \bar{r}_2),$$

the three cases are as follows:

a)  $D_K \equiv D_L:$

$$2\langle D_K | \sum_{u>v} \hat{O}(u,v) | D_K \rangle$$

$$= 2 \sum_{k>l} \langle \phi_k(u) \phi_l(v) | \hat{O}(u,v) (\hat{1} - \hat{P}_{uv}) | \phi_k(u) \phi_l(v) \rangle;$$

in which  $k$  and  $l$  run over the sets of occupied spin-orbitals in each determinant, and  $\hat{P}_{uv}$  is the transposition operator for the particles  $u$  and  $v$ . It is through this case that every determinant has the potential to contribute.

b) In place of  $\phi_a$  in  $D_K$ ,  $\phi'_a$  appears in  $D_L$  (1 dissonant orbital, 1DO);

$$2\langle D_K | \sum_{u>v} \hat{O}(u,v) | D_L \rangle$$

$$= 2 \sum_{k \neq a} \langle \phi_k(u) \phi_a(v) | \hat{O}(u,v) (\hat{1} - \hat{P}_{uv}) | \phi_k(u) \phi'_a(v) \rangle.$$

c)  $\phi_a$  and  $\phi_b$  in  $D_K$  are replaced by  $\phi'_a$  and  $\phi'_b$  in  $D_L$  (2DO):

$$2\langle D_K | \sum_{u>v} \hat{O}(u,v) | D_L \rangle$$

$$= 2\langle \phi_a(u) \phi_b(v) | \hat{O}(u,v) (\hat{1} - \hat{P}_{uv}) | \phi'_a(u) \phi'_b(v) \rangle.$$

Any other situation yields a result of zero.

Since each case reduces to a sum of integrals of orbital products over  $\hat{O}(u,v) (\hat{1}-\hat{P}_{uv})$ , it is useful to evaluate a general integral of that type. For the integral

$$\langle \phi_a(u) \phi_b(v) | \hat{O}(u,v) (\hat{1}-\hat{P}_{uv}) | \phi_p(u) \phi_q(v) \rangle,$$

two possibilities arise; the four spin-orbitals involved have the same spin or both  $\alpha$  and  $\beta$  spin are involved. Considering the first possibility (like spins):

$$\begin{aligned} & \langle \phi_a(u) \phi_b(v) | (2\hat{s}_{uz}\hat{s}_{vz} - \frac{1}{2}(\hat{s}_{u+}\hat{s}_{v-} + \hat{s}_{u-}\hat{s}_{v+})) \delta(\bar{r}_u - \bar{r}_1) \\ & \quad \times \delta(\bar{r}_v - \bar{r}_2) (\hat{1}-\hat{P}_{uv}) | \phi_p(u) \phi_q(v) \rangle \\ & = \langle \phi_a(u) \phi_b(v) | [2(\frac{1}{4}) - \frac{1}{2}(0)] \delta(\bar{r}_u - \bar{r}_1) \delta(\bar{r}_v - \bar{r}_2) (\hat{1}-\hat{P}_{uv}) | \phi_p(u) \phi_q(v) \rangle \\ & = \frac{1}{2} \{ \chi_a(\bar{r}_1) \chi_b(\bar{r}_2) \chi_p(\bar{r}_1) \chi_q(\bar{r}_2) - \chi_a(\bar{r}_1) \chi_b(\bar{r}_2) \chi_q(\bar{r}_1) \chi_p(\bar{r}_2) \}. \end{aligned}$$

For mixed spins, i.e., one  $\alpha$  and one  $\beta$  in each orbital product, the result is:

$$\begin{aligned} & \langle \phi_a(u)_{\beta}^{\alpha} \phi_b(v)_{\alpha}^{\beta} | [2\hat{s}_{uz}\hat{s}_{vz} - \frac{1}{2}(\hat{s}_{u+}\hat{s}_{v-} + \hat{s}_{u-}\hat{s}_{v+})] \delta(\bar{r}_u - \bar{r}_1) \\ & \quad \times \delta(\bar{r}_v - \bar{r}_2) (\hat{1}-\hat{P}_{uv}) | \phi_p(u)_{\beta}^{\alpha} \phi_q(v)_{\alpha}^{\beta} \rangle \\ & = \langle \phi_a(u)_{\beta}^{\alpha} \phi_b(v)_{\alpha}^{\beta} | \delta(\bar{r}_u - \bar{r}_1) \delta(\bar{r}_v - \bar{r}_2) \{ 2(-\frac{1}{4}) (\hat{1}-\hat{P}_{uv}) | \phi_p(u)_{\beta}^{\alpha} \phi_q(v)_{\alpha}^{\beta} \rangle \end{aligned}$$

$$\begin{aligned}
& - \frac{1}{2} (\hat{1} - \hat{P}_{uv}) | \phi_p(u) \phi_q(v) \rangle \\
& = - \frac{1}{2} \chi_a(\bar{r}_1) \chi_b(\bar{r}_2) \chi_p(\bar{r}_1) \chi_q(\bar{r}_2) - \frac{1}{2} [ -\chi_a(\bar{r}_1) \chi_b(\bar{r}_2) \chi_q(\bar{r}_1) \chi_p(\bar{r}_2) ] \\
& = - \frac{1}{2} \chi_a(\bar{r}_1) \chi_b(\bar{r}_2) (\hat{1} - \hat{P}_{12}) \chi_p(\bar{r}_1) \chi_q(\bar{r}_2).
\end{aligned}$$

Using these expressions, it is now possible to write out the results for each pair of determinants.

Case a):

$$\begin{aligned}
& 2 \langle D_K | \sum_{u>v} \hat{O}(u,v) | D_K \rangle \\
& = \sum_{k_\alpha > \ell_\alpha} \chi_{k_\alpha}(\bar{r}_1) \chi_{\ell_\alpha}(\bar{r}_2) [\hat{1} - \hat{P}_{12}] \chi_{k_\alpha}(\bar{r}_1) \chi_{\ell_\alpha}(\bar{r}_2) \\
& + \sum_{k_\beta > \ell_\beta} \chi_{k_\beta}(\bar{r}_1) \chi_{\ell_\beta}(\bar{r}_2) [\hat{1} - \hat{P}_{12}] \chi_{k_\beta}(\bar{r}_1) \chi_{\ell_\beta}(\bar{r}_2) \\
& - \sum_{k_\alpha > \ell_\beta} \chi_{k_\alpha}(\bar{r}_1) \chi_{\ell_\beta}(\bar{r}_2) [\hat{1} - \hat{P}_{12}] \chi_{k_\alpha}(\bar{r}_1) \chi_{\ell_\beta}(\bar{r}_2) \\
& - \sum_{k_\beta > \ell_\alpha} \chi_{k_\beta}(\bar{r}_1) \chi_{\ell_\alpha}(\bar{r}_2) [\hat{1} - \hat{P}_{12}] \chi_{k_\beta}(\bar{r}_1) \chi_{\ell_\alpha}(\bar{r}_2) .
\end{aligned}$$

With respect to the index running over the spin-orbitals in the orbital product of  $D_K$ ,  $k_\alpha$  is the subset labelling the  $\alpha$  spin-orbitals and similarly for  $\ell_\alpha$ ,  $k_\beta$ , and  $\ell_\beta$ .

Case b):

$$2 \langle D_K | \sum_{u>v} \hat{O}(u,v) | D_L \rangle$$

$$\begin{aligned}
&= (-1)^{P_{KL} + (m_s - \frac{1}{2})} \sum_{k\alpha \neq a} \chi_a(\bar{r}_1) \chi_{k\alpha}(\bar{r}_2) (\hat{1} - \hat{P}_{12}) \chi'_a(\bar{r}_1) \chi_{k\alpha}(\bar{r}_2) \\
&- (-1)^{P_{KL} + (m_s - \frac{1}{2})} \sum_{k\beta \neq a} \chi_a(\bar{r}_1) \chi_{k\beta}(\bar{r}_2) (\hat{1} - \hat{P}_{12}) \chi'_a(\bar{r}_1) \chi_{k\beta}(\bar{r}_2).
\end{aligned}$$

$P_{KL}$  is the number of transpositions required to bring the dissonant orbitals,  $\phi_a$  and  $\phi'_a$ , to the same position in the orbital products of each determinant,  $D_K$  and  $D_L$ .  $M_s$  is the  $\hat{S}_z$  eigenvalue of the dissonant orbitals ( $\frac{1}{2}$  for  $\alpha$ ;  $-\frac{1}{2}$  for  $\beta$ ).

Case c):

$$\begin{aligned}
&2 D_K | \sum_{u>v} \hat{O}(u,v) | D_L \\
&= \pm (-1)^{\sigma_{KL}} \chi_a(\bar{r}_1) \chi_b(\bar{r}_2) (\hat{1} - \hat{P}_{12}) \chi'_a(\bar{r}_1) \chi'_b(\bar{r}_2)
\end{aligned}$$

$\sigma_{KL}$  is the number of transpositions required to bring the dissonant orbitals into corresponding positions in their respective determinants; such that their spin functions match in the case of mixed spins. The (+) applies if all the spins are the same; the (-) if both spin functions are involved.

The above completes the details of how each integral over each pair of determinants contributes to the function  $S(\bar{r}_1, \bar{r}_2)$ . It is significant to note that although the summations involve all the spin-orbitals in each determinant, in practice there is usually a "core" of closed shells,

spatial MO's doubly occupied in every determinant. Due to a theorem by McConnell,<sup>39</sup> the core, as a contributor to the spatially symmetric part of the two-particle density matrix, can be ignored as a cause of ZFS. This will also be true for any closed shell common to both determinants when evaluating the contributions from the sum over determinant pairs. Depending on the wave function employed, these considerations can effect significant savings in computation.

## **BIBLIOGRAPHY**

## BIBLIOGRAPHY

1. Geuther, A., Justus Siebig's Ann. Chem., 123, 121 (1862).
2. Standinger, H., and Kupfer, O., Ber., 45, 501 (1912).
3. Mulliken, R. S., Phys. Rev., 41, 751 (1932).
4. Venkateswarlu, P., Phys. Rev., 77, 79, and 676 (1950).
5. Andrews, F. B., and Barrow, R. F., Nature (London), 165, 890 (1950).
6. Herberg, G., and Shoosmith, J., Nature (London), 183, 1801 (1959).
7. Herzberg, G., Proc. Roy. Soc. (Ser. A), 262, 291 (1961).
8. Herzberg, G., and Johns, J. W. C., Proc. Roy. Soc. (Ser. A), 295, 107 (1967).
9. Harrison, J. F., and Allen, J. C., J. Am. Chem. Soc., 91, 807 (1969).
10. Bender, C. F., Schaefer, H. F. III, O'Neil, S. V., J. Chem. Phys. 55, 162 (1971).
11. Bernheim, R. A., Bernard, H. W., Wang, P. S., Wood, L. S., and Skell, P. S., J. Chem. Phys. 53, 1280 (1970).
12. (a) Wasserman, E., Yager, W. A., and Kuck, V. J., Chem. Phys. Lett., 7, 409 (1970).  
(b) Wasserman, E., Kuck, V. J., Hutton, R. S., and Yager, W. A., J. Am. Chem. Soc., 92, 7491 (1970).  
(c) Wasserman, E., Kuck, V. J., Hutton, R. S., Yager, W. A., J. Chem. Phys., 55, 2593 (1971).
13. Herzberg, G., and Johns, J. W. C., J. Chem. Phys. 54, 2276 (1971).
14. Hoffman, R., Zeiss, G. D., and VanDine, G. W., J. Am. Chem. Soc., 90, 1485 (1968).
15. Staemmler, V., Theor. Chim. Acta., 31, 49 (1973).
16. Harrison, J. F., Int. J. Quant. Chem., 5, 285 (1971).
17. Hine, J., Divalent Carbon, The Ronald Press Co., New York (1964).

18. Kirmse, W., Carbene Chemistry (2nd Ed.), Academic Press (1971).
19. Harrison, J. F., Accts. Chem. Res., 7, 378 (1974).
20. Pople, J. A., Hehre, W. J., Stewart, R. F., J. Chem. Phys., 51, 2657 (1969).
21. Shalhoub, G., and Harrison, J. F., J. Am. Chem. Soc., 97, 000 (1975).
22. Csizmadia, I. G., J. Chem. Phys., 44, 1849 (1966).
23. Powell, F. X., Lide, D. R., Jr., J. Chem. Phys., 45, 1067 (1966).
24. Bodor, N., and Dewar, M. J. S., J. Am. Chem. Soc., 94, 9103 (1972).
25. Mulliken, R. S., J. Chem. Phys., 23, 1833 (1955).
26. Harrison, J. F., J. Am. Chem. Soc., 93, 4112 (1971).
27. Williams, J. E., Chem. Phys. Lett., 25, 507 (1974).
28. Griffith, J. S., Mol. Phys., 3, 79 (1960).
29. McLachlan, A. D., Mol. Phys., 6, 441 (1963).
30. McWeeny, R., J. Chem. Phys., 34, 399 (1961).
31. Higuchi, J., J. Chem. Phys., 38, 1237 (1963); 39, 1339 (1963); 39, 1847 (1963).
32. Harrison, J. F., J. Chem. Phys., 54, 5413 (1971).
33. Hameka, H. F., and Hall, W. R., J. Chem. Phys., 58, 226 (1973).
34. Bender, C. F., and Davidson, E. R., J. Chem. Phys., 70, 2675 (1966).
35. Langhoff, S. R., and Davidson, E. R., Int. J. Quantum. Chem., VII, 759 (1973).
36. Huzinaga, S., Approximate Atomic Functions I (1971), Div. of Theoretical Chemistry, University of Alberta.
37. Dunning, T. H., Jr., J. Chem. Phys., 53, 2823 (1970).
38. Roothaan, C. C. J., Rev. Mod. Phys., 32, 179 (1960).
39. McConnell, H. M., Proc. Nat. Acad. Sci (Wash), 45, 172 (1959).



MICHIGAN STATE UNIVERSITY LIBRARIES



3 1293 03145 4642